

# A Generalized Procedure for Generating Flaw-Related Inputs for the FAVOR Code

---

---

Prepared by  
F. A. Simonen, S. R. Doctor, G. J. Schuster, and P. G. Heasler

**Pacific Northwest National Laboratory**  
Operated by  
Battelle Memorial Institute

Prepared for  
Division of Engineering Technology  
Office of Nuclear Regulatory Research  
U.S. Nuclear Regulatory Commission  
Washington, DC 20555-0001  
NRC Job Code Y6604

---

---

# A Generalized Procedure for Generating Flaw-Related Inputs for the FAVOR Code

---

---

Manuscript Completed: October 2003  
Date Published:

Prepared by  
F. A. Simonen, S. R. Doctor, G. J. Schuster, and P. G. Heasler

Pacific Northwest National Laboratory  
Richland, WA 99352

D. Jackson, NRC Project Manager

**Prepared for**  
**Division of Engineering Technology**  
**Office of Nuclear Regulatory Research**  
**U.S. Nuclear Regulatory Commission**  
**Washington, DC 20555-0001**  
**NRC Job Code Y6604**

## **ABSTRACT**

The U.S. Nuclear Regulatory Commission (NRC) has supported research to re-evaluate regulations for pressurized thermal shock. In addition to a severe overcooling transient and an embrittled material, a factor critical to reactor pressure vessel (RPV) failure is a crack-like flaw near the inner vessel surface. This report documents research on fabrication flaws performed at Pacific Northwest National Laboratory as part of a larger multiyear program sponsored by the NRC to address issues related to the reliability of ultrasonic testing and the development of improved programs for inservice inspection. These studies have generated data on flaws in RPVs in terms of flaw densities, flaw locations, and flaw sizes (through-wall depth dimensions and lengths). This report describes data from these studies, results from an expert judgment elicitation on RPV fabrication practices, and probabilistic models that characterize flaws that may exist in RPVs. A procedure is described for generating flaw-related parameters for use as inputs to probabilistic fracture mechanics calculations. This revision to NUREG/CR-6817 incorporates documentation of how welding flaws can be treated using the flaws per unit area concept and describes additional details of the flaw model used in the FAVOR probabilistic fracture mechanics code.



# CONTENTS

ABSTRACT.....	iii
EXECUTIVE SUMMARY .....	xv
ACKNOWLEDGMENTS .....	xvii
ABBREVIATIONS .....	xix
1 INTRODUCTION.....	1.1
1.1 Probabilistic Fracture Mechanics Codes .....	1.1
1.2 Domestic Reactor Pressure Vessel Fabrication .....	1.3
1.3 Historical Sources of Fabrication Flaw Data.....	1.3
1.4 Overview of Report .....	1.4
2 OVERVIEW OF FLAW ESTIMATION PROCEDURE .....	2.1
2.1 Vessel Regions and Flaw Categories.....	2.1
2.1.1 Seam Welds.....	2.1
2.1.2 Base Metal.....	2.2
2.1.3 Repair Welds.....	2.3
2.1.4 Cladding .....	2.3
2.1.5 Underclad Cracking.....	2.4
2.2 Treatment of Flaws by FAVOR Code.....	2.4
2.3 Monte Carlo Simulation .....	2.4
2.4 Estimation Procedure for Welds.....	2.5
2.5 Estimation Procedure for Base Metal .....	2.6
2.6 Estimation Procedure for Clad/Surface Flaws.....	2.7
2.7 Flaw Locations .....	2.7
2.8 Treatment of Uncertainties .....	2.8
2.9 Sample Flaw Distributions .....	2.8
2.10 Summary and Conclusions .....	2.9
3 EXAMINATIONS OF VESSEL MATERIAL .....	3.1
3.1 Procedures Used to Detect and Size Flaws .....	3.2
3.2 Characterization of Flaws for Fracture Mechanics Models.....	3.8
3.3 Treatment of Large Repair Flaws.....	3.8
3.4 Validated Flaw Densities and Size Distributions .....	3.11
3.4.1 Shielded Metal Arc Weld .....	3.12
3.4.2 Submerged Arc Weld .....	3.13
3.4.3 Repair Weld.....	3.13
4 EXPERT JUDGMENT PROCESS FOR FLAW DISTRIBUTION .....	4.1
4.1 Expert Judgment Process.....	4.1
4.1.1 Selection of Issues and Experts .....	4.1
4.1.2 Presentation of Issues to the Experts.....	4.1
4.1.3 Elicitation Training .....	4.2

4.1.4	Preparation of Issue Analyses by the Experts .....	4.2
4.1.5	Discussion of Issue Analyses .....	4.2
4.1.6	Elicitation of the Experts .....	4.2
4.2	Recomposition and Summary of Results.....	4.3
4.3	Flaw Characteristics from Elicitation .....	4.3
5	PRODIGAL WELD SIMULATION MODEL .....	5.1
5.1	Types of Defects.....	5.1
5.2	Defect Density .....	5.3
5.3	Defect Characteristics.....	5.3
5.4	Inspection Model.....	5.3
5.5	Computer-Based Implementation.....	5.3
5.6	Calculations and Results.....	5.4
5.7	Flaw Characterization by PRODIGAL Code .....	5.7
5.8	Discussion and Conclusions .....	5.7
6	WELD FLAWS - DATA AND STATISTICAL CORRELATIONS .....	6.1
6.1	Approach and Assumptions.....	6.1
6.2	Statistical Functions for Flaw Distributions .....	6.5
6.2.1	Flaw Densities .....	6.6
6.2.2	Conditional Depth Distribution for Small Flaws .....	6.8
6.2.3	Conditional Depth Distribution for Large SAW and SMAW Flaws .....	6.11
6.2.4	Conditional Depth Distribution for Large Repair Flaws.....	6.13
6.2.5	Length Distribution for Small SAW Flaws in PVRUF Vessel .....	6.15
6.2.6	Length Distribution for Small SMAW and Repair Flaws in PVRUF Vessel .....	6.17
6.2.7	Length Distribution for Small SAW Flaws in Shoreham Vessel .....	6.17
6.2.8	Length Distribution for Small SMAW and Repair Flaws in Shoreham Vessel .....	6.21
6.2.9	Length Distribution for Large SAW Flaws in PVRUF Vessel .....	6.22
6.2.10	Length Distribution for Large SMAW and Repair Flaws in PVRUF Vessel .....	6.22
6.2.11	Length Distribution for Large SAW Flaws in Shoreham Vessel .....	6.23
6.2.12	Length Distribution for Large SMAW and Repair Flaws in Shoreham Vessel .....	6.24
7	BASE METAL FLAWS - DATA AND STATISTICAL CORRELATIONS .....	7.1
7.1	Approach and Assumptions.....	7.1
7.2	Inputs from Expert Elicitation .....	7.3
7.3	Flaw Data from PNNL Base Metal Examinations .....	7.4
7.4	Flaw Estimation Procedure for Plate Materials .....	7.5
8	CLAD FLAWS - DATA AND STATISTICAL CORRELATIONS .....	8.1
8.1	Approach and Assumptions.....	8.1
8.2	Sources of Information Cladding Flaws.....	8.2
8.2.1	PVRUF Data .....	8.2
8.2.2	Data from Bettis Laboratory .....	8.3
8.2.3	Expert Judgment Elicitation .....	8.4
8.2.4	PRODIGAL Predictions.....	8.4
8.2.5	Vessel-Specific Considerations.....	8.6
8.3	Flaw Length Distribution for Clad Flaws.....	8.7
8.4	Flaw Inputs to Fracture Mechanics .....	8.11

8.5	Probabilistic Fracture Mechanics Calculations .....	8.13
8.5.1	Fracture Mechanics Methodology .....	8.14
8.5.2	Description of Reference Vessel .....	8.15
8.5.3	Results of Probabilistic Fracture Mechanics Calculations .....	8.15
8.5.4	Concluding Discussion.....	8.17
9	ALGORITHM TO GENERATE FLAW INPUT FILES FOR FAVOR.....	9.1
9.1	FAVOR Code Structure and Organization.....	9.1
9.1.1	FAVLoad Module .....	9.1
9.1.2	FAVPFM Module .....	9.3
9.1.3	FAVPost Module.....	9.8
9.2	Required Input Files .....	9.8
9.3	Computer Code for Generating Flaw Input Files .....	9.9
9.3.1	Input File to PNNL Algorithm .....	9.9
9.3.2	Output File from PNNL Algorithm.....	9.13
9.3.3	Output File from PNNL Algorithm for Inputs to FAVOR.....	9.14
9.4	Procedure for Weld Regions.....	9.14
9.4.1	Treatment of Weld Flaws.....	9.14
9.4.2	Flow Chart for Welds.....	9.15
9.4.3	Sample Input and Output File for Welds.....	9.17
9.5	Procedure for Base Metal Regions .....	9.20
9.5.1	Treatment of Base Metal Flaws.....	9.20
9.5.2	Flow Chart for Base Metal.....	9.21
9.5.3	Sample Input and Output Files for Base Metal .....	9.21
9.6	Procedure for Surface/Clad Flaws.....	9.24
9.6.1	Treatment of Surface/Clad Flaws.....	9.24
9.6.2	Flow Chart for Surface/Clad Flaws.....	9.24
9.6.3	Sample Input and Output Files for Surface/Clad Flaws.....	9.24
10	CONCLUSIONS.....	10.1
11	REFERENCES.....	11.1
Appendix A - STATISTICAL EQUATIONS FOR FLAW DISTRIBUTION FUNCTIONS AND UNCERTAINTY ANALYSIS .....		A.1
Appendix B - LIST OF EXPERTS ON VESSEL FLAWS .....		B.1

## FIGURES

1.1	Elements of Computational Model for Predicting Vessel Failure Probabilities and Its Application to Regulations for Pressurized Thermal Shock .....	1.2
2.1	Conceptual View of Material Regions of a Vessel and the Categories of Flaws That Can Impact Structural Integrity .....	2.1
2.2	Metallographic Cross Section of a Circumferential Weld Showing Adjacent Regions of Base Metal and Cladding .....	2.2
2.3	Flaw Locations Relative to Vessel Inner Surface .....	2.7
2.4	Sample Flaw Distribution for Use in Probabilistic Fracture Mechanics Calculations .....	2.9
3.1	Sequence of Techniques Used To Detect and Size Flaws .....	3.2
3.2	Techniques Used for Detailed Characterization of Flaws .....	3.2
3.3	Metallographic Cross Section of a Circumferential Weld from PVRUF Vessel Showing Adjacent Regions of Base Metal and Cladding .....	3.3
3.4	Location of Flaw in the Fusion Zone of a Weld with the Base Metal .....	3.3
3.5	Inside View of the PVRUF Vessel During SAFT-UT Inspections .....	3.4
3.6	Weld Normal Inspections .....	3.5
3.7	Examinations of Plate Specimens .....	3.5
3.8	Image of a Fabrication Flaw Using Conventional Radiography .....	3.5
3.9	Micrograph of 25-mm Cube Containing a Failed Weld Bead .....	3.7
3.10	Electron Microscope Image of Cracked Weld Bead .....	3.7
3.11	Composition of a Complex Flaw .....	3.9
3.12	Shape and Orientation of 14-mm PVRUF Flaw - Relevant to Structural Integrity Assessment .....	3.9
3.13	Shape and Orientation of 32-mm Shoreham Repair Flaw with Less Conservative Treatment B of Flaw Dimensions .....	3.11
3.14	SMAW Metal, Through-Wall Size Distribution of Cumulative Flaw Densities .....	3.12
3.15	SAW Metal, Through-Wall Size Distribution of Cumulative Flaw Densities .....	3.13

3.16	Repair Metal, Through-Wall Size Distribution of Cumulative Flaw Densities .....	3.14
3.17	Comparison of Through-Wall Size Distributions of Cumulative Flaw Densities.....	3.14
4.1	Relative Flaw Densities of Base Metal Compared to Weld Metal as Estimated by Expert Judgment Process .....	4.4
5.1	Types of Crack-Like Defects .....	5.2
5.2	Cross Section of Thickness Transition Single V Weld for PVRUF Vessel.....	5.5
5.3	Model of Thickness Transition Single V Weld for PVRUF Vessel.....	5.6
5.4	Calculated Flaw Frequencies for PVRUF Weld Showing Effects of Inspection and Repairs .....	5.7
5.5	Distributions of Flaw Aspect Ratio and Flaw Length as Predicted by PRODIGAL Weld Simulation .....	5.8
6.1	Uncertainty in Flaw Densities for Flaws in PVRUF Vessel .....	6.8
6.2	Uncertainty in Flaw Densities for Flaws in Shoreham Vessel.....	6.8
6.3.	PVRUF Weld Metal Specimen Cut into 25-mm Plate.....	6.9
6.4	Depth Distribution for Small Flaws Including Uncertainty Analysis .....	6.11
6.5	Uncertainty Evaluation for Complementary Conditional Depth Distribution for Large SAW and SMAW Flaws .....	6.13
6.6	Uncertainty Evaluation for Complementary Conditional Depth Distribution for Large Repair Flaws .....	6.14
6.7	Lengths of Small Flaws in SAW and SMAW Welds of PVRUF Vessel.....	6.16
6.8	Lengths of Small Flaws in SAW Welds of PVRUF Vessel Showing Exponential Distribution Along with Uncertainties .....	6.16
6.9	Lengths of Small Flaws in SMAW Welds of PVRUF Vessel Showing Exponential Distribution Along with Uncertainties .....	6.17
6.10	Lengths of Small Flaws in SAW and SMAW Welds of Shoreham Vessel .....	6.18
6.11	Lengths of Small Flaws in SAW Welds of Shoreham Vessel Showing Exponential Distribution Along with Uncertainties .....	6.18
6.12	Lengths of Small and Large Flaws in SMAW and Repair Welds of Shoreham Vessel Showing Exponential Distribution Along with Uncertainties.....	6.22

6.13	Lengths of Large Flaws in SMAW and Repair Welds of PVRUF Vessel Showing Exponential Distribution Along with Uncertainties.....	6.23
6.14	Lengths of Large Flaws in SAW Welds of Shoreham Vessel Showing Exponential Distribution Along with Uncertainties.....	6.25
7.1	A Flaw Detected in Plate Material .....	7.3
7.2	Flaw Frequencies for Plate Materials with Comparisons to Data for Weld Flaws .....	7.5
8.1	Examples of Flaws in Cladding of PVRUF Vessel.....	8.1
8.2	Summary of Data on Flaws in Vessel Cladding .....	8.2
8.3	Lengths of Clad Flaws in PVRUF and Hope Creek II Vessels.....	8.11
8.4	Proposed Curves for Estimating Number and Sizes of Flaws in Vessel Cladding .....	8.12
8.5	Probability of Flaw Initiation in Vessel with Axial Welds as Limiting Material .....	8.16
8.6	Probability of Flaw Initiation in Vessel with Plates as Limiting Material .....	8.16
9.1	Data Streams for FAVOR Code Modules (1) FAVLoad, (2) FAVPFM, and (3) FAVPost .....	9.2
9.2	Flaw Models in the FAVOR Code.....	9.3
9.3	Fabrication Configurations of PWR Vessel Beltline Shells.....	9.4
9.4	Input of User-Supplied Data on Flaw Distributions and Embrittlement and Output of Data on Vessel Failure Probabilities.....	9.5
9.5	Weld Fusion Area Definitions for (a) Axial-Weld Subregion Elements and (b) Circumferential Subregion Elements .....	9.7
9.6	Input Instructions for Flaw Distribution Algorithm.....	9.10
9.7	Flow Chart for Weld Flaws.....	9.16
9.8	Sample Flaw Distribution Input File for Weld Region .....	9.18
9.9	Sample from Flaw Distribution File for Weld Region.....	9.18
9.10	Sample Flaw Data Output File for Weld Region .....	9.19
9.11	Flaw Distribution for Various Vessel Regions .....	9.20
9.12	Sample from Flaw Distribution Input File for Base Metal Region.....	9.22
9.13	Sample Flaw Distribution Output File for Base Metal Region.....	9.22

9.14	Sample Flaw Data from Output File for Base Metal Region .....	9.23
9.15	Sample Flaw Distribution Input File for Surface/Clad Flaws .....	9.25
9.16	Output File for Surface/Clad Flaws .....	9.25
9.17	Data from Output File for Surface/Clad Flaw .....	9.26

## TABLES

3.1	Weld Material Evaluated To Generate Data on Flaw Rates .....	3.1
3.2	Base Metal Material Evaluated To Generate Data on Flaw Rates .....	3.1
3.3	Presence of Metallic and Nonmetallic Oxides in Failed Weld Bead .....	3.7
3.4	Flaw Dimensions, Validated by Use of Multiple Techniques.....	3.8
6.1	Flaw Density Parameters.....	6.7
6.2	Gamma Distribution Used To Sample for Parameter of Poisson Distribution for Flaw Densities .....	6.7
6.3	Weld Bead Dimensions for PVRUF and Shoreham Welds .....	6.7
6.4	Data from Radiography of 25-mm-Thick Plates from PVRUF Welds .....	6.10
6.5	Data and Parameters of the Uncertainty Distribution for Depth Distribution for Small Flaws .....	6.11
6.6	Large SAW and SMAW Flaws in PVRUF and Shoreham Vessels.....	6.12
6.7	Large Repair Flaws in PVRUF and Shoreham Vessels .....	6.14
6.8	Lengths of Small Flaws in SAW Welds of PVRUF Vessel.....	6.16
6.9	Lengths of Small Flaws in SMAW Welds of PVRUF Vessel .....	6.17
6.10	Lengths of Small Flaws in SAW Welds of Shoreham Vessel .....	6.19
6.11	Lengths of Small and Large Flaws in SMAW and Repair Welds of Shoreham Vessel .....	6.21
6.12	Lengths of Large Flaws in SMAW and Repair Welds of PVRUF Vessel.....	6.23
6.13	Lengths of Small Flaws in SAW Welds of Shoreham Vessel .....	6.24
7.1	Flaws Detected and Sized in PNNL Examinations of Inner 1 Inch of Plate Material .....	7.4
8.1	Flaws in Cladding of PVRUF Vessel.....	8.3
8.2	Parameters of Representative PWR Reactor Pressure Vessel for PRODIGAL Calculations .....	8.5
8.3	RR-PRODIGAL Predictions for Surface-Breaking Flaws in Cladding by Submerged Arc Process (with and without PT).....	8.5

8.4	RR-PRODIGAL Predictions for Buried Flaws in Cladding Applied with Manual Metal Arc and Submerged Arc Process .....	8.6
8.5	Clad Product Form and Inspection Results .....	8.8
8.6	Dimensions of Flaws in Cladding as Reported in Appendix A of Schuster et al. (1998).....	8.8
8.7	Validated Dimensions of Flaw in Cladding as Reported in Schuster et al. (2000).....	8.8
8.8	Amount of Multi-Wire Clad in Specimen HC2A2B.....	8.8
8.9	Length of Flaws in Cladding for Specimen HC2A2B .....	8.8
8.10	Amount of 4-in. Strip Clad in Specimen 5-10D.....	8.9
8.11	Length of Flaws in Cladding for Specimen 5-10D .....	8.9
8.12	Data Used to Develop Length Distribution for Clad Flaws .....	8.10
9.1	Applied Flaw Orientations by Major Regions .....	9.4



## EXECUTIVE SUMMARY

Pacific Northwest National Laboratory (PNNL) is conducting a multiyear program for the U.S. Nuclear Regulatory Commission (NRC) to assess the reliability of ultrasonic testing (UT) in detecting flaws in piping and pressure vessels and to develop improved programs for inservice inspection (ISI). This involves establishing the accuracy and reliability of UT for ISI and includes efforts to apply improved methods to ensure the integrity of vessels and piping at commercial nuclear power plants. This report summarizes studies that have measured and characterized fabrication flaws in the welds and base metal of reactor pressure vessel (RPV) materials.

The present work is coordinated with other research by the NRC that is re-evaluating regulations for pressurized thermal shock (PTS) of RPVs. In determining the significance of a PTS event, the critical factors for the integrity of an RPV are the severity of the overcooling transient, the level of material embrittlement, and the presence of a crack-like flaw near the inner vessel surface. This report documents research on fabrication flaws that has generated data on flaws in RPVs covering the vessel fabrication permit from the late 1960s through the early 1980s when most vessels in commercial operation were fabricated. The fabrication flaw data was developed to quantify the flaw densities, flaw locations, and flaw sizes (through-wall depth dimensions and lengths). In addition to data from vessel examinations, the report presents results from an expert judgment elicitation on RPV fabrication practices and presents probabilistic models that characterize the flaws that may exist in vessels. Also described is a procedure for generating flaw-related parameters for use as inputs to probabilistic fracture mechanics calculations. This revision to NUREG/CR-6817 incorporates documentation of how welding flaws can be treated using the flaws per unit area concept and describes additional details of the flaw model used in the FAVOR probabilistic fracture mechanics code.

PTS events consist of a severe overcooling along with an increase in pressure in the RPV, which challenges the integrity of the reactor vessel's inner wall. Such transients are a significant concern as plants approach the end of their operating license and for periods of license renewal because the material of the vessel wall can become increasingly embrittled at elevated levels of neutron fluence. PNNL has participated in research to address PTS issues by performing examinations of RPV materials to detect and measure the numbers and sizes of fabrication flaws in weld cladding and base metal. Experimental work has provided fabrication flaw data from nondestructive and destructive examinations using material from vessels fabricated for cancelled nuclear power plants.

The current treatment of fabrication flaws considers different vessel regions including seam welds, base metal, and cladding. Welding processes include submerged metal arc, shielded metal arc, and repair welding procedures. Depending on known details for the fabrication process, the resulting flaw distributions can, if desired, be generated to apply to a particular vessel. Most of the smaller flaws, which can be significant to the integrity of highly embrittled vessels, are related to common lack-of-fusion defects and slag that occurs from the normal welding process. The largest observed flaws are, however, associated with repair welding. The probabilistic model realistically assumes that flaws are at random locations through the thickness of the vessel wall rather than being conservatively placed at the inner vessel surface. Inner surface-breaking flaws are those associated with only the vessel cladding process.

Measured flaw data show vessel-to-vessel differences regarding the numbers and sizes of flaws. Consequently, the flaw treatment allows the application of data trends from either the Pressure Vessel

Research User Facility (PVRUF) vessel<sup>a</sup> or the Shoreham vessel. Because the limited data did include occurrences of very large flaws, the treatment truncates flaw distributions at flaw depths that significantly exceed the maximum observed depths. Flaw lengths (or aspect ratios) are not assumed to be very large as has been the practice in past treatments, with flaw lengths being assigned on the basis of the measured lengths of observed flaws.

The number and sizes of flaws in base metal regions are assigned using the limited flaw data from PNNL's examinations of plate and forging materials, as well as by applying insights gained from the expert judgment elicitation. Flaws in base metal, compared to weld material, have significantly lower densities in terms of flaws per unit volume of material. In addition, the maximum possible depth dimensions of base metal flaws are significantly less than the corresponding maximum depths of weld flaws.

To supplement the limited data from flaw measurements, PNNL has applied an expert judgment elicitation process and has applied the PRODIGAL flaw simulation model developed in the United Kingdom by Rolls-Royce and Associates. Using these data, PNNL has developed statistical distributions to characterize the number and sizes of flaws in the various regions of RPVs. The available data have been applied in combination with insights from the expert elicitation and PRODIGAL flaw simulation model to generate computer files using a Monte Carlo simulation that generates flaw-related inputs for probabilistic fracture mechanics calculations. The end objective of the PNNL work on flaw distributions has therefore been to support research at Oak Ridge National Laboratory that has developed the probabilistic fracture mechanics code titled FAVOR (**F**racture **A**nalysis of **V**essels: **O**ak **R**idge). This computer code predicts failure probabilities for embrittled vessels subject to PTS transients.

This report begins with a summary of the available empirical inspection and validated data on flaws in seam welds, repair welds, base metal, and cladding materials and describes the treatment of these data to estimate flaw densities, flaw depth distributions, and flaw aspect ratio distributions. In each case, there are statistical treatments of uncertainties in the parameters of the flaw distributions, which have been included as part of the inputs to the probabilistic fracture mechanics calculations. The report concludes with a presentation of some sample inputs for flaw distributions that have supported NRC evaluations of the risk of vessel failures caused by PTS events.

---

<sup>a</sup> The PVRUF vessel was fabricated by Combustion Engineering but was never put into use after fabrication was completed in December 1981. The vessel was later transported to Oak Ridge National Laboratory and was used for research programs related to the structural integrity of RPVs.

## ACKNOWLEDGMENTS

The authors wish to thank the U.S. Nuclear Regulatory Commission Office of Nuclear Regulatory Research for supporting this work and, in particular, the NRC Program Manager, Ms. Deborah A. Jackson.

The authors thank Dr. Lee Abramson, Dr. Mark Kirk, and Dr. Ed Hackett of the U.S. Nuclear Regulatory Commission Office of Nuclear Regulatory Research for discussions and guidance during the development of the generalized procedure for estimating vessel-specific flaw distributions. Terry Dickson of Oak Ridge National Laboratory provided constructive interactions that ensured that the flaw estimation procedure was compatible with current fracture mechanics developments. Finally, we acknowledge the insights gained from discussions with the members of the expert elicitation panel.

The authors also acknowledge the contributions of PNNL staff members Ms. Kay Hass for assistance in preparing this manuscript and Ms. Andrea Currie for editorial support.



## ABBREVIATIONS

ASME	American Society of Mechanical Engineers
BWR	boiling water reactor
CAT	computer-assisted tomography
CCDF	complementary conditional depth distribution
CPF	conditional probability of failure
CPI	conditional probability of initiation
EPRI	Electric Power Research Institute
ESW	electro slag welding
FAVOR	Fracture Analysis of Vessels: Oak Ridge
GDF	generalized flaw distribution
GMAW	gas metal arc welding
GTAW	gas tungsten arc welding
HAZ	heat-affected zone
ISI	in-service inspection
LQ	lower quartile
NDE	nondestructive evaluation
NDT	nondestructive testing
NRC	U.S. Nuclear Regulatory Commission
ORNL	Oak Ridge National Laboratory
PFM	probabilistic fracture mechanics
PNNL	Pacific Northwest National Laboratory
PRA	probabilistic risk assessment
PT	dye penetrant
PTS	pressurized thermal shock
PVRUF	Pressure Vessel Research User Facility
PWR	pressurized water reactor
RPV	reactor pressure vessel
RRA	Rolls-Royce and Associates
RT	radiographic testing
RVID	reactor vessel integrity data

SAFT-UT	synthetic aperture focusing technique for ultrasonic testing
SAW	submerged arc welding
SMAW	shielded metal arc welding
UQ	upper quartile
UT	ultrasonic testing

# 1 INTRODUCTION

The U.S. Nuclear Regulatory Commission (NRC) has supported research to re-evaluate the regulations for pressurized thermal shock (PTS) within the framework of modern probabilistic risk assessment techniques (Dickson et al. 1999). A PTS event or transient consists of a severe overcooling along with an increase in pressure in the reactor pressure vessel (RPV), which challenges the integrity of the reactor vessel's inner wall. Such transients are a significant concern as plants approach the end of their operating license and for periods of license renewal because the material of the vessel wall can become increasingly embrittled at elevated levels of neutron fluence. In addition to the severe overcooling transient and embrittled vessel material, a factor critical to vessel failure is the presence of a crack-like flaw within the embrittled material of the inner surface region of the vessel. This report focuses on the fabrication flaws in RPVs in terms of the number of flaws (flaw density), the locations of flaws (relative to the vessel inner surface), the sizes of the flaws (through-wall depth dimensions and lengths), and orientations of flaws (axial or circumferential).

Pacific Northwest National Laboratory (PNNL) has participated in research to address PTS issues by performing examinations of RPV materials to detect and measure the numbers and sizes of fabrication flaws in welds and base metal. To supplement the limited data from flaw detection and measurements, PNNL has applied an expert judgment elicitation process (Jackson and Doctor 2000; Jackson and Abramson 2000) and the PRODIGAL flaw simulation model (Chapman and Simonen 1998) developed in the United Kingdom by Rolls-Royce and Associates. The experimental work on flaw distributions has provided fabrication flaw data from nondestructive and destructive examinations. Using these data, PNNL has developed statistical distributions to characterize the number and sizes of flaws in the various regions of RPVs. The work on flaw distributions has been coordinated with another research program at Oak Ridge National Laboratory (ORNL) that has developed a probabilistic fracture mechanics (PFM) code titled FAVOR (Fracture Analysis of Vessels: Oak Ridge) (Dickson 1994). This computer code predicts failure probabilities for embrittled vessels subject to PTS transients. Critical inputs to FAVOR are the number and sizes of fabrication flaws in the vessels of interest. To this end, PNNL has provided computer files to ORNL that describe the flaws in various vessel regions. The present report describes how PNNL applied the available data on fabrication flaws in combination with insights from the expert elicitation and PRODIGAL flaw simulation model to computer files that serve as inputs to the FAVOR.

## 1.1 Probabilistic Fracture Mechanics Codes

Since the early to mid 1980s, there have been significant advancements and refinements in the relevant technologies associated with the physics of PTS events that impact RPV integrity assessment. Updated computational models have evolved through interactions among experts in the relevant disciplines of thermal hydraulics, probabilistic risk assessment, statistics, material embrittlement, fracture mechanics, and inspection (flaw detection and characterization). These updated models have been integrated into the FAVOR computer code, which is an applications tool for performing risk-informed structural integrity evaluations of aging reactor pressure vessels. Figure 1.1 diagrams the major elements that enter into a PFM evaluation of a RPV subjected to conditions of pressurized thermal shock. Each of these elements has been reviewed and revised as part of an effort to update the technical bases for revision of current NRC regulations for PTS. In this methodology, the loads due to thermal and pressure transients come from detailed probabilistic risk assessments (PRAs) and thermal hydraulic calculations.

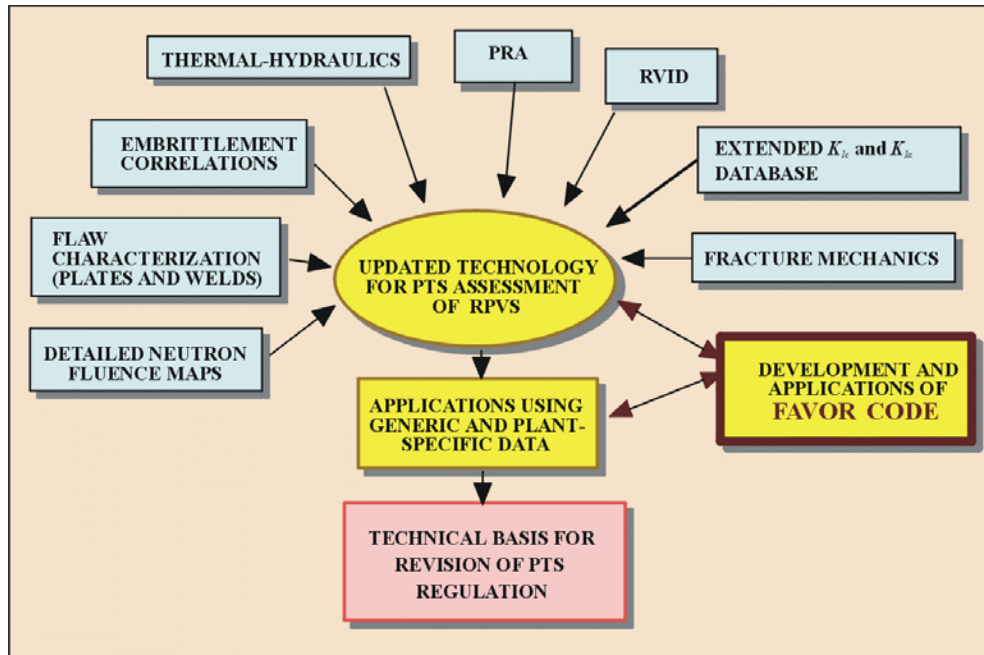


**Figure 1.1. Elements of Computational Model for Predicting Vessel Failure Probabilities and Its Application to Regulations for Pressurized Thermal Shock**

Material properties (fracture toughness estimates) are based on calculated neutron fluence maps, embrittlement correlations, databases on fracture toughness measurements, and vessel parameters from reactor vessel fabrication records (RVID).

The model used in the previous PFM analyses, from which the current PTS regulations were derived, conservatively postulated that all fabrication flaws were inner-surface breaking flaws. It was also recognized that the fabrication flaw data had the greatest level of uncertainty of the inputs required for the PTS evaluations. This report discusses an improved model that PNNL developed for postulating fabrication flaws in RPVs and describes the treatment of that data by the FAVOR code. The discussion presents a methodology that has been developed to estimate the number and sizes of fabrication flaws in RPVs. The methodology has been applied to generate flaw-related inputs for probabilistic fracture mechanics calculations that have been performed as part of an effort to update pressurized thermal shock regulations. NRC-funded research at PNNL has generated data on fabrication flaws from nondestructive and destructive examinations of RPV material (Crawford et al. 2000; Schuster et al. 1998, 1999, 2000a,b). Statistical distributions have been developed to describe the flaws in each material region (Jackson and Doctor 2000; Jackson and Abramson 2000; Jackson et al. 2001). Results from an expert elicitation (Jackson and Abramson 2000) helped to fill gaps in the measured data on fabrication flaws. The regions include the main seam welds, repair welds, base metal of plates and forgings, and the cladding at the inner surface of the vessel.

This report includes a summary of the available data on fabrication flaws in seam welds, repair welds, base metal, and cladding materials and describes the treatment of these data to estimate flaw densities, flaw depth distributions, flaw aspect ratio distributions, flaw orientation, and flaw location. In each case, there have been statistical treatments of uncertainties in the parameters of the flaw distributions, which have been included as part of the inputs to the PFM calculations. The report includes a presentation of

some sample inputs for flaw distributions that have supported evaluations by NRC of the risk of vessel failures caused by PTS events. This report is a revision of a previous NUREG/CR report. Revisions provide additional emphasis and documentation of how welding flaws are treated using the approach of flaws per unit area of weld fusion surface. The FAVOR code has adopted this approach, and revisions to this report ensure consistency with documentation of the FAVOR code. Additional discussion of the flaw model used in the FAVOR probabilistic fracture mechanics code also has been incorporated into this revision, along with a number of other changes of an editorial nature.

## **1.2 Domestic Reactor Pressure Vessel Fabrication**

The fabrication process involves a number of variables or characteristics that must be considered, some of which have a significant bearing on the introduction of flaws into the RPV. There were three major manufacturers of domestic RPVs: Combustion Engineering, which fabricated approximately 45% of the domestic RPVs; Babcock and Wilcox, which fabricated about 35%; and Chicago Bridge and Iron, which fabricated the remaining 20%. Although each vessel was inspected to American Society of Mechanical Engineers (ASME) standards prior to operation, the fabrication and inspection processes were different for each manufacturer. The fabrication processes for pressurized water reactors (PWRs) and boiling water reactors (BWRs) is very similar, but PTS is a concern only for PWRs.

Most RPVs in the United States were constructed by welding together plate material and forgings. The shell courses of the RPVs were constructed either by welding three sections of formed plate, resulting in axial weldments, or using forged rings for the shell courses. The base metal materials used for most plates and forgings were A533B and A508, respectively. The welding process used in the fabrication of the reactor vessels varied with each manufacturer. For the vast majority of PWRs, three welding processes were used in assembling the reactor vessels: shielded metal arc welding (SMAW), gas metal arc welding (GMAW), and submerged arc welding (SAW). The rarely used GMAW process was for cladding repairs. Both SMAW and SAW were used for axial and circumferential welds. A fourth process, electroslag, is an automatic process that was used mainly for axial welds in a few BWR vessels. Before, during, and following the welding, both surface and volumetric inspections were performed. A stainless steel cladding was applied to the inside of each shell course. The formed rings were then stacked and welded to form the cylinder. These circumferential weld preparation surfaces were inspected prior to welding, and the welds were subjected to inspections during and following welding. Finally, cladding was applied to the inside of the vessel to cover the newly formed circumferential weld, and the clad surface was then inspected.

## **1.3 Historical Sources of Fabrication Flaw Data**

The current rules that govern the generic PTS screening limit and plant-specific vessel evaluations were derived from models that utilized the Marshall distribution for flaws in the welds of RPVs. The documents on the Marshall study (Marshall Committee 1982) indicate that the flaw distribution was based on flaw data from a limited population of nuclear vessels and many non-nuclear vessels. The flaw measurements were part of the customary nondestructive preservice examinations as performed 25 or more years ago at vessel fabrication shops. Due to limitations of the nondestructive evaluation (NDE) technology, the Marshall flaw distribution provides a reasonable representation only for flaws having depth dimensions of about 1 in. (25.4 mm) or greater. The Marshall distribution has nevertheless been applied to PTS evaluations by extrapolation of curves to the much smaller flaws of concern to PTS calculations (flaw depths of 0.25 in. [6 mm] and smaller).

The objective of the recent NRC research on vessel flaws has been to examine RPV materials using more sensitive NDE techniques and to collect data on flaws of all sizes, including those with depth dimensions as small as a few millimeters. These efforts have exploited advanced NDE methods with high levels of sensitivity. Another advantage came from the use of material from surplus RPVs from cancelled plants. In this regard, ultrasonic scans were not limited to access from the clad inner surface of the vessels but exploited the use of smaller samples of material removed from intact vessels along with high-resolution synthetic aperture focusing technique for ultrasonic testing (SAFT-UT) scans from sectioned surfaces that were optimized to detect flaws with orientations normal to the vessel inner surface. The current database provides dimensions for a large number of relatively small flaws of the sizes identified as the major contributors to potential vessel failures for PTS events. Such flaw sizes were not addressed by the data used to develop the Marshall distribution.

Other papers have described the methods used to examine RPV materials and have documented the actual detection and sizing of the flaws in these materials. The flaw measurements have included through-wall depth dimensions, flaw lengths (aspect ratios), and locations of inner flaw tips relative to the inner surface of the vessel. Where limitations in the measured data were identified, other approaches, including expert elicitation (Jackson and Doctor 2000; Jackson and Abramson 2000) and the PRODIGAL weld simulation model (Chapman and Simonen 1998), were applied to supplement the measured data or to otherwise guide the development of flaw-related inputs to the fracture mechanics model. The objective of the current report is to describe how new sources of information on RPV flaws were used to support the improved model for postulating fabrication flaws in RPV. The discussion describes the conceptual framework of the PFM in terms of vessel regions and the types of flaws that are important to each region.

In the PTS evaluations, the flaws of concern are assumed to be present at the time of vessel fabrication but not detected and repaired before the vessel was placed into service. The evaluations assume that there are no credible mechanisms to cause service-related cracking of the RPV materials. It is also assumed that crack growth mechanisms of fatigue and stress corrosion cracking can be neglected due to the relatively benign operating conditions of pressurized water reactors.

## **1.4 Overview of Report**

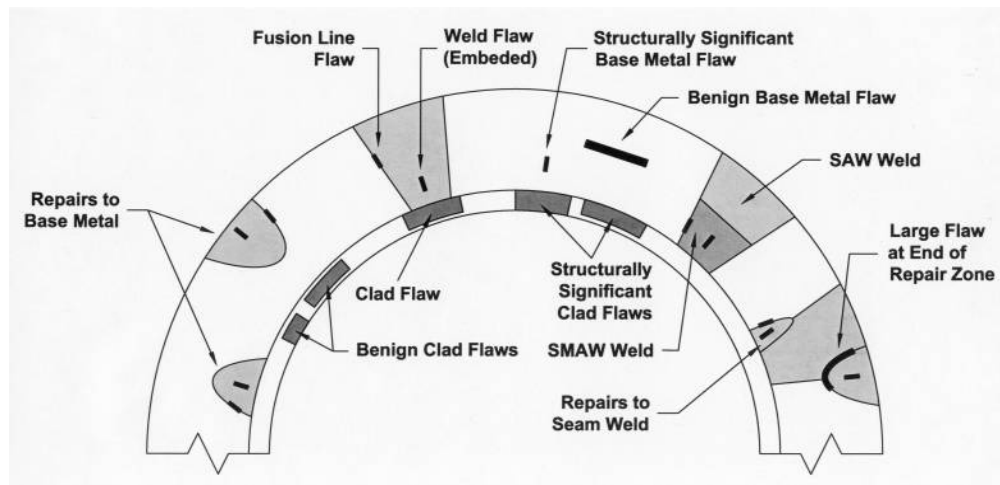
This report provides a systematic documentation of how flaw-related inputs have been generated for the FAVOR probabilistic fracture mechanics code. Section 2 describes the basic structure of the flaw estimation model, with a focus on key assumptions made in developing the methodology. Section 3 presents experimental work on examinations of vessel material that provided a database on fabrication flaws in welds, base metal, and cladding. Section 4 describes the expert judgment process used to augment the gaps in the empirical database and Section 5 provides a detailed description of and results from the PRODIGAL model. The treatment of these data to develop statistical distribution functions is documented in Sections 6, 7, and 8 for weld metal, base metal, and cladding, respectively. Integration of the flaw estimation model into a computer algorithm to generate input files for the FAVOR code is described in Section 9. Most of the revisions to the previous NUREG/CR report consist of additional material incorporated into Section 9. The new material provides additional documentation of how welding flaws can be treated using the flaws per unit area concept and describes in greater detail about the flaw model used in the FAVOR probabilistic fracture mechanics code. Section 10 provides conclusions.

## 2 OVERVIEW OF FLAW ESTIMATION PROCEDURE

This section provides an overview of the flaw estimation model and summarizes a number of assumptions made in the development of the model.

### 2.1 Vessel Regions and Flaw Categories

Figure 2.1 depicts the various regions of a RPV and the flaws that are addressed by the PFM model. This conceptual cross-sectional view shows axial welds in a vessel. A corresponding cross section to show circumferential welds would illustrate the same categories of flaws but with flaw orientations rotated by 90 degrees.



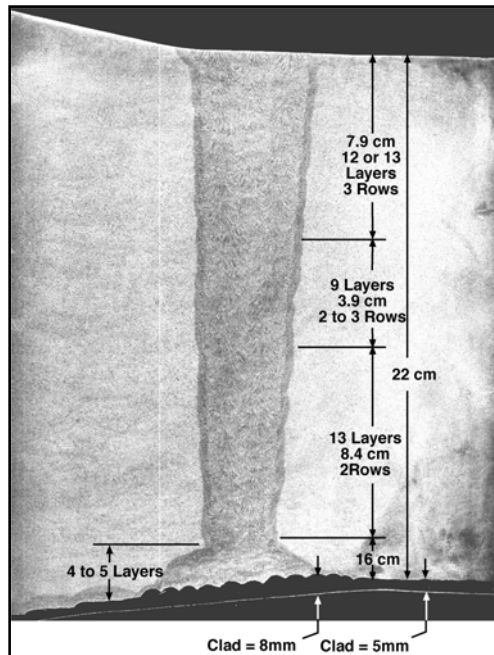
**Figure 2.1. Conceptual View of Material Regions of a Vessel and the Categories of Flaws That Can Impact Structural Integrity**

Figure 2.2 is a metallographic cross section of a circumferential weld from a RPV. This view shows all the major material regions of concern to vessel integrity, which include weld metal, base metal, weld fusion lines, and the cladding at the vessel inner surface. The flaws of concern are those present at the time of vessel fabrication and not detected and repaired before the vessel is placed into service. It is assumed in this report that there are no credible mechanisms to cause service-related cracking and that crack growth mechanisms of fatigue and stress corrosion cracking can be neglected.

In developing inputs for fracture mechanics calculations, the vessel material regions described in Sections 2.1.1 through 2.1.5 were addressed.

#### 2.1.1 Seam Welds

Major weld regions of concern to RPV integrity are the axial and circumferential seam welds in the high neutron fluence region of the vessel beltline. These welds can be fabricated by the SAW process or by the SMAW process. Typically, a given seam weld will have some welding from both processes but the largest fraction (e.g., >90%) of the weld would be deposited by the automatic SAW process. The improved flaw model accounts for separate flaw densities and flaw size distributions for each weld



**Figure 2.2. Metallographic Cross Section of a Circumferential Weld Showing Adjacent Regions of Base Metal and Cladding**

process. However, the identification of specific local weld regions as being produced by particular processes requires information not generally available from vessel fabrication records. Calculations with the FAVOR code have therefore been based on an assumption of a random mixture of SAW and SMAW materials along with a small fraction of repair welding. The fractions have been based on trends observed from examinations of vessels at PNNL.

Flaws in seam welds can be located randomly within the volume of deposited weld metal or along the fusion lines between the weld metal from the adjoining base metal (plate or forging material). Although some flaws are distributed within the volume of the weld joint, the measured data have shown very few of these flaws to have significant through-wall dimensions. Most flaws are located along the weld fusion line. These flaws (lack-of-fusion or entrapped slag) are usually relatively small. However, a small fraction of these flaws has through-wall dimensions approaching or exceeding the size of a single weld bead. Based on observed flaw locations, the probabilistic fracture mechanics analysis assumes that all weld-related flaws are located along weld fusion lines. Flaws for axial welds are assumed to have axial orientations, and flaws for circumferential welds are assumed to have circumferential orientations.

### 2.1.2 Base Metal

Flaws within base metal are observed to occur at much lower rates (per unit volume of metal) than in welds. Figure 2.1 shows two flaw categories that were identified. It is well known that the largest flaws in plate and forging materials have orientations parallel to the surface of the vessel. This orientation comes from the rolling and other operations used to fabricate the vessel plates and forged rings. Although such flaws can be quite large, their orientations are such that they have no significance to vessel integrity. As indicated in Figure 2.1, the only base metal flaws of concern are those that have some through-wall dimension. Data from limited examinations at PNNL of plate materials indicate that such flaws occur at

lower rates per unit volume (by a factor of ten or greater) in plate materials than in welds (Crawford et al. 2000; Schuster and Doctor 2001a).

Another significant feature of the flaw model for plate materials relates to the fusion line flaws located at the region between the base metal and weld metal. The FAVOR code assumes that these fusion line flaws can propagate into either embrittled weld metal or into embrittled plate material, depending on which material has the lower level of fracture toughness.

### **2.1.3 Repair Welds**

Although repair welds make up only a small percentage of the weld metal in a typical vessel, most of the larger flaws (depth dimensions greater than a weld bead) have been observed in weld repairs. As depicted in Figure 2.1, typical repairs consist of a ground-out region that has been filled by a manual welding process. The repairs can be entirely within seam welds, entirely within base metal, but will most typically span both weld metal and base metal because repairs are generally made to defects along the weld fusion lines. Repairs have been observed to occur at both the inside and the outside of vessels.

Flaws in repair welds have been observed along fusion lines between the metal of the weld repair and the original vessel material. These flaws will usually impinge on both seam welds and base metal. The largest flaws found during PNNL examinations have been located at the ends of repair cavities and have been attributed to the difficulties in manual welding within the confined spaces at the ends of the ground-out cavities.

In modeling of weld repairs with the FAVOR code, it has not been practical to identify specific locations of repairs such as may be documented by construction records. The repairs have been assumed to occur at random locations, such that the repair flaws are blended into the other population of flaws associated with the normal welding processes. The small amount of material from repair welding nevertheless makes a disproportionate contribution to the estimated numbers of larger flaws.

### **2.1.4 Cladding**

The number and size of surface-breaking flaws at the inner surface of a vessel have been estimated from data on flaws that have been detected during examinations of vessel cladding (Simonen et al. 2001). As indicated in Figure 2.1, such flaws can occur randomly in the cladding applied over both weld and base metal. Because the vessel inner surface consists mostly of base metal, all but a small fraction of the clad (or surface-related) flaws will be associated with base metal rather than with weld metal.

Figure 2.1 shows four categories of clad flaws. The FAVOR code assumes that the fracture toughness of the cladding material is sufficiently high such that flaws entirely within the cladding will not propagate. Hence, some configurations of clad flaws labeled in Figure 2.1 are benign. Structurally significant flaws are only those flaws (either buried flaws or large through-clad flaws) that extend to the clad-to-base metal interface. The vessel examinations show that the majority of such structurally significant flaws are of the buried type because the probability for the larger through-clad flaws is low and because shop examinations of clad surfaces will detect and repair most of the surface-breaking flaws that may occur from the weld depositing of cladding. All flaws in cladding are assumed to have circumferential orientations because cladding is applied using weld beads that have a circumferential orientation.

### **2.1.5 Underclad Cracking**

A final type of flaw, not yet addressed by the FAVOR code, is underclad cracks resulting from unfavorable conditions during the weld deposition of the cladding material. Underclad cracks have been observed in some vessels, particularly within the base metal of forged rings. Such flaws are precluded for most PWR vessels by consideration of the chemical compositions of the base metal.

## **2.2 Treatment of Flaws by FAVOR Code**

The FAVOR code simulates the sizes and locations of flaws and makes use of three input files for (1) flaws in weld regions, (2) flaws in base metal regions, and (3) surface-related flaws in the vessel cladding. In each case, the number of flaws per unit volume of material is specified using numerical tables of data. Statistical uncertainties in the estimated flaw-related parameters are treated by generating 1000 possible tables to characterize the estimated uncertainties in the flaw distributions. The elements of the tables correspond to flaws with given depth dimensions as a percentage of the vessel wall thickness and given aspect ratios (flaw length divided by flaw depth). The locations of flaws in weld and base metal regions are assumed to be randomly distributed through the thickness of the vessel wall.

All of the planar-type flaws that have been observed during the vessel examinations are treated by FAVOR as exhibiting ideal crack-like behavior. For planar flaws, it was not possible to consider the morphology of cracks in detail such as to account for flaws whose tips were somewhat blunted relative to idealized cracks such as sharpened by fatigue crack growth.

User input data to FAVOR PFM analyses includes the volume of metal or weld fusion areas for each of the RPV subregions. Each of these subregions has its own embrittlement-related properties. From the assigned metal volumes and areas and the inputs for the number of flaws per unit volume of each size category, the total number of flaws in each weld, base metal region, or clad region is calculated. Flaw locations relative to the vessel inner surface are assigned randomly. The FAVOR code also divides the vessel wall thickness into regions with the first region being the inner one-eighth of the wall thickness, and the second region being the region from one-eighth to three-eighths of the vessel wall thickness. FAVOR assumes that flaws located beyond three-eighths of the wall thickness make negligible contributions to the vessel failure probabilities.

## **2.3 Monte Carlo Simulation**

A computer code was developed by PNNL to generate input files for probabilistic fracture mechanics calculations. The flaw distribution code decomposed the data on measured flaws into a set of flaw categories (large and small flaws, SAW, SMAW, and repair welds) and separated the data measured from the Pressure Vessel Research User Facility (PVRUF) and Shoreham vessels. The objective was to allow vessel-specific flaw distributions to be estimated by consideration of the actual processes used to complete the welds, the sizes and number of weld beads for each weld, and the statistical uncertainties in the parameters that describe the characteristics of each category of welds.

To address uncertainties in the parameters of the statistical correlations that characterize the densities and sizes of the various categories of flaws, a Monte Carlo simulation was used to generate a large number of possible flaw distributions that are consistent with the uncertainties arising from the limited amount of data. The FAVOR code takes samples from these datasets in calculating vessel failure probabilities.

## 2.4 Estimation Procedure for Welds

The procedure assumes that seam welds consist of various amounts of weld metal deposited by different welding processes (SAW, SMAW, and manual repair welding). However, the FAVOR code does not attempt to identify the specific locations of materials from each process but assumes that each weld process can occur randomly within the volume of the completed weld. The procedure therefore blends the contributions from the three welding processes in accordance with the relative fractions of material deposited by each process. User inputs are required for the fraction of weld metal from each welding process. Characterization of welds in the PVRUF and Shoreham vessels indicates that at least 90% of the weld will be of the SAW type, 5% to 10% of the SMAW type, and 1% to 2% will consist of repair welding.

In evaluating the data from weld examinations, the flaw dimensions were first normalized with respect to the estimated thickness of the weld beads to account for vessel-to-vessel differences in welding procedures. This approach permitted the data from PVRUF and Shoreham vessels to be applied to welds with smaller or larger bead sizes.

The first step in the estimation procedure assigns values for the flaw densities (e.g., flaws per cubic meter or per square meter) for each of the weld types. Each sampling of the Monte Carlo simulation assigns six values of flaw density corresponding to the two flaw size categories (large and small) and the three weld processes (SAW, SMAW, and repair). The estimation procedure also includes a specification that determines if flaw densities should be based on the observed densities from the PVRUF vessel or from the Shoreham vessel.

The second step in the estimation procedure addresses the through-wall depths of simulated flaws. As part of this step, a user input is required to specify a through-wall bead size for each weld process. These bead sizes are used as the basis for distinguishing “small flaws” from “large flaws.” There are potentially six statistical distributions for the through-wall dimensions of flaws corresponding to the small and large flaws and the three welding processes. Because there were limited data from high-accuracy measurements for the sizes of very small flaws, a single depth distribution was assumed to apply to all three welding processes. For large flaws, there was a clear difference in the depth distributions for flaws in repair welds as compared to the flaw depths for SMAW and SAW welds. Two depth distribution functions were developed for large flaws. Given the relatively small number of large flaws, the uncertainties in the parameters of the distribution functions (exponential distributions) were relatively large, and these parameter uncertainties were an important element of the Monte Carlo simulation.

The next step of the flaw estimation procedure addressed flaw lengths (or aspect ratios). Again the procedure allows separate consideration of the trends from the PVRUF and Shoreham vessels and deals separately with the six flaw categories corresponding to small and large flaws and three weld processes (SAW, SMAW, and repair welds). The data indicated that flaw dimensions are best described in terms of flaw length rather than in terms of flaw aspect ratios (i.e., ratio of flaw length to flaw depth dimension). The important parameter was the amount by which the flaw lengths exceeded the flaw depth dimensions. This procedure produced distributions of flaw aspect ratios that were a function of the depth dimensions. The data showed interesting trends for flaw lengths. For example, small flaws in the SAW welds of the PVRUF vessel were all nearly 1:1, whereas the corresponding flaws in the Shoreham vessel had relatively large aspect ratios. Another significant trend was that flaws with relatively large through-wall depth dimensions had small aspect ratios. Flaws with large aspect ratios were primarily those with relatively small depth dimensions.

A final step in the estimation procedure allows a truncation on the possible through-wall depths of large flaws. The truncation values of flaw depths are user inputs to the estimation procedure. Different truncation values can be specified for each of the three welding processes. For example, the maximum depth dimension for repair flaws can be set at a much larger value than the maximum value for flaws associated with SAW welds.

Consistent with the flaw orientations observed during the PNNL examinations of vessel welds, the orientations of flaws in axial welds are treated as having axial orientations. Similarly, flaws in circumferential welds were treated as circumferential flaws.

## **2.5 Estimation Procedure for Base Metal**

The base metal flaws of interest were those with sufficient through-wall dimensions to potentially impact the structural integrity of an RPV. This consideration excluded the common types of planar flaws seen in plate and forging material (e.g., laminations) that may be relatively large but whose through-wall dimensions are negligible. Therefore, the examinations of vessel base metal specimens at PNNL were designed to detect and size flaws with measurable through-wall dimensions.

In summary, the inputs for flaws within the volume of base metal regions (plate and forging materials) were estimated by applying reduction factors to the flaw densities for weld metal. A factor of 10 reduction was applied for densities of small flaws (depth dimensions less than or equal to 6 mm) and a factor of 40 reduction for large flaws. A truncation of the distribution is applied to flaws greater than 11 mm in depth dimension, which depth corresponds to about 5% of a PWR vessel wall thickness. The resulting inputs for base metal flaws are otherwise identical to those for weld flaws, including the elements of flaw aspect ratios and uncertainty distributions applied to flaw densities. The procedure allows the parameters of the flaw density and depth distributions to be based on either the data from the PVRUF or the Shoreham vessels. Because the flaw aspect ratios observed during PNNL's base metal examinations had consistently small values, the assigned distribution of aspect ratios had values of 2:1 or less.

The reduction factors of 10 and 40 corresponded to values from an expert elicitation (Jackson and Abramson 2000). These values are also generally consistent with available data from nondestructive examinations of plate materials. Future work may provide additional validated flaw data for plate materials and may also address forging material. Data from plate taken from four different vessels show considerable variation in the number and sizes of flaws. However, the reduction factors of 10 and 40 have been found to be generally consistent with the range of the data obtained from the various samples of vessel plate material. It should also be noted that the FAVOR code assumes that failures caused by low-toughness plate and forging materials are potentially associated with (1) flaws distributed within the volume of the base metal itself, (2) flaws located along the fusion line between base metal and weld metal, or (3) clad/surface flaws within the clad material that extend up to the clad/base metal interface. The relative importance of each of these flaw categories will be determined by vessel-specific calculations with the FAVOR code.

There was no consistent trend in the observed base metal flaw orientations during the PNNL examinations of base metal materials. Therefore, in the probabilistic fracture mechanics model, it was assumed that half of the base metal flaws had axial orientations and the other half was assigned circumferential orientations.

## 2.6 Estimation Procedure for Clad/Surface Flaws

Flaws located in the clad/inner surface region are addressed using the methodology described in an ASME conference paper (Simonen et al. 2001). There is no quantitative treatment of uncertainties in the inputs for surface flaws. Flaw aspect ratios are assigned by application of data on flaw lengths as measured for clad flaws detected in the cladding of the PVRUF and Hope Creek vessels. The estimation procedure can address specific clad configurations as defined by the number of clad layers along with the thickness and width of the weld beads that make up the cladding.

All of the observed flaws in the cladding had the circumferential orientation. This trend was consistent with expectations because weld-deposited cladding is applied to vessel inner surfaces as a series of circumferential weld passes. The fracture mechanics model treated all inner surface flaws as being in the circumferential direction. Inputs for clad/surface flaws have been generated for the FAVOR code. Inputs to address both buried clad flaws and surface-breaking flaws were developed to match the fracture mechanics model used in FAVOR, which addresses only the contributions of surface-breaking flaws. Because the flaws detected by PNNL in vessel cladding were exclusively buried flaws, the number of such flaws was reduced to values consistent with the FAVOR fracture mechanics model that treats only flaws that penetrate the full thickness of the clad. Based on sensitivity calculations (Simonen et al. 2001), only about one of a thousand buried clad flaws was estimated to impact vessel integrity as much as the limiting surface flaw having a depth equal to the full clad thickness. The FAVOR code expresses the density of surface-breaking flaws as the number of surface flaws per unit area of underlying material of the vessel wall.

## 2.7 Flaw Locations

Figure 2.3 presents data on the observed locations of flaws in the welds of the Shoreham vessel as measured relative to the inner surface of the vessel. There was a similar trend for flaw locations in the PVRUF vessel. There were no observed flaws from the PNNL examinations that were true inner-surface

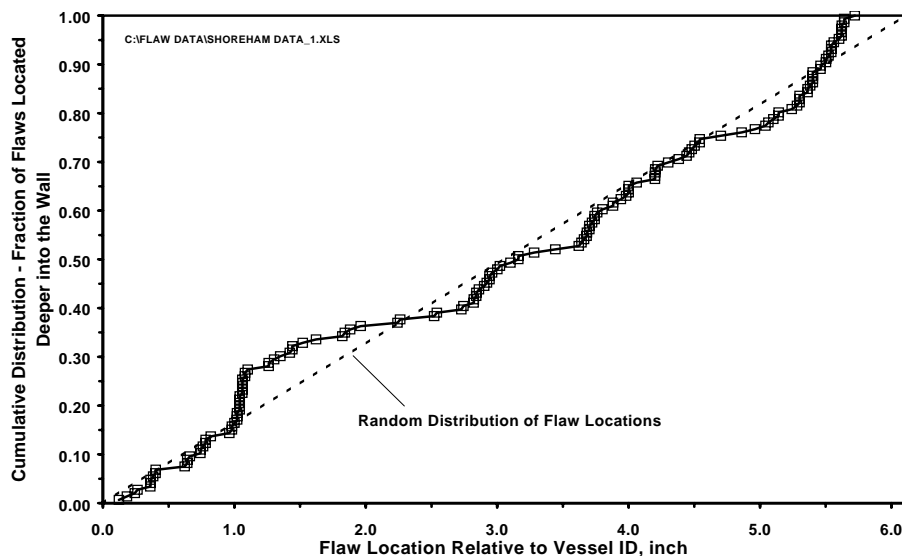


Figure 2.3. Flaw Locations Relative to Vessel Inner Surface

breaking. All observed flaws near the inner vessel surface could be classified as buried flaws. These data had important implications to the fracture mechanics calculations because there was no indication that weld flaws occur preferentially at the locations at or near the embrittled inner surface of the vessel. Based on the trends such as shown by Figure 2.3, it was assumed that weld flaws occur at random locations within the thickness of the weld.

## 2.8 Treatment of Uncertainties

Two broad areas of uncertainty were identified in the treatment and application of the PNNL flaw data. One area of uncertainty was how well the flaws in other vessels are described by the flaws that were observed in the PVRUF or Shoreham vessels. The second area of uncertainty is that the measurements from the PVRUF and Shoreham vessels provide only a finite number of data points for use in establishing the parameters of statistical distributions that describe the densities and sizes (through-wall depth dimensions and aspect ratios) for each of the flaw categories of interest (large and small flaws, SAW, SMAW, and repair flaws). The uncertainty analyses focused on this second area of uncertainty.

The uncertainty analysis selected an appropriate distribution function and used the available data to establish the numerical parameters for the selected distribution functions that provided the best fit of the data. If the number of data points was relatively small, the established distribution is subject to large uncertainties. A formal procedure (described in Appendix A) quantified the uncertainties in the estimated parameters of the statistical distributions making use of a Bayesian methodology based on unbiased prior distributions.

## 2.9 Sample Flaw Distributions

The methodology as described above is a generalized procedure for generating a flaw distribution applicable to a specific vessel. Figure 2.4 presents some sample flaw distributions coming from applications of the generalized procedure. Presentations of these results become somewhat complicated because the uncertainty analysis provides not one distribution but a series of sample distributions, with each distribution being consistent with the statistical variability of the observed data.

Figure 2.4 presents 50th percentiles of the uncertainty analyses. These flaw distributions were based on the trends of the data from the Shoreham vessel, which gave a somewhat more conservative estimate of the number and sizes of flaws than would estimates based on the PVRUF data. It was assumed that the weld of interest consisted of a mixture of SAW, SMAW, and repair welding with volume fractions for these weld processes being 93%, 5%, and 2%, respectively. The depth distributions were truncated to avoid unreasonable extrapolations beyond the flaw depths actually observed in the vessel examinations. The curves for SAW and SMAW flaws were truncated at a depth of 25 mm, which is a depth about two times greater than the measured depth of any flaws detected in either the Shoreham or PVRUF vessel. The depths for repair flaws were truncated at a depth of 50 mm, which is a factor of two or more greater than any observed flaws in repair welds. The 50-mm depth is also a physical limitation on the largest repair flaw imposed by the width dimensions of a large cavity associated with a large weld repair. A final curve of Figure 2.4 is a plot of the flaw distribution for surface or clad-related flaws. The maximum possible flaw depth is constrained by the thickness of the cladding.

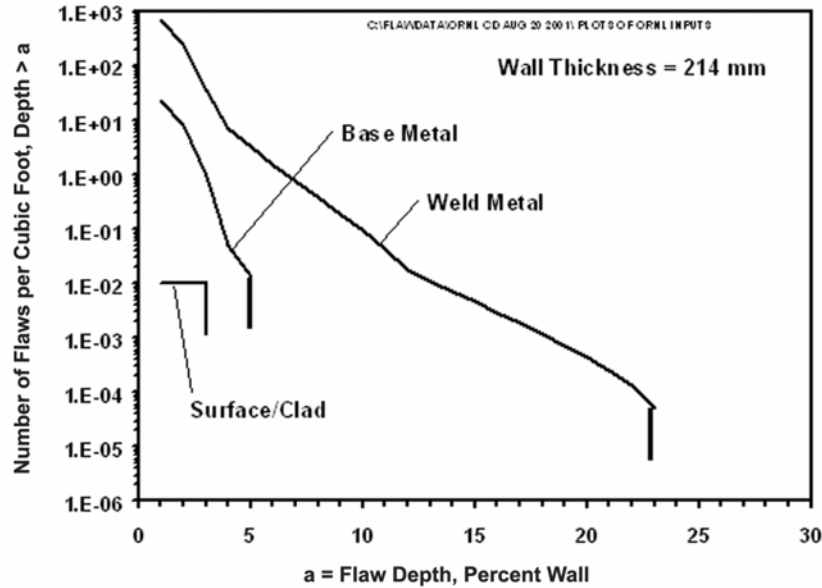


Figure 2.4. Sample Flaw Distribution for Use in Probabilistic Fracture Mechanics Calculations

## 2.10 Summary and Conclusions

The objective was to develop fracture mechanics inputs for the number, sizes, and locations of fabrication flaws that may exist in the belt-line regions of reactor pressure vessels. The approach has been to maximize the use of data on vessel flaws obtained from examinations of material taken from cancelled nuclear power plant RPVs fabricated from the late 1960s to the early 1980s. The examined material is therefore believed to be typical of the material in vessels at currently operating plants in the United States that are of concern for potential failure due to PTS events.

The improved model for postulating fabrication flaws in RPVs addresses three broad categories of vessel material regions and the flaws within these regions, namely (1) weld flaws, (2) base metal flaws, and (3) cladding flaws. A separate set of input data corresponding to each of these flaw categories is provided as input to the probabilistic fracture mechanics calculations. These input files describe the number of flaws per unit area or unit volume, the distribution of flaw depth dimensions, and the distribution of flaw aspect ratios. Other key features of the flaw model are as follows:

1. The flaw model treats the flaw locations as uniformly distributed through the thickness of the vessel wall and does not assume, as in previous PTS calculations, that the flaws are inner-surface breaking.
2. Weld flaws are assumed to lie along the weld fusion line between weld and base metal; fracture mechanics calculations then allow these fusion line flaws to grow into either the weld material or into the base metal, whichever is more limiting from the standpoint of fracture toughness.
3. Flaws of potential concern to failure of base metal regions are (1) flaws within the base metal itself, (2) flaws associated with the weld fusion line, and (3) flaws associated with the cladding.

4. Clad materials are assumed to have sufficient fracture toughness to preclude the growth of flaws if the flaws are entirely within the cladding material; clad flaws are therefore structurally significant only if they extend up to or penetrate beyond the clad-to-base metal interface.
5. Underclad cracks in base metal are not addressed; the present model would need to be enhanced in the future to evaluate vessels for which underclad cracking is considered to be a credible source of flaws.

Data files have been prepared for use by ORNL for PTS calculations with the FAVOR code. Calculations have been performed for several representative vessels that will address plants from the major nuclear steam supply system (NSSS) suppliers and with various levels of embrittlement. Although most calculations have been for vessels, for which the weld material is the most limiting material from the standpoint of embrittlement, other calculations have addressed a vessel that has base metal as the most limiting material.

### 3 EXAMINATIONS OF VESSEL MATERIAL

Recent NRC research on vessel flaws has examined RPV materials using sensitive NDE techniques and has collected data on flaws with depth dimensions as small as a few millimeters. This research has exploited advanced NDE methods with high levels of sensitivity and has used material from surplus RPVs from cancelled plants. Ultrasonic scans were not limited to access from the clad inner surface of the vessels but used smaller samples of material removed from intact vessels. High-resolution SAFT-UT has scanned from sectioned surfaces in a manner optimized to detect flaws with critical orientations normal to the vessel inner surface.

The examinations of vessel welds and base metal used vessel materials from cancelled plants as listed in Tables 3.1 and 3.2. The examined weld metal (Table 3.1) totaled about 50% of the beltline weld material for the Shoreham and PVRUF vessels; for the Hope Creek II and River Bend II vessels, only relatively small samples of weld metal were examined. The sampling of plate material was limited to the inner 1 in. of the vessel wall because this region of the vessel is the primary concern for PTS fracture mechanics calculations. The total volume of examined plate material as listed in Table 3.2 approached 10% of the plate material of the beltline of a typical PWR vessel.

The newly developed database provides dimensions for a large number of smaller flaws of the sizes identified to be the major contributors to potential vessel failures for PTS events. Several reports and papers have described the methods used to examine RPV materials and have documented the detection and sizing of the flaws in these materials (Schuster et al. 1998, 1999, 2000a,b; Crawford et al. 2000; Jackson and Doctor 2000; Jackson and Abramson 2000; Pardini et al. 2000; Jackson et al. 2001; Schuster and Doctor 2001b).

**Table 3.1. Weld Material Evaluated To Generate Data on Flaw Rates**

Cancelled Plant	Manufacturer	Reactor Type	Years of Construction	Total Weld Length Available for Examination, m	Volume of Weld Metal Examined, m <sup>3</sup>	Indication Density, indications/m <sup>3</sup>
Shoreham	CE	BWR	1968 to 1974	24	0.15	30,000
Hope Creek II	CB&I	BWR	1971 to 1975	3	0.004	40,000
River Bend II	CB&I	BWR	1974 to 1978	15	0.04	10,000
PVRUF	CE	PWR	1976 to 1981	20	0.17	9,000

**Table 3.2. Base Metal Material Evaluated To Generate Data on Flaw Rates**

Cancelled Plant	Plate or Forging Vendor	Year of Fabrication	Material	Volume of Material Available for Examination, m <sup>3</sup>	Volume of Material Available for Examination, m <sup>3</sup>
Shoreham	Lukens	1968	A533B Plate	0.9	0.016
Hope Creek II	Lukens	1971	A533B Plate	6.8	0.009
River Bend II	Lukens	1974	A533B Plate	1.0	0.024
PVRUF	Marrel Freres	1976	A533B Plate	0.6	0.014
Midland	Ladish	1969	A508 Forging	0.4	pending

### 3.1 Procedures Used to Detect and Size Flaws

PNNL’s methodology for flaw detection and size measurements consisted of four stages of increasing refinement. The first two stages form a general category wherein PNNL selected material for the later stages for more refined measurements. The final two stages produced the validated measurements for best estimates of flaw densities and size distributions.

A combination of techniques was applied as indicated in Figures 3.1 and 3.2. A cross section of an examined circumferential weld of the PVRUF vessel is shown in Figure 3.3. The validation results showed that most flaws were located in the fusion zone of the weld to the adjacent base metal (Figure 3.4) and that the largest flaws were associated with repairs.

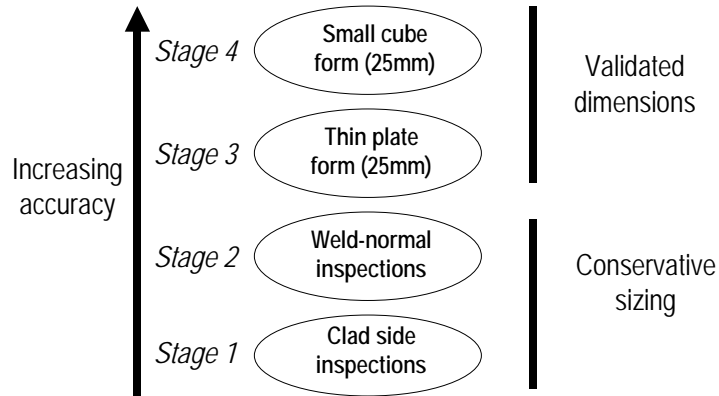


Figure 3.1. Sequence of Techniques Used To Detect and Size Flaws

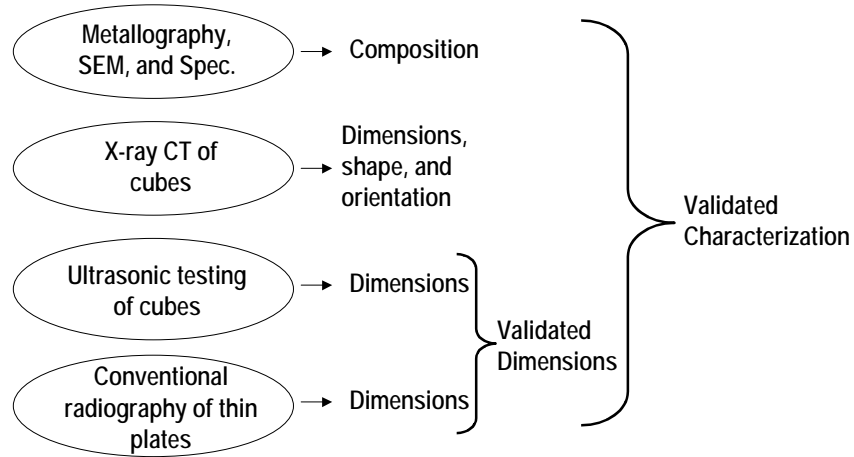


Figure 3.2. Techniques Used for Detailed Characterization of Flaws

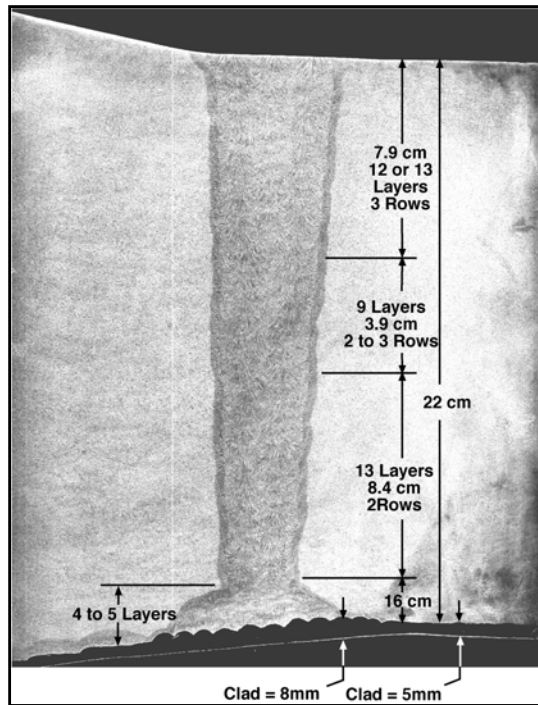


Figure 3.3. Metallographic Cross Section of a Circumferential Weld from PVRUF Vessel Showing Adjacent Regions of Base Metal and Cladding

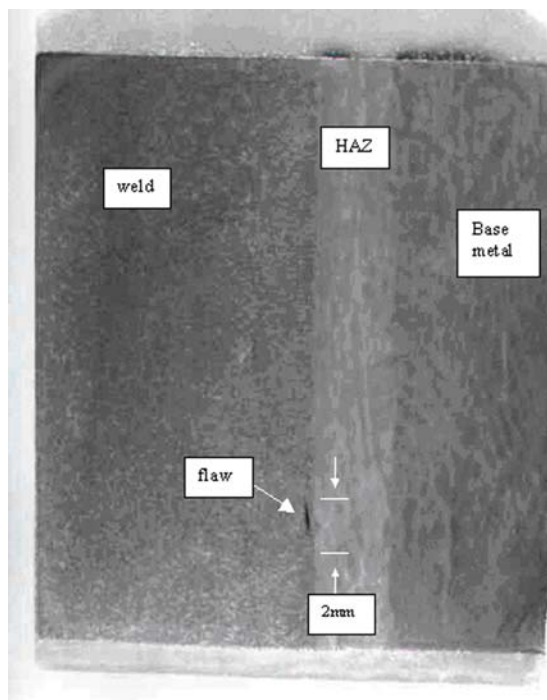


Figure 3.4. Location of Flaw in the Fusion Zone of a Weld with the Base Metal

Metallography provided good information on flaw composition. Electron microscopy confirmed the metallographic results and provided additional magnification. The X-ray computed tomography gave additional shape information for the complex repair flaws. Metallography provided information on flaw composition. Electron microscopy confirmed the metallographic results and provided additional magnification. X-ray spectroscopy provided chemical composition. The repair flaws were shown to be a combination of cracks, lack of fusion, porosity, and slag. X-ray spectroscopy provided chemical compositions.

The initial inspections of the PVRUF vessel were performed by SAFT-UT from the clad inner surface as shown in Figure 3.5. Data from these inspections were analyzed, and sizing rules as reported by Schuster et al. (1998) were consistently applied for two purposes. Most important, the material that contained the largest indications was identified for later validation. The sizing rules were needed also to generate the tabulation of 2500 flaws inspected with 10 modalities in a reproducible way. These rule statements and the results of their application to SAFT-UT inspections formed PNNL's two-part conservative sizing methodology.

The second stage in developing validated flaw rates for RPVs used weld-normal SAFT-UT inspections (see Figure 3.6) of weld-bearing specimens removed from the vessels (Schuster et al. 1999). The amount of vessel material examined with weld-normal testing was reported in Schuster et al. (1999). For the weld-normal inspections, it was assumed that no large flaws were missed. Of equal importance, the flawed material was rank-ordered to set priorities of the subsequent validation testing.

The measurements of the final validated dimensions of the larger fabrication flaws in the PVRUF vessel began with radiographic inspections of thin, weld-bearing plates as shown in Figure 3.7. The weldments were sectioned into 25-mm-thick plates and radiographed using a 450-kV X-ray machine. The flaws in the welds were centered within the plate thickness, and the through-wall dimensions were recorded. Figure 3.8 shows an example of a digitized radiograph of a fabrication flaw using conventional radiography.



**Figure 3.5. Inside View of the PVRUF Vessel During SAFT-UT Inspections**



**Figure 3.6. Weld Normal Inspections**



**Figure 3.7. Examinations of Plate Specimens**

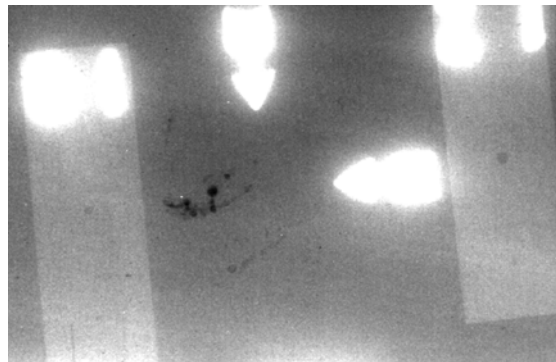


**Figure 3.8. Image of a Fabrication Flaw Using Conventional Radiography**

Dimensions for the lack-of-fusion flaws were recorded to the nearest 1.0 mm. The shapes and orientations were evident in the image of the flaw, and the lack of fusion could be observed to follow the fusion zone between the weld and the base metal. The composition of the flaw was evidenced by a low-density shape in the radiograph. Rounded and linear features of the radiographic testing (RT) indication separated porosity from lack of fusion. However, tight cracks not in a single plane were not imaged on the radiographic film.

The fourth and last stage of the validation was accomplished by centering flaws in small cubes as shown by Figure 3.4. Dimensions for the flaws in the cubes were measured by ultrasonic, radiographic, and computer-assisted tomographic (CAT) scans, as well as metallography techniques. In cube form, the measurements by each technique confirmed the measurements by the other techniques. Because of the small variance in measurements from the cubed flaws, PNNL was able to dispense with the conservative sizes established in stages one and two of the validation.

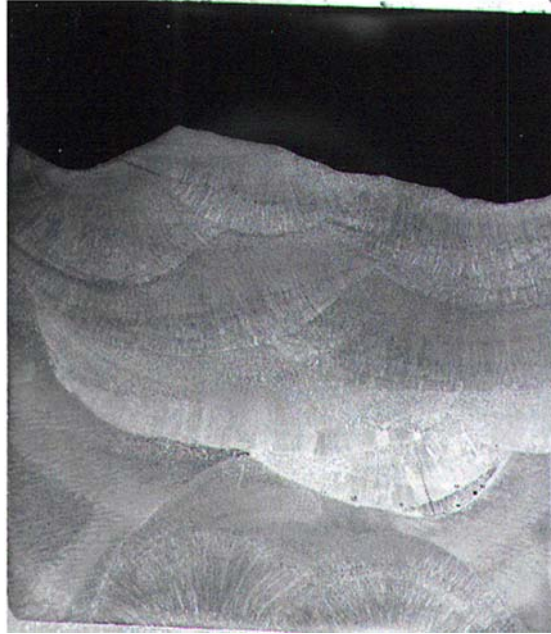
The cubes were inspected in an immersion tank with 10-MHz high-resolution SAFT (Schuster et al. 2000b). The horizontal resolution for the probe was 1 mm, and the images were full-volume focused. The scanner's steps were 0.25 mm in both scan and increment directions. The majority of the flaws examined were lack of fusion. The inspection surface was chosen to favorably orient the flaw to the ultrasonic beam. The location and dimensions of the flaws in the cubes were determined to within  $\pm 0.5$  mm and recorded to the nearest 1.0 mm. The shapes and orientations were evident in the image of the flaw, and the lack of fusion could be observed to follow the fusion zone of the weld with the base metal. Changes in composition of the flaw were evident where the lack of fusion contained more or less slag.

Small specimens were sent to the Electric Power Research Institute NDE Center for characterizing the shape and orientation of the flaws. The specimens contained large flaws from the ends of weld repairs and small flaws from the fusion zone of SAW material with the base metal. The data showed that X-ray CAT is capable of imaging complex flaws and giving the extent of the flaws as it followed the three-dimensional contour of the end of the repair (Jackson and Doctor 2000).

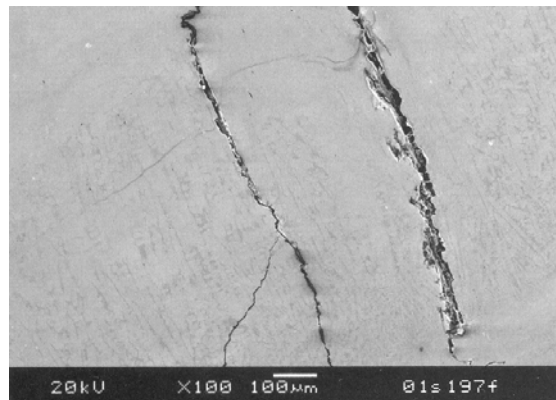
Six cubes were examined with metallography. The micropolish produced a surface finish of approximately 1  $\mu$  (a mirror finish). The etchant was a solution of 20% nitric acid and 80% ethyl alcohol. Lighting sources were adjusted to produce the necessary contrast for the photomicrographs. Dimensions for the flaws were recorded to the nearest 1.0 mm. The composition of the flaws was generally shown to be lack of fusion and cracks. Figure 3.9 shows a micrograph of SMAW weld passes at the inner near-surface zone of a vessel. A cracked weld pass can be seen in the micrograph.

Figure 3.10 shows an image from one of PNNL's electron microscopes. A portion of the cracked weld pass was imaged using 20-kV electrons, and the magnification is shown with a 100- $\mu$  scale. The crack morphology is shown in the image to be branched and filled with segregates.

Table 3.3 shows the distribution of atomic elements in the cracked portion of the SMAW weld pass shown in Figure 3.10. The measurements were made with the electron microscope using the X-ray emissions from the electron bombardment and the spectroscopic features of the microscope. The concentrations of elemental oxygen, aluminum, and silicon are evidence of metallic and nonmetallic oxides in the failed weld bead.



**Figure 3.9. Micrograph of 25-mm Cube Containing a Failed Weld Bead**



**Figure 3.10. Electron Microscope Image of Cracked Weld Bead**

<b>Table 3.3. Presence of Metallic and Nonmetallic Oxides in Failed Weld Bead</b>		
<b>Proportions in Crack</b>		
<b>Element</b>	<b>Weight %</b>	<b>Atomic %</b>
C	3.73	9.30
Mn	1.22	0.66
Fe	55.62	29.83
O	22.57	42.25
Al	1.65	1.84
Si	14.80	15.78
S	0.14	0.13
K	0.26	0.20

### 3.2 Characterization of Flaws for Fracture Mechanics Models

The purpose of characterizing flaws was to provide accurate data for developing flaw density and size distributions for use in probabilistic fracture mechanics calculations. The final characterization used a combination of techniques for measurements of location, dimensions, shape, and orientation. The data showed that most flaws are located in the weld fusion zone and that repair regions contained the largest flaws. The measured dimensions of the flaws were consistent across all techniques used to validate through-wall dimensions, lengths, and widths. The flaws were not truly elliptical as assumed in fracture mechanics calculations. Flaws in repairs were particularly irregular and unique in shape. In the case of fusion line flaws in the normal seam welds (Figure 3.4), it nevertheless was reasonable to approximate the flaws as planar elliptical cracks. However, flaws in repairs were determined to be trapped impurities along the irregular shape of the fusion zone, most notably for the flaws located at the ends of the repairs.

Metallography provided the best information for flaw characterization. A 17-mm repair flaw was shown to be a continuous flaw composed of a combination of cracks, lack of fusion, elongated tubular gas pocket (blow hole), and slag. Metallography provided the only clear evidence of the crack. The crack was detected because it was associated with nearby lack of fusion, slag, and contamination.

Figure 3.4 showed the location of a small flaw in the fusion zone of an SAW weld. The weld is to the right in Figure 3.4, and the heat-affected zone (HAZ) of the base metal is just right of image center. The flaw is located in the weld metal, where fusion occurs with the heat-affected zone.

Flaw dimensions in the coordinate system of the vessel were recorded for the small specimens removed from three product forms. Table 3.4 lists depth (relative to the vessel inner surface) locations and dimensions of flaws with values listed for metallography, radiography, and ultrasound. Good agreement was found in the validated flaw dimensions as measured by the independent techniques.

<b>Table 3.4. Flaw Dimensions, Validated by Use of Multiple Techniques</b>			
<b>Vol 1 name: HAZ V1</b>			
<b>Vol 1 TWD: 7 mm</b>			
	<b>Metallography</b>	<b>RT</b>	<b>UT of Cubes</b>
Depth location	20 mm	19 mm	22 mm
TWD	4 mm	4 mm	5 mm
Length	Not Measured	17 mm	16 mm
Width	6 mm	6 mm	6 mm

Figure 3.11 shows the composition of a complex flawed region as measured by metallography. The two images shown are from the same region of a vessel but are from different micropolished and etched cross sections. The flawed region is shown to be composed of a crack, lack of fusion, contamination, and slag.

### 3.3 Treatment of Large Repair Flaws

The large repair flaws found in the PVRUF and Shoreham vessels were subjected to special detailed evaluations. In all cases, these flaws occurred at the ends of repair cavities, and the SAFT-UT images showed complex flaw geometries. Figure 3.12 exemplifies such a flaw, designated as the “14-mm Shoreham repair flaw” because of initial examinations showing it to have a 14-mm through-wall dimension. The flaw was clearly not a planar elliptical crack with a radial orientation. Additional evaluations addressed the size, shape, and orientation of the flaw. The treatment of this flaw illustrates

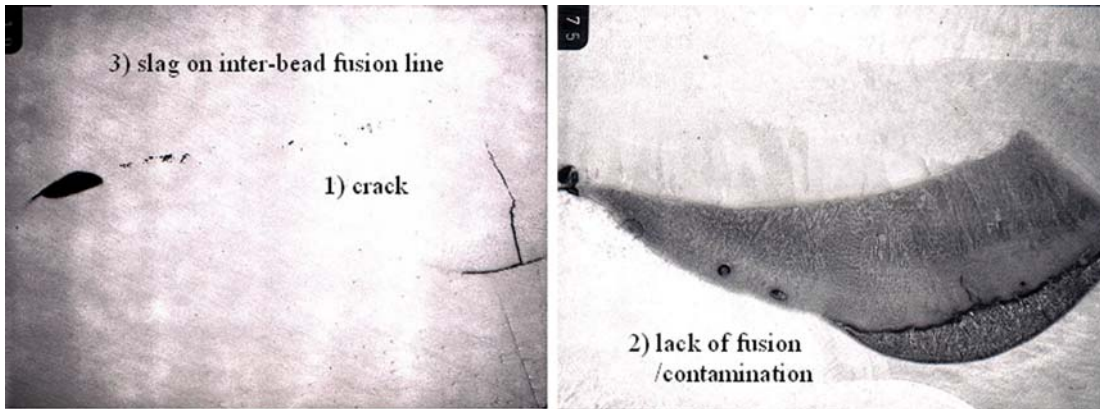


Figure 3.11. Composition of a Complex Flaw

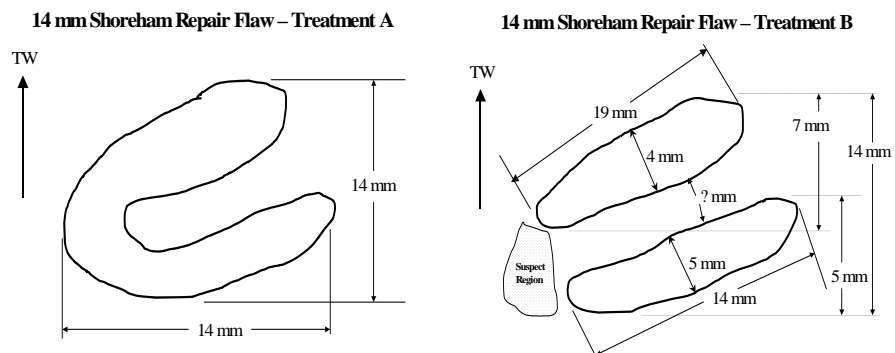
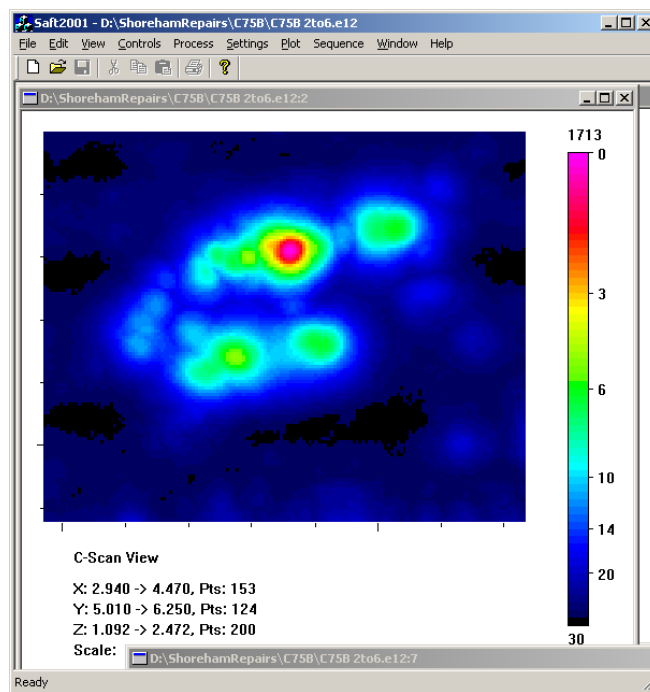


Figure 3.12. Shape and Orientation of 14-mm PVRUF Flaw - Relevant to Structural Integrity Assessment

the approach used for all large repair flaws. In all cases, the characterizations made use of refined SAFT scans that were performed after the flaws had been removed from the welds and placed into the form of small cube samples.

The sketches of Figure 3.12 represent projections of the complex flaw onto a radial plane for idealization of the flaw as potentially an axial or circumferential planar flaw. The sketch of the flaw labeled Treatment A shows an estimate of shape and orientation where the ultrasonic indication is assumed to be one connected flaw.

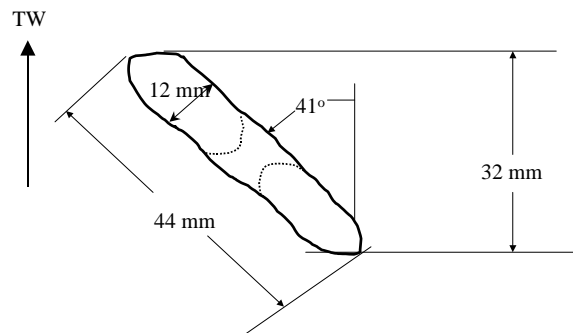
The sketch labeled Treatment B shows a characterization of the indication as two separate flaws oriented at approximately 60 degrees from surface normal. The dimensions as measured along the orientation of the flaw (rather than the coordinates of the cylindrical vessel) are considered to be the most useful for structural integrity assessments.

The nominal flaw sizes (in terms of through-wall extent) were established to be conservative relative to the subsequent measurements made during the validation. The initial sizing measurements did not necessarily show the presence of a single planar crack as opposed to a cluster of cracks or other NDE indications such as due to inclusions or material contamination. The images used to draw the sketches such as Figure 3.12 showed more detail as to the structure of the flaws and defined dimensions of possible multiple flaws and their relative proximity to each other.

The original measurements of the flaw in Figure 3.12 characterized this flaw as approximately circular with a maximum through-wall dimension of about 14 mm. The more refined SAFT examinations showed a more complex shape having two major subregions that could be connected (Figure 3.12 – Treatment A) or unconnected (Figure 3.12 – Treatment B). Fracture mechanics calculations would show that the flaw interpretation of Figure 3.12b would have a significantly smaller impact on structural integrity because the critical flaw dimensions have been reduced from a single flaw of 14 mm to separate flaws with dimensions of 4 mm and 5 mm. However, there are significant uncertainties regarding the separation distance between the legs of the complex flaw and with the structural soundness of the region joining the ends of the two subregions. Therefore, the recommendation for this particular flaw was to describe the flaw with the same dimension of 14 mm as originally estimated.

A very different result was obtained from the detailed characterization for the “32-mm Shoreham repair flaw,” as shown by Figure 3.13. The original measurements characterized this flaw as approximately circular with a maximum through-wall dimension of about 32 mm. The more refined SAFT examinations showed a flawed region bounded by dimensions of 12 mm and 44 mm. The 32-mm maximum through-wall extent was confirmed. However, the images did not show evidence of the circular flaw but rather an elongated flaw at an angle of about 45 degrees. The proper characterization of this flaw for fracture mechanics calculations of stress intensity factors was a smaller flaw with a depth of 12 mm and a length of 44 mm. There remained uncertainties regarding the possible separation of the single elongated flaw into separate flaws as indicated in Figure 3.13 – Treatment B. However, the dimension of the ligament between the separate flaws is subject to uncertainties such that ASME Code flaw proximity rules would need to combine the two flaws into one flaw. The recommendation was to describe the flaw as a single flaw with dimensions of 12 mm and 44 mm. This characterization removes a large measure of conservatism from the earlier evaluation by dealing with the large apparent through-wall dimension of 32 mm with recognition of the 45-degree flaw orientation or rotation. The rotation increases the measured maximum through-wall dimension of the flaw but does nothing to increase the value of the calculated crack-tip stress intensity factor.

### 32 mm Shoreham Repair Flaw – Treatment A



### 32 mm Shoreham Repair Flaw – Treatment B

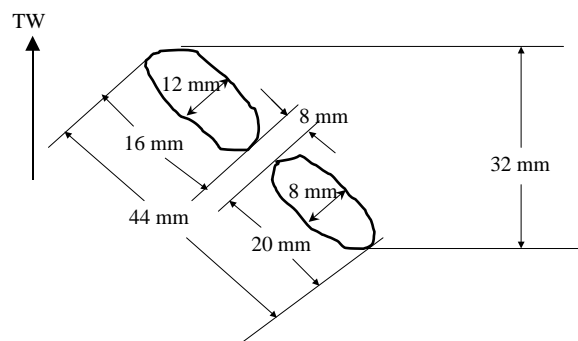


**Figure 3.13. Shape and Orientation of 32-mm Shoreham Repair Flaw with Less Conservative Treatment B of Flaw Dimensions**

In summary, the validation effort generally confirmed the original characterizations of many of the large repair flaws but, in most cases, the flaw dimensions recommended for fracture mechanics calculations were significantly reduced. The primary consideration for the less conservative treatments was recognition of the importance of flaw orientation, and how a rotated orientation can impact the measured through-wall dimension of a flaw. The validation measurements significantly reduced the dimensions of the 32-mm Shoreham repair flaws as well as the dimensions of a number of other flaws.

## 3.4 Validated Flaw Densities and Size Distributions

Best estimates of flaw density and size distributions were made using the validated flaw characteristics for larger flaws combined with the measured characteristics for smaller flaws. The smaller flaws were validated on a more limited sampling basis. Distributions are given here for flaw through-wall dimensions for the different product forms. The discussion presents the data as collected from the vessel exams without the use of statistical evaluations. Sections 6, 7, and 8 present the statistical analyses of the data along with the development of statistical distribution functions to describe the data trends and the uncertainties in the derived statistical distributions.

The construction of best estimates of flaw distributions required measurements to determine that large flaws are not present in the bulk of the examined material and that the larger detected flaws are accurately

characterized. For this reason, the larger flaw indications from PNNL’s conservative sizing methodology were selected for the validation cubes. Eighteen such flaw-bearing cubes were removed from the welds. The cubes were approximately 25 mm on a side. This specimen size permitted accurate measurement of flaw characteristics using ultrasound, radiography, computed tomography, and metallography.

Consideration of pressurized thermal shock dictated that the inner near-surface zone material receive special emphasis in the selection of the validation cubes. Fourteen cubes were removed from the SMAW of the inner near-surface zone. Three of these cubes were removed from repair metal. One cube and 30 thin plates were removed from the SAW material.

The results illustrated in Figures 3.14 through 3.17 show the impact of the validation on the flaw distributions for the three product forms. Flaw densities are shown before and after validation. Because all of the small flaws were not selected for the validation with cubes, separate densities are shown with and without the cube data.

### 3.4.1 Shielded Metal Arc Weld

Figure 3.14 compares three flaw distributions for SMAW material. The first distribution, shown by circles, is from the validation cubes. The second uses the data given in Jackson and Abramson (2000) and is labeled *Best* (for best estimate). The third is labeled *Step 1* and is taken from the SAFT-UT inspections as performed through the vessel’s cladded surface (Schuster et al. 1998). As shown in Figure 3.14, no flaws were validated to be 6 mm in size or greater. Reasonable agreement is evident between 3 mm and 5 mm in through-wall size. The density of small flaws in SMAW was not selected for validation in the cubes, so the 2-mm data point for the cubes is artificially low. The data from Jackson and Abramson (2000) is PNNL’s best estimate for the flaw rate in SMAW material of the PVRUF vessel’s inner near-surface zone.

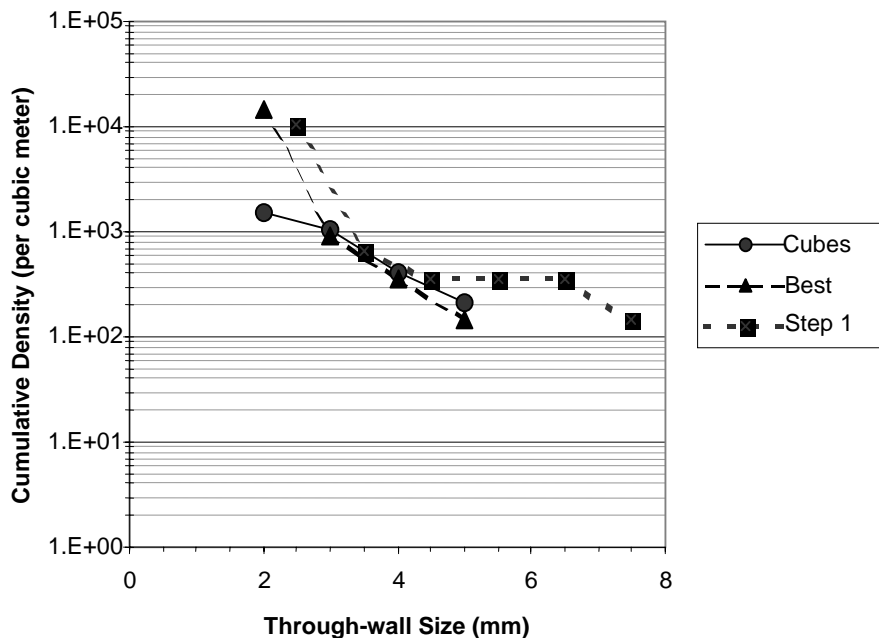


Figure 3.14. SMAW Metal, Through-Wall Size Distribution of Cumulative Flaw Densities

### 3.4.2 Submerged Arc Weld

Figure 3.15 compares three flaw density distributions for SAW. The first uses the validated data from the thin plates given (Schuster et al. 1998). The second, labeled *Best* (for best estimate), uses the plate data plus the flaw indications that were not available for validation. PNNL received all flaw-indications that were 8 mm in through-wall size or larger in the SAW material. A third flaw distribution data set, labeled *Step 1*, is taken from Schuster et al. (1998). All flaw indications were confirmed to be smaller than 8 mm. For flaws between 1 mm and 4 mm in through-wall size, reasonable agreement can be seen in Figure 3.15.

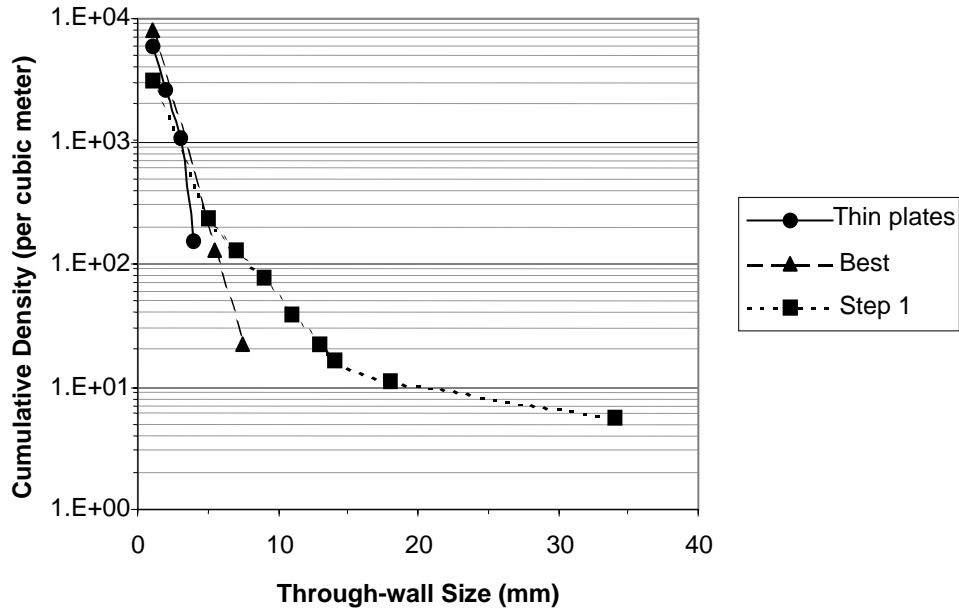


Figure 3.15. SAW Metal, Through-Wall Size Distribution of Cumulative Flaw Densities

### 3.4.3 Repair Weld

Figure 3.16 compares flaw distributions for repair metal. The first distribution uses the through-wall dimensions from the three validation cubes. The second uses the cube data plus four flaw indications as given in Jackson and Abramson (2000). The third data set is from Schuster et al. (1998) for SAW material including the HAZ. No flaws larger than 17 mm were found in the vessel. For flaws 12 mm to 17 mm in through-wall size, the flaw density is high for repair metal compared to the unvalidated (Step 1) SAW flaw densities. Smaller flaws in repair metal were not selected for the validation cubes, making the data point at 4 mm appear artificially low.

Figure 3.17 shows a comparison of PNNL's best estimates of flaw density distributions for the three product forms and the rate estimated by the Marshall Committee (1982). The density distribution for SMAW and SAW are in reasonable agreement with each other. The distribution of flaws in repair metal is shown to be significantly different from those of the other two product forms.

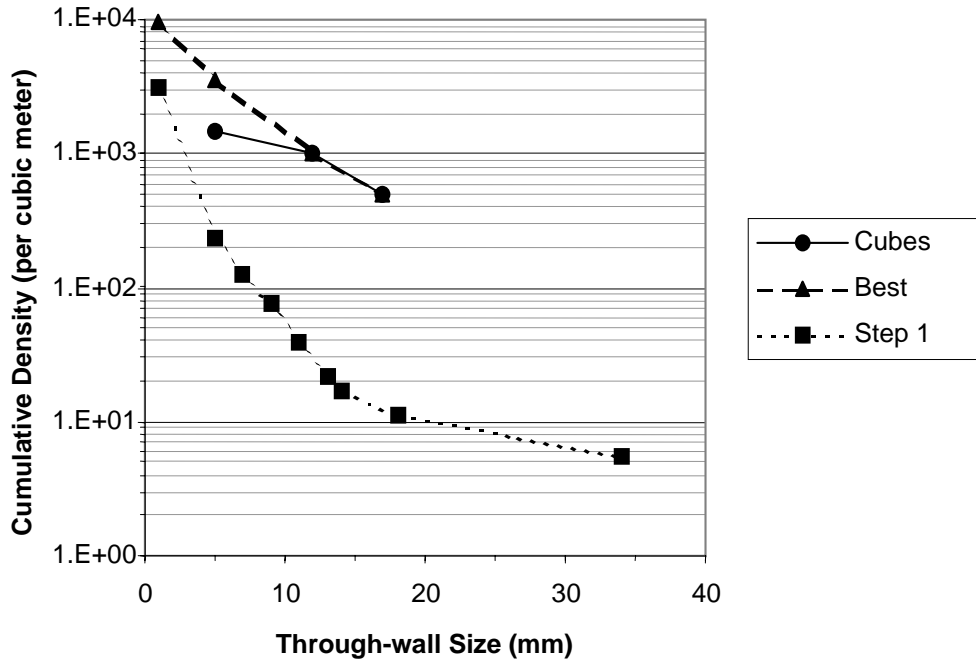


Figure 3.16. Repair Metal, Through-Wall Size Distribution of Cumulative Flaw Densities

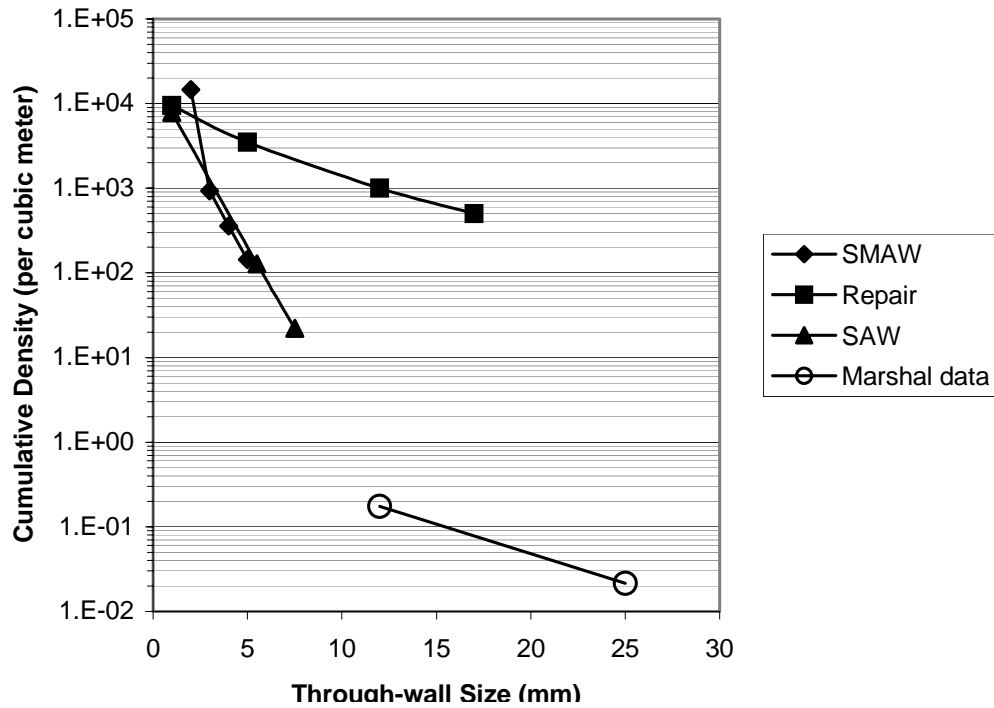


Figure 3.17. Comparison of Through-Wall Size Distributions of Cumulative Flaw Densities

The results of the selected application of four techniques to the characterization of flaws in 25-mm cubes showed that accurate validated dimensions were achieved. The conservative oversizing, used for the long metal paths of the preliminary inspections, was not needed for the measurements of flaw dimensions in the cubes. X-ray computed tomography was able to show a complex three-dimensional shape for a repair flaw and revealed that the flaw followed the fusion surface between the repair metal with the base metal. Metallography was able to show the complex composition of fabrication flaws.

Sizes for lack-of-fusion flaws were easily measured by all of the techniques used. For one flaw, a weld bead solidification crack was validated. A recommendation for use of CAT is made to overcome the alignment limitations of only the three viewing directions used in RT. Porosity was reliably detected in weld-normal ultrasound but was excluded from the cubes because it was small and its volumetric nature reduced the importance to structural integrity assessment. Validated flaw distributions were achieved using the best data for each point in the distribution. Best estimates are based on the validated dimensions in the 25-mm cubes, from weld-normal testing, and from ultrasonic flaw indications.

For SMAW, the flaw indications from the early exams had a density distribution that was in reasonable agreement with the validated distribution. This shows that the rule statements used in the analysis of the inspections through the vessel's cladded surface worked reasonably well.

## **4 EXPERT JUDGMENT PROCESS FOR FLAW DISTRIBUTION**

This section provides an overview of an expert judgment process that was used to support the development of flaw distributions. An expert judgment elicitation was used in conjunction with the empirical data from PNNL vessel examinations and the PRODIGAL model for weld flaws to develop a generalized approach to flaw distributions. A report prepared by NRC staff documents details of the elicitation (Jackson and Abramson 2000).

### **4.1 Expert Judgment Process**

The formal use of expert judgment (sometimes referred to as expert opinion) has been extensively applied to a number of major studies in the nuclear probabilistic risk assessment area. Scientific inquiry and decision-making have always relied informally on expert judgment, but the formal use of expert judgment is a well-documented systematic process. For the development of a generalized flaw distribution, 17 experts participated as the panel. The panel was needed to review, interpret, and supplement the available information on vessel fabrication processes and the data on vessel flaw distributions. The experts also reviewed the comprehensive work to date by PNNL.

The expert judgment process involved eight steps: (1) selection of issues and experts, (2) presentation of issues to the experts, (3) elicitation training, (4) preparation of issue analyses by the experts, (5) discuss of issue analyses, (6) elicitation of the experts, (7) recomposition, and (8) documentation.

#### **4.1.1 Selection of Issues and Experts**

The selections of issues and experts were closely related. The initial selection of issues was developed by NRC and PNNL staff and was used to guide the selection of experts. The experts reviewed an initial list of issues and proposed additions, deletions, or modifications to the list. It was essential that the experts be knowledgeable about the state of the art in their respective fields. The expert panel was chosen to represent a diversity of backgrounds, with a wide variety of viewpoints (e.g., academic, consulting, vessel fabricators, forging manufacturers). The specific areas of needed expertise were ASME Code for construction, failure analysis, forgings, metallurgy, NDE, reactor vessel fabrication, statistics, and welding. The 17 experts were selected on the basis of their recognized expertise in the issue areas, as demonstrated by their work experience, publications, and professional reputations. In most cases, the experts were individuals, many retired, who were employed by organizations involved during the 1960s, 1970s, and 1980s in the fabrication of the RPVs that are in service at currently operating nuclear power plants in the United States. Appendix B provides the names and qualifications of the experts.

#### **4.1.2 Presentation of Issues to the Experts**

Presentation of issues to the experts provided a mechanism to discuss the state of the art for each issue. An essential aspect of issue presentation was a decomposition of the issues, which allowed the experts to make a series of simpler assessments rather than one overall assessment of a complex issue. This step was crucial, as the decomposition of an issue can vary by expert and can thereby significantly affect its assessment. Upon initial review of the issues, extensive feedback was provided by the experts. This feedback was critical to NRC and PNNL staff in making revisions to the format in which the issues were presented to the experts during their individual elicitation sessions.

### **4.1.3 Elicitation Training**

Elicitation training assisted the experts with encoding their knowledge and beliefs into a quantitative form. Such training can significantly improve the quality of the expert's assessments by avoiding psychological pitfalls that can lead to biased and/or other overconfident assessments. The training was conducted by a normative expert who was knowledgeable about decision theory and the practice of probability elicitation. In addition to elicitation training, NRC and PNNL staff gave presentations on the background of the PTS work and the empirical NDE data from RPV inspections. The definition of a flaw for use during the expert judgment process was developed. A flaw was defined as an unintentional discontinuity that has the potential to compromise vessel integrity and is present in the vessel after pre-service inspection.

### **4.1.4 Preparation of Issue Analyses by the Experts**

In order to perform a comprehensive issue analysis, the experts were given time and resources to analyze all of the issues before their individual elicitation sessions. If an expert's preparation required additional technical support, it was provided by NRC and PNNL staff. Each expert was given a set of documents to review, which supplemented the information presented during the three-day orientation meeting.

### **4.1.5 Discussion of Issue Analyses**

Before the elicitation session, the experts were invited to discuss their issue analyses and to present the results of their analyses and research. Some of the experts engaged in discussions of the characteristics of vessels and flaws prior to their individual elicitation sessions. The ensuing discussions served to ensure a common understanding of the issues and available data.

### **4.1.6 Elicitation of the Experts**

The experts were elicited by a team consisting of a normative expert, two substantive experts, and a recorder. The elicitation team met separately with each expert, to avoid pressure to conform and other group dynamic interactions that might occur if the expert judgments were elicited in a group setting. The elicitation focused on a number of quantitative and qualitative characteristics (see Sections 4.3 and 4.4). The experts were asked to rank each characteristic in order from highest to lowest in terms of contributing to or having a flaw after preservice inspection. They were then asked for a quantitative assessment, if appropriate. For example, the experts were asked which product form is most likely to have a flaw remaining after preservice inspection. Suppose the response was that weld metal is the most likely to have a flaw remaining, followed by cladding, plate, and forgings. The expert was then asked to assess the relative likelihood of a flaw in cladding, plate, and forgings, each compared with the likelihood of a flaw in weld metal. For each relative likelihood (expressed as a ratio or percentage change), the expert was asked to supply low, high, and median values. For characteristics for which the ranking or quantitative assessment did not apply, the experts were asked what effect the characteristic would have on the introduction of a flaw. They were asked which vessels are more likely to have a large number of flaws and what elements of fabrication are most affected by field versus shop fabrication.

As the sessions continued, it became apparent to the members of the elicitation team that the experts were not able to provide quantitative data such as ranking of the characteristics and/or pairwise comparisons for all characteristics. For example, welder skill and inspector skill are dominated by human factors issues, and quantitative data was not easily provided. The experts also provided the elicitation team with

feedback that some of the characteristics should be further subdivided to accurately classify a particular characteristic. Flaw size and cladding process are examples of two characteristics that needed further division.

## **4.2 Recomposition and Summary of Results**

Recomposition and summaries of results was performed by the normative and substantive experts who recomposed the results into a form suitable for further analysis. This was completed after each session. Upon completion of the 17 elicitation sessions and a preliminary review of the responses, it was apparent that the characteristics had to be divided into quantitative and qualitative categories. There was a need to re-elicite the experts on a number of quantitative characteristics and obtain additional information on flaw size. The experts were re-elicited to obtain responses regarding flaw size, density of large flaws versus small flaws, flaw density in cladding versus weld metal, flaw density in base metal versus weld metal, repaired versus nonrepaired weld metal and base metal for small and large flaws, underclad cracking, flaw density of SAW and electro slag welding (ESW) versus SMAW, flaw density of three cladding processes (strip, multi-wire, and single-wire) versus SMAW.

Quantitative characteristics were those for which the experts were able to provide numerical comparisons. In most cases, records and data are available to verify information for quantitative characteristics. The quantitative characteristics were product form, weld process, flaw mechanisms, repairs, and flaw size. Qualitative characteristics were those for which the experts could not provide any meaningful numerical comparisons. Records and corresponding information are not readily available. The qualitative characteristics are field versus shop fabrication, weld procedure, weld materials, welder skill, inspection procedure, inspection skill, base metal properties, surface parameters and preparation, and flaw location.

The final step in the expert judgment process was to document the entire process. Documentation had several purposes. First, it can be used by the experts involved to assure them that their judgments were correctly reflected. Second, it can be used by potential users of the results to enhance their understanding. Third, it can be used by peer reviewers of the process to provide an informed basis for their review. And finally, documentation can be extremely useful to update the analyses, when future research on other vessel material becomes available. Technical rationales for the responses from each expert were recorded during the elicitation sessions.

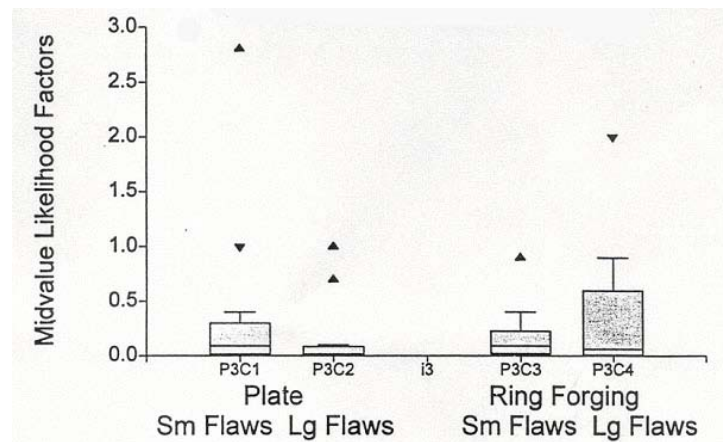
## **4.3 Flaw Characteristics from Elicitation**

Information on the quantitative characteristics can also be obtained from construction and QA records for most vessels. Many experts provided similar or identical rationales to justify their assessments. Some of the vessel fabrication characteristics addressed whose effects were addressed on a quantitative basis by the elicitation were as follows:

- flaw size
- product form - base metal ring forgings
- product form - base metal plate
- product form - cladding
- product form - weld metal
- repairs to weld metal
- repairs to base metal

- repairs to cladding
- weld process - SMAW
- weld process - SAW
- weld process - ESW (used mainly in BWRs but information was provided by experts)
- weld process - cladding
- flaw location.

Figure 4.1 shows a typical set of results (from Jackson and Abramson 2000). In this example the experts were asked to estimate the number of flaws in plate and forging materials. The estimates were expressed as flaw densities (flaws per unit volume) relative to flaw densities for weld metal. Figure 4.1 indicates individual estimates along with minimum, maximum, median, lower quartiles (LQ) and upper quartiles (UQ) from the group of experts. For example, the median values indicate one-tenth as many small flaws in plates as in welds. The corresponding ratio for large flaws (>6 mm) was even smaller (40:1). Similar estimates were provided for ring forgings, with a consensus that the occurrence of large flaws is more likely in forgings than in plate materials.



	Base Metal vs. Weldmetal			
	Plate vs. Welds		Ring Forgings vs. Welds	
	Small Flaws	Large Flaws	Small Flaws	Large Flaws
MIN	.0004	.001	.001	.002
LQ	.015	.01	.02	.007
MED	.1	.025	.1	.07
UQ	.3	.09	.2	.6
MAX	12.0	1.0	.9	2.0

**Figure 4.1. Relative Flaw Densities of Base Metal Compared to Weld Metal as Estimated by Expert Judgment Process (from Jackson and Abramson 2000)**

For qualitative characteristics, it is not possible to quantify the effect the characteristic will have on the introduction of a fabrication flaw, and no records are readily available to document information on these characteristics. However, qualitative knowledge can help guide application of existing data to other vessels. Some of the technical rationales for the qualitative characteristics are as follows:

- field versus shop fabrication
- weld procedure
- weld materials
- welder skill
- inspection procedure
- inspector skill
- base metal properties
- surface preparation and parameters.

In summary, the expert judgment process was not a consensus process. Responses and data were obtained from each expert during individual elicitation sessions. The entire set of data and responses from the process was an important input to the generalized flaw distribution methodology as described in this report for the fleet of domestic reactor vessels.

## 5 PRODIGAL WELD SIMULATION MODEL

This section describes a method originally developed at Rolls-Royce and Associates (RRA) in the mid 1980s to create an expert system (PRODIGAL) that generates a defect size distribution and density for multi-pass welds up to approximately four inches in thickness (Chapman 1993). The model accounted for fabrication factors such as differences in welding processes, materials being welded, restraint, access, welding position, and shop versus field conditions. Parameters to quantify the effects of each factor were established by an elicitation process that involved experts on welding processes and the procedures used to fabricate vessels. On an NRC-funded research program, PNNL collaborated with RRA to extend the PRODIGAL method to address welds in thick section reactor pressure vessels as built for the nuclear power industry in the United States (Chapman et al. 1996; Chapman and Simonen 1998).

A number of specific benefits were gained from the PRODIGAL model:

1. physical insights into the nature of welding defects
2. a basis for estimating flaw densities and size distributions for cases for which no data are available
3. a basis for extrapolating the data from detailed characterizations studies such as that for the PVRUF vessel—One such extrapolation is needed to estimate the probabilities for large flaw sizes greater than the sizes observed in the examination of the limited volume of PVRUF and Shoreham weld material.
4. a basis for extrapolating the data from vessels such as PVRUF and Shoreham to other vessels.

The discussion below describes the extension of the PRODIGAL model to U.S. vessels, explains the role of this model as a complement to data on welding flaws (Schuster et al. 2000b) and to perform expert elicitations that address vessel fabrication practices (Jackson and Doctor 2000), presents results of some applications to predict distributions of flaws in vessel welds made using particular welding and inspection processes, and proposes further development of the model to better simulate inspection and repair procedures. A detailed description of PRODIGAL and example applications of the code are given in Chapman and Simonen (1998).

### 5.1 Types of Defects

The PRODIGAL model addresses defects that occur and that may or may not be detected and repaired during the buildup of a weld. The methodology is based on the concept that a weld is made of individual weld runs (beads) and layers. Figure 5.1 shows the specific defects of concern to welds in reactor pressure vessels as identified by the experts.

Most flaws are confined to a single weld layer, and the characteristic flaw sizes are related to the bead dimensions. Larger flaws are associated with processes that cause the forward propagation of a given defect from one weld layer into the next layer as the weld is built up. Based on discussions with stress engineers and fracture mechanics experts, defect types such as single pores that are unlikely to impact structural integrity were excluded from consideration in the modeling of the defect distributions. In addressing vessel welds, the original list of defects identified by the RRA experts was reviewed and

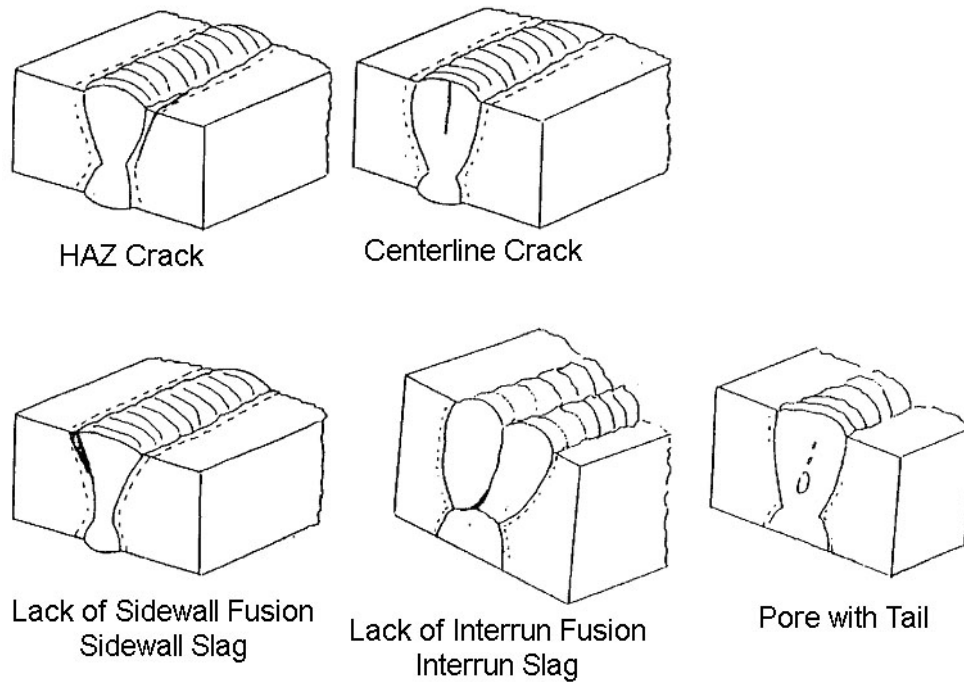


**Figure 5.1. Types of Crack-Like Defects**

modified by a group of experts on U.S. vessel fabrication. These experts were individuals from the major U.S. vessel manufacturing facilities and who were involved on a first-hand basis during the 1960s and 1970s with the welding and inspection of the vessels that are currently in use at operating nuclear power plants.

The defect types for reactor vessel welds as indicated in Figure 5.1 include the following:

- centerline cracking - As a weld solidifies and contracts, any impurities tend to collect at the top center of the bead. The stresses present may then cause a centerline crack to initiate along the weld bead due to the presence of low strength or low melting point phases.
- heat-affected zone cracking - During the formation of a weld, hydrogen is usually absorbed on cooling. The hydrogen may form hydrogen gas, which exerts a bursting pressure within the metal. If this effect is combined with the formation of a hardened structure, cracking may result. This usually occurs in the heat-affected zone (HAZ).
- lack of fusion - The lack of fusion defect is a lack of union between the weld metal and the parent plate or (in multi-run welds) between successive weld runs.
- nonmetallic slag inclusions - Linear slag inclusions are normally due to incomplete slag removal between weld runs but may occasionally be caused by slag laminations within the parent plate. Isolated slag inclusions can be caused by mill scale or rust on the plate, or damaged electrode coatings that denude the weld metal of slag-forming elements of adequate floatability; i.e., slag is left within the weld bead rather than floating to the top for removal.

- porosity - A welded joint usually will contain gas-forming elements; these evolve into phases as the temperature decreases and result in formation of cavities or porosity.

## **5.2 Defect Density**

The defect occurrence frequencies (per unit length of weld bead) for the resulting set of crack-like defect types were estimated by welding metallurgists and inspection engineers. The experts were asked to rank the defects from 1 to 10 against the factors that define the specific welding process used in constructing a weld. The ranking numbers were intended to quantify the relative rates of occurrence of each type of defect as a function of each welding condition (e.g., process, restraint). In this step of the evaluation, the occurrence rates are those prior to any inspection and repair of defects. The welding conditions were selected to be attributes for welding processes (e.g., shop versus field weld) that could be assigned by a structural analyst without access to detailed data from archived shop records. The data for the different scorings under different conditions for a given type of defect should be added or multiplied. It was decided that the individual scorings reflected independent probabilities of producing the defect, and multiplication was appropriate.

## **5.3 Defect Characteristics**

The first step in developing the model was to estimate the numbers of each type of defect, without defining the various characteristics (e.g., size, location) of these defects. The principal parameters and defect types for thick vessels are described by Chapman and Simonen (1998). Through-wall and length dimensions are defined for purposes of fracture mechanics calculations. Defect location within the vessel wall is defined by application of the simulation model with the assumption that defects occur randomly within the individual runs that make up the completed weld.

A significant question was the probability that a defect, once initiated, would propagate on to the next layer or additional layers of the weld. An important part of the model was designed to predict the number of small defects initiated early in the welding process that would grow to become larger defects before the weld was completed.

## **5.4 Inspection Model**

A final aspect of the weld simulation model addresses the effects of inspections that are performed in the shop both during the welding process and after the welding process is completed. The details of the inspection models are not documented here. The original RRA model included methods for calculating inspection efficiency curves for each type of defect in the weld of interest, with the inspection efficiency being a function of the defect size and its through-wall location. Both radiographic and surface (dye penetrant) inspection methods are addressed. Radiography is simulated using the model of Halmshaw and Hunt (1975).

## **5.5 Computer-Based Implementation**

The expert system model of weld buildup, as adapted to address reactor pressure vessel welds, uses a Monte Carlo simulation procedure. A computer code (PRODIGAL) has been written for application on a

UNIX-based workstation with the parameters for the simulated welds specified through interactive menu-driven inputs.

A weld is described as a series of activities. One type of activity consists of the stepwise process of constructing the weld as a set of building blocks, with each block corresponding to a single pass of the multi-pass weld. Other activities are as follows:

- inspections - Radiographic or surface inspections can be performed at any stage, either during the partial weld buildup or after all weld runs have been completed. It is assumed that all detected defects are repaired. It is assumed in PRODIGAL that new flaws are not introduced by the repair process.
- machining - Post-weld machining is considered as a factor for the surface finish that impacts the effectiveness of surface inspections. Machining can also expose near-surface buried defects and thereby increase the number of surface-breaking defects.
- post-weld heat treatment - The sizes of heat-affect-zone cracks can be extended by the effects of post-weld heat treatment.
- code outputs - Data outputs from the RRA PRODIGAL simulation model currently include information on flaw depth, flaw length or aspect ratio, and flaw locations within the vessel wall. All outputs are in the form of frequency distributions that indicate the number of flaws in each category per meter of finished weld (after inspections and weld repairs).

## 5.6 Calculations and Results

The flaw simulation model of the PRODIGAL computer code has been used to estimate the numbers and sizes of flaws in the welds of reactor pressure vessels. The cross section of a single V weld taken from the PVRUF vessel (Figure 5.2) was idealized for the PRODIGAL calculations as the configuration of weld layers and individual beads shown by Figure 5.3. Further details of the model and the input used to describe the welding and inspection processes are described in Chapman and Simonen (1998).

All comparisons of predicted versus observed flaw densities are made on a per unit volume or unit length basis. The simulated flaw densities were calculated using the PRODIGAL code for the submerged arc weld as described Figures 5.2 and 5.3. A weld cross-sectional area of  $0.0054 \text{ m}^2$  was used to convert the calculated flaw densities from flaws per meter of weld length to flaws per cubic meter.

Figure 5.4 shows the results of the PRODIGAL calculations expressed as the number of flaws greater than a given depth per meter of weld length. This plot shows the predicted effects of various assumptions regarding radiographic examinations and the associated repairs. It is noted that the PRODIGAL code simulates the detection of flaws and then assumes that all material with detected flaws is replaced with material that has no flaws. Computer runs were made first for the limiting assumption of radiographic examinations and then by assuming there were no radiographic examinations. The difference in the flaw distributions predicted by these two limiting cases was calculated outside the PRODIGAL code to establish the depth and length dimensions of the flaws that were detected by the RT examinations.

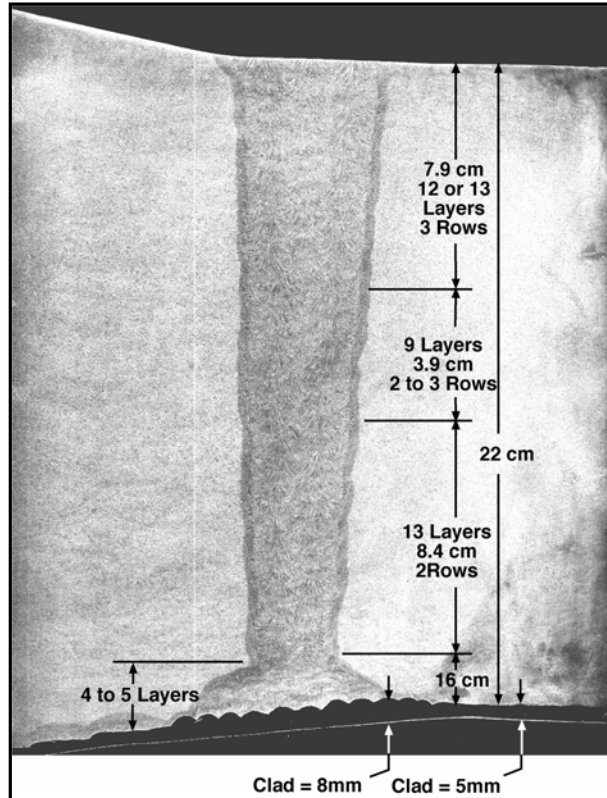


**Figure 5.2. Cross Section of Thickness Transition Single V Weld for PVRUF Vessel**

The family of curves of Figure 5.4 corresponding to various repair criteria was then generated. It is noted that the repair criteria of the ASME Section III and XI Codes require repairs of flaws between 19 and 33 mm in measured length. It was recognized, however, that there are uncertainties in both the ability of radiographic methods to accurately measure flaw lengths and the ability of the PRODIGAL code to predict the distribution of flaw lengths. Therefore, the range of the curves from  $L = 0$  mm to 33 mm is believed to represent the range of how much the flaw depth distribution can be influenced by inspections and repairs. Accordingly, a best estimate from the PRODIGAL calculations would be somewhere intermediate to the two limiting curves of Figure 5.4.

In comparing results of PRODIGAL calculations with measured data, several observations can be made:

- The observed data show a much larger number of very small flaws (1- to 2-mm range) than predicted by PRODIGAL. This occurs because the scope of the PRODIGAL model is limited to crack-like flaws that have a potential to affect structural integrity. Flaws of very small sizes (less than about half a weld bead in depth dimension) were excluded from the predicted flaw distribution.
- The measured and predicted flaw distributions are in relatively good agreement for flaw sizes of about 5 mm, which corresponds to about the dimensions of weld beads.
- If flaws associated with weld repairs are excluded from the PVRUF data, no data remain to make comparisons for flaw depths greater than 7 mm.

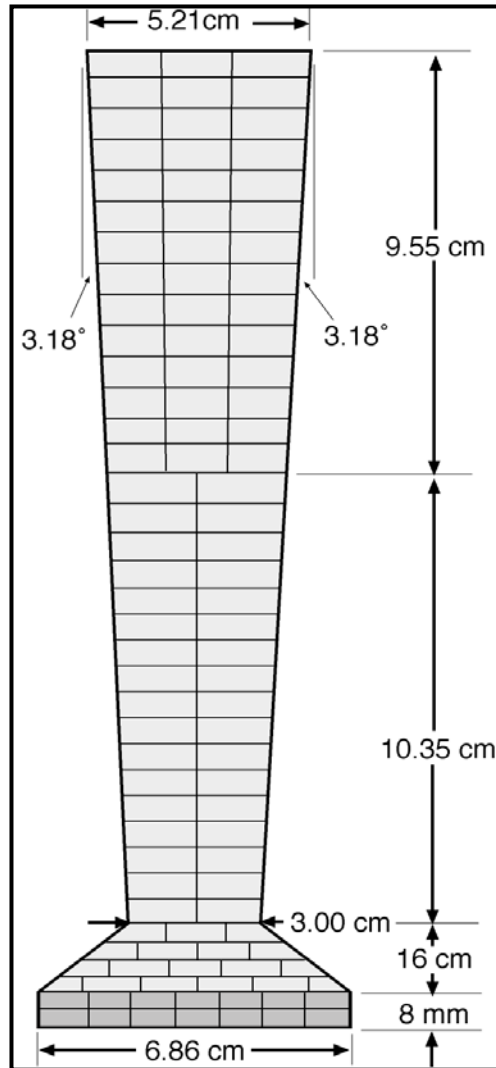


**Figure 5.3. Model of Thickness Transition Single V Weld for PVRUF Vessel**

- With the inclusion of the larger measured flaws associated with repairs, the measured data are seen to follow the upper bound curve of the PRODIGAL calculations (effects of radiography neglected), rather than following a trend between the two limiting curves from PRODIGAL. This disagreement with the expected trend is likely the result of the assumption in PRODIGAL that weld repairs are made without introducing any new flaws in the repaired material. In contrast, the PNNL examinations show that the largest detected flaws have been associated with weld repairs.

The comparisons of PVRUF data with PRODIGAL predictions show a reasonable level of agreement. Observed differences are within the level of accuracy expected, based on the fact that PRODIGAL was designed to predict the average flaw distribution for populations of welds and was not intended to address random weld-to-weld differences.

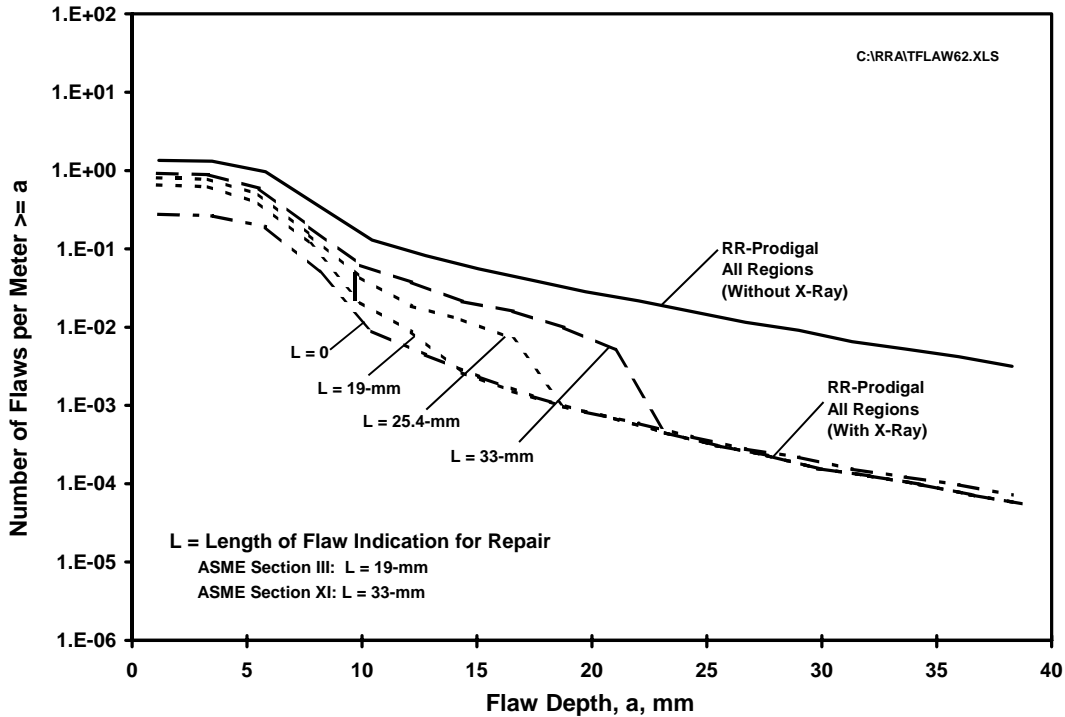


Figure 5.4. Calculated Flaw Frequencies for PVRUF Weld Showing Effects of Inspection and Repairs

## 5.7 Flaw Characterization by PRODIGAL Code

PRODIGAL provides detailed outputs for both flaw lengths and locations within the vessel wall that can provide a source of input data for probabilistic fracture mechanics calculations.

Figure 5.5 shows predictions of flaw lengths and aspect ratios (ratio of total flaw length to total flaw depth dimension). It is seen that the predicted aspect ratios become significantly smaller as the flaw depths become larger. The same data, when plotted in terms of flaw lengths, show that the predicted lengths of shallow flaws are about the same as the corresponding lengths of much deeper flaws. This trend differs from the (conservative) assumption commonly used in probabilistic fracture mechanics models, which assigns the same aspect ratios to deep flaws as for shallow flaws. Trends as seen in Figure 5.5 are a direct result of an assumption in the PRODIGAL model that grows flaws in the depth direction from one weld bead to the next bead but provides for no corresponding increase in the flaw length. Data on flaw lengths such as from the PVRUF and Shoreham vessels (as described in Section 6) is consistent with the PRODIGAL assumption of flaw length being relatively independent of the through-wall depth of the flaw.

## 5.8 Discussion and Conclusions

The PRODIGAL code provides a simulation model to estimating flaw densities and size distributions for welds in reactor pressure vessels. This model is founded on empirical knowledge of the flaws that have been observed by the welding and inspection experts who were responsible for the fabrication of the

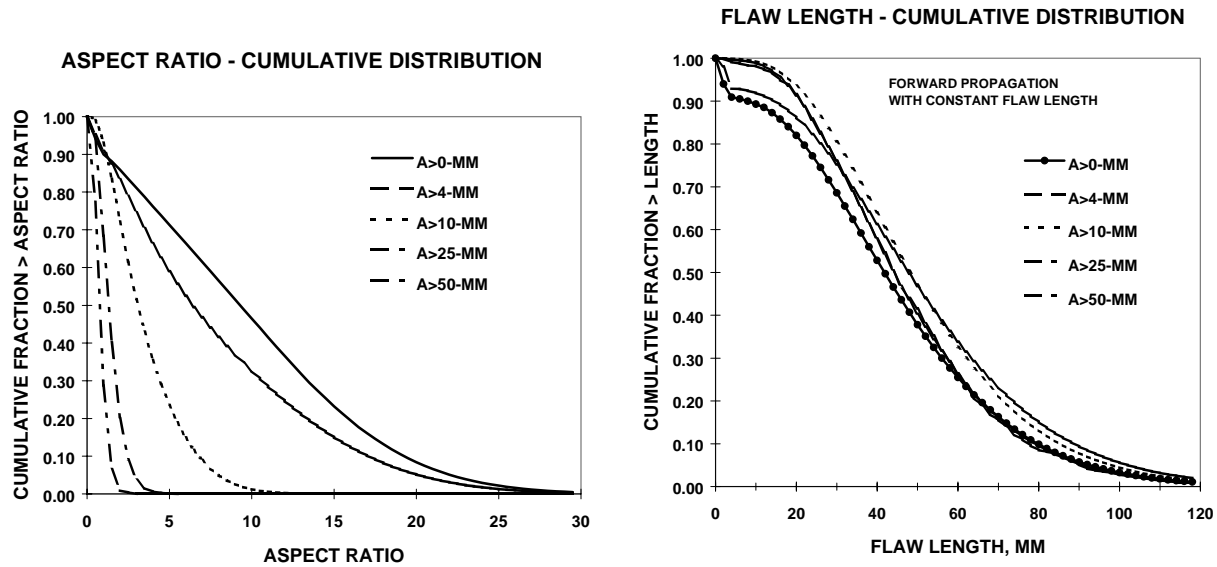


**Figure 5.5. Distributions of Flaw Aspect Ratio and Flaw Length as Predicted by PRODIGAL Weld Simulation**

vessels now in use at operating nuclear power plants. Efforts to validate the simulation model with data from inspections of vessel welds have shown relatively good agreement between the NDE and destructive examination data for the PVRUF vessel.

NRC's interest in the PRODIGAL methodology began before data from examinations of the PVRUF and Shoreham vessels were available, and the flaw simulation model was viewed as a parallel and/or alternative approach for estimating flaw distributions should examinations of vessel materials prove to be impractical. As the work at PNNL moved forward, both with PRODIGAL and with examinations of vessel welds, the quantity and quality of the flaw data from vessel examinations became sufficient to support the generation of flaw estimates without reference to PRODIGAL calculations. Nevertheless, the PRODIGAL methodology had an important role in the final methodology of estimating flaw distributions as follows:

1. Quantitative predictions of flaw densities and size distributions from PRODIGAL provided an independent benchmark for comparisons with flaw distributions generated on the basis of examinations of the PVRUF and Shoreham vessels. The estimates from PRODIGAL were based on an independent set of judgments from welding experts drawn from organizations in the United Kingdom. In addition, the PRODIGAL model was based in part on data for welding flaws not covered by the examinations performed at PNNL.
2. Insights from the PRODIGAL model guided the interpretation of the data from the PVRUF and Shoreham vessels. The depth dimensions of flaws were normalized with respect to weld bead dimensions, and the data were separated in terms of flaws less than a weld bead in size and those greater than a weld bead in size. The data for measured flaw lengths were described in terms of a distribution of flaw lengths independent of the flaw depth dimensions rather than as a distribution of flaw aspect ratios, as had been the past practice in the treatment of flaws in probabilistic fracture mechanics.

3. The PRODIGAL model provided a systematic approach to relate flaw occurrence rates and size distributions to the parameters of welding processes that can vary from vessel-to-vessel. Application of the model showed the sensitivity of calculated flaw distributions to changes in the welding process conditions. Calculations with PRODIGAL and consideration of known differences in fabrication procedures used to manufacture U.S. vessels indicated that data from PVRUF and Shoreham can reasonably be applied to all vessels at U.S. plants.
4. Insights from the PRODIGAL model supported the assumption that locations of flaws relative to the vessel inner surface should be described by a uniform or random distribution.
5. The development of distributions for clad/surface flaws was in large measure guided by the insights and quantitative predictions of PRODIGAL calculations. As a result, the probability of a clad flaw (in a multilayer clad) having depth dimension greater than the thickness of a single layer was assigned very small values. A tendency of clad flaws to be originated at the clad-to-base metal interface was based largely on the approach used in the PRODIGAL model. An approach for estimating densities of clad flaws using observed flaw densities for flaws in seam welds came from the approach used in the PRODIGAL code.
6. The assumption that essentially all larger flaws in seam welds are along the weld fusion line was reinforced by the insights provided by the PRODIGAL model.

## 6 WELD FLAWS - DATA AND STATISTICAL CORRELATIONS

The flaw distribution model was designed to generate three input files for the FAVOR code with one file used to describe flaws in seam welds, another file to describe flaws in base metal regions, and a final file to describe surface-breaking flaws that reside in the vessel cladding. This section addresses flaws in seam welds and describes the measured flaw data along with the correlations that characterize the data.

### 6.1 Approach and Assumptions

The basic considerations that apply to the development of flaw distributions for weld regions are described in the following paragraphs.

**Scope of Generalized Distribution** - Although the data available to PNNL for weld flaws were from two specific vessels (PVRUF and Shoreham), the flaw distribution model was developed to allow some specific attributes of other vessels to be addressed if the attributes differ from the attributes of the two reference vessels.

Evaluations of data on observed flaws took several steps to allow for the construction of generalized flaw distributions. PNNL did not combine the data from the PVRUF and Shoreham vessels. In developing statistical correlations, all flaw dimensions were normalized by the estimated dimensions of the weld beads for the weld regions of interest.

Inputs to the computer code that generates input files to FAVOR allow the following vessel-specific considerations to be addressed:

1. The user can specify if the desired flaw distribution should be based on data trends from the PVRUF vessel or from trends from the Shoreham vessel.
2. The user can specify volume fractions for the amount of the total seam weld that is made up of welding by the SAW, SMAW, and repair welding processes.
3. The user can specify dimensions for the through-wall dimensions of weld beads, with independent inputs allowed for bead sizes of SAW, SMAW, and repair welds.
4. The user can specify maximum flaw depths at which the extrapolations of flaw distributions for SAW, SMAW, and repair welding material regions are to be truncated.

In most cases, the user will lack the detailed knowledge needed to make vessel-specific inputs for the above factors. The suggested approach would be to use the same values of inputs used to characterize the welds in the PVRUF or Shoreham vessels, thereby allowing the flaw distribution model to produce a distribution of flaws as measured for either the PVRUF or Shoreham vessel.

**Flaws per Unit Volume Versus Flaw per Unit Area** - Past approaches, including that of early versions of the FAVOR code, quantify flaw densities in terms of flaws per unit volume. PNNL's weld examinations, however, indicated that essentially all of the flaws with significant through-wall dimensions were located along weld fusion lines. Therefore, it was recognized that it would be best to describe weld flaw densities in terms of flaws per unit area of fusion zone. However, the flaw

distribution algorithm allows the user to specify which measure of flaw density is to be used in generating the input for files for the probabilistic fracture mechanics code.

The original reduction of data from the PVRUF and Shoreham vessels was performed to estimate flaw densities on a per-unit volume basis. The flaw distribution algorithm makes appropriate transformations (based on the average widths of the weld joints) of the PVRUF and Shoreham data to go from flaws per unit of volume to flaws per unit area. The transformation used weld widths of 1.61 in. and 1.52 in. for the PVRUF and Shoreham vessels, respectively.

**Use of Data Versus Models and Expert Elicitation** - In developing flaw distributions, measured data were used to the maximum extent possible. The PRODIGAL flaw simulation model and results of the expert judgment elicitation were used only when the data were inadequate. In the case of seam welds, there was a relatively large amount of data, and the PRODIGAL model and expert elicitation were not used to quantify estimates of flaw densities and sizes. The PRODIGAL model did, however, suggest the normalization of flaw dimension by the dimensions of weld beads and the separation of data into subsets corresponding to small and large flaws (as defined by flaw depth dimensions relative to the weld bead dimensions). In addition, the expert elicitation and the PRODIGAL model helped to justify the application of data from the PVRUF and Shoreham vessels to the larger population of vessels at U.S. nuclear plants.

**Rule of Mixtures** - PNNL's examinations showed that final welds will typically consist of weld metal deposited by the SAW, SMAW, and repair welding processes. In most cases, the weld consists mainly of SAW-deposited material with a few percentage of SMAW and repair weld. The flaw distribution algorithm uses a "rule of mixtures" that first calculates flaw densities and size distributions for each of the three weld types and then combines these contributions in proportion to the relative volumes of material coming from each process. In estimating the flaw locations relative to the vessel inner surface, the resulting flaws are assumed to occur randomly within the volume of the weld. In application of the FAVOR code, the level of knowledge of the welds has made it necessary to assume random locations for the flaws coming from the various welding processes. However, the generalized flaw model can be used to generate inputs that identify specific weld regions produced by given welding processes. For example, such a model could, for example, identify a region of SMAW weld with relatively low levels of embrittlement and then assign an appropriate distribution of flaws for the region of interest.

**Decomposition of Flaw Data** - The flaw data from PNNL's examinations were separated into subsets according to the following three attributes:

- PVRUF versus Shoreham vessel
- small flaws versus large flaws based on through-wall flaw dimensions relative to the estimated sizes of the weld passes
- flaws in SAW, SMAW and repair-welded material.

This approach is more detailed than that of other studies (such as that of the Marshall Committee [1982]) that have combined the data and approximated the trends with a single statistical distribution function such as an exponential distribution. The current approach avoids difficulties of using single distribution functions to achieve good statistical fits over wide ranges of flaw sizes. The current approach allowed

each subset of data to be described by a simple statistical function such as an exponential distribution, with the overall distribution coming from a summation of distributions from the subsets of data.

**Use of Combined Datasets** - In some cases, it was necessary and/or desirable to work with combined datasets from PVRUF and Shoreham in developing statistical distributions to describe the data. In estimating flaw densities, it was not necessary to combine data from the various subsets of flaws. However, for flaw size distributions, the data were more limited because the flaw sizes were measured with a high level of accuracy for only a small number of flaws. As one example, the flaw size measurements combined SAW and SMAW data to establish the statistical size distribution for small flaws.

**Approach to Statistical Correlations** - Once the flaw data were separated into subsets corresponding to relatively narrow categories of flaws, it was possible to describe the data in terms of simple statistical distribution functions. The evaluations also characterized the uncertainties in the parameters of the distributions associated with the finite number of data points in the samples. The Poisson distribution was used to treat the flaw density. Exponential distributions were found to be suitable to characterize distributions of flaw depths and lengths. The exception was the use of a multi-nomial distribution for the depth dimensions of small flaws (flaws one weld bead size or smaller).

The use of statistical distribution functions served two purposes that could not be accomplished by simple numerical histograms or binning of the flaw data. Common statistical functions allowed uncertainties associated with small sample sizes to be quantified with a Bayesian approach as described in Appendix A to this report. The statistical functions also provided a consistent basis for extrapolating flaw distributions to flaws larger than could be observed in the limited volume of vessel material that could be examined.

**Vessel-to-Vessel Variability** - The PNNL examinations of vessel material focused on two vessels (PVRUF and Shoreham), with only limited examinations of material from other vessels (Hope Creek, River Bend, and Midland). The Shoreham flaws showed some clear differences from the PVRUF flaws with somewhat greater flaw densities and longer flaws (larger aspect ratios). However, there was no basis for relating these differences in flaw densities and sizes to other vessels. With only two examined vessels it was not possible to statistically characterize vessel-to-vessel differences such that the differences could be simulated as a random factor in Monte Carlo calculations. The decision was to develop separate procedures to generate flaw distributions for the PVRUF and Shoreham vessels. Following the conservative approach taken in other aspects of the PTS evaluations where data and/or knowledge is lacking, it was recommended that the Shoreham version of the flaw distribution be used in PTS calculations, which served to ensure conservatism in the predictions of vessel failure probabilities.

**Locations of Flaws Relative to Vessel Inner Surface** - Weld flaws were assumed to be buried flaws with the locations of their inner tips relative to the vessel inner surface distributed in a random manner. The limiting case would be a flaw with its inner tip at the clad-to-base metal interface, which would statistically have a zero probability of occurrence. A separate flaw distribution was defined for the flaws in the vessel cladding.

**Fusion Line Flaws** - PNNL's examinations of vessel material showed that most weld flaws of significant size were located at weld fusion lines and had orientations to follow weld fusion lines. This trend occurred for flaws in original seam welds and for flaws associated with weld repairs. This information was used to modify assumptions used in fracture mechanics calculations performed with the

FAVOR code. Flaws associated with seam welds or repair welds are assumed to propagate into either weld metal or base metal. Cracks are assumed to propagate into the material with the lowest level of fracture toughness.

**Crack Shape** - All flaws are assumed to be crack-like flaws, which is consistent with the generally planar nature of the flaws observed in the PNNL examinations. There was no detailed consideration of the truly sharp nature of flaw tips. It was recognized that the treatment of flaws by the FAVOR code assumes planar flaws having ideal elliptical shapes. The plane of the cracks and the major and minor axes in FAVOR of the flaws are aligned with the radial and axial coordinates of the vessel. The PNNL measurements of flaws gave dimensions of the flaws in terms of a “box” that would contain the flaw. In the case of fusion line flaws in seam welds, the dimensions of this box provide a realistic representation of the flaw for the fracture mechanics calculations. However, complex repair flaws tended to have major and minor axes that did not align with the vessel coordinate system. PNNL described these flaws in terms of dimensions of major and minor axes (relative to the orientation of the flaw) to preclude an overly conservative treatment of such flaws by the FAVOR code.

**Flaw Proximity Considerations** - The weld examinations by SAFT-UT gave special consideration to indications that would give the appearance of one or more flaws that may in fact be one larger flaw. Subsequent validation efforts focused on these regions for more accurate characterization of flaw dimensions. ASME Code flaw proximity rules were then applied to the refined NDE results. The dimensions of multiple flaws were tabulated as a single larger flaw if so dictated by application of the code proximity rules. The database on flaws should therefore be considered as accounting for random occurrences of small flaws that are sufficiently close to each other to be properly treated as a single larger flaw in fracture mechanics calculations. The flaws as given by the input files from generalized flaw distribution procedure should be treated as single isolated flaws. There should therefore be no further steps in the fracture mechanics models to simulate random locations of flaws in order to identify occurrences of adjacent flaws that should be treated as a single larger flaw.

**Flaw Orientation** - Flaws in axial seam welds are assumed to have axial orientations, and flaws in circumferential seam welds are assumed to have circumferential orientations. These orientations correspond to the assumptions made in the development of the FAVOR code and are consistent with the orientations of flaws as observed in the PNNL examinations. These orientations were imposed without regard to whether the flaw was associated with the original seam weld or with a subsequent repair to the weld. Given the complex geometries and orientations of repair flaws, these assumptions may be overly simplified and could be subject to revision as more refined fracture mechanics models are developed in the future.

**Truncation of Flaw Distributions** - Flaw inputs for use in the FAVOR code calculations were truncated to avoid excessive extrapolations of the statistically based depth distributions. The truncations were such to preclude flaws that are greater than about two times the depth dimensions of any of the observed flaws upon which the statistical correlations were based. This approach was a compromise that allowed consideration of low-probability flaws larger than could be detected in the limited volume of examined material addressed by the PNNL work. On the other hand, the truncations avoided arbitrary extrapolations to larger flaw depths outside the range of the cracking mechanisms covered by the databases.

**Service-Related Flaws** - The flaw distribution methodology addresses only fabrication flaws, with no consideration of service-initiated cracks or service-induced growth of fabrication flaws (by fatigue or

stress corrosion cracking). In this regard, the material examined by PNNL was from vessels that had never been placed into operation. Inservice inspections of PWR vessels and fracture mechanics calculations provide no reason to believe that crack initiation or growth for flaws in the vessel beltline region are likely.

## 6.2 Statistical Functions for Flaw Distributions

Statistical distribution functions were developed to describe the data obtained from PNNL's examinations of vessel weld material. The evaluations were also to address the uncertainties in the parameters for the distribution functions. The following matrix identified the potential need for a total of 36 functions ( $3 \times 2 \times 3 \times 2$ ) as follows:

Variable	Values	N
Flaw Characteristics	Flaw Density Through-Wall Depth Flaw Length (Aspect Ratio)	3
Source of Flaw Data	PVRUF Shoreham	2
Weld Process	SAW SMAW Repair Weld	3
Flaw Depth Category	Small Large	2

In many cases, one function served more than one purpose, which reduced the number of independent statistical correlations that were needed. The following commonality in the functions was employed:

- One conditional depth distribution described the small flaws in both the PVRUF and Shoreham vessels, including all three welding processes.
- One conditional depth distribution described all large repair flaws in the PVRUF and Shoreham vessels.
- One conditional depth distribution described all large SAW and SMAW flaws in both the PVRUF and Shoreham vessels.
- One length distribution described all large flaws in the PVRUF and Shoreham vessels, including all three welding processes.
- One length distribution described the small SMAW and repair flaws in the PVRUF vessel.
- One length distribution described the small SMAW and repair flaws in the Shoreham vessel.

This commonality reduced the number of independent functions to 20, including 12 functions to describe flaw densities. In all cases, flaw density was described by a Poisson distribution. Exponential distributions were used to describe flaw depth dimensions and flaw lengths, except that a multi-nomial distribution was used for the depth dimensions of small flaws.

The distribution functions that described the measured dimensions of flaws included the following considerations:

1. Flaw dimensions were first normalized with respect to the estimated through-wall dimensions of the weld bead associated with the flaw being addressed.
2. Only datasets for which the flaw dimensions were measured with the highest degree of accuracy were used to develop the statistical distribution functions; in many cases this approach resulted in a relatively small collection of data for use in the statistical evaluations.
3. Whenever possible, a single distribution function were used to address (1) both the PVRUF and Shoreham vessels, (2) several weld types (SAW, SMAW, and repair) and (3) ranges of flaw sizes (large and small flaws). In some cases, the data indicated common trends for the normalized dimensions of two or more categories of flaws; in other cases, the very limited amount of data dictated that datasets be combined for the statistical evaluations.

The discussion below describes the derivation of the individual distribution functions. The data used to establish the parameters of each distribution are listed. Mean values of the distribution parameters are given along with the parameters use to simulate the uncertainties in the estimated parameters. Appendix A provides equations for the distribution functions and the equations used to simulate the uncertainties in the parameters of the distribution functions.

### **6.2.1 Flaw Densities**

Flaw densities were expressed in terms of flaws per cubic meter. Options with PNNL's algorithm for generating flaw input files for FAVOR convert the output to units of flaws per cubic foot and allow flaw densities to be expressed on the basis of flaws per unit area of fusion surface. It should also be noted that the development of the distribution functions was originally performed in terms of flaws per unit volume based on data from the PVRUF and Shoreham vessels. It was later recognized that flaws per unit area of the weld fusion zone is a better measure of flaw density. The algorithm has the option for output files in units of flaws per unit area. Conversion factors for the PVRUF and Shoreham vessels are embedded in the algorithm to make the conversion from a volume basis to an area basis. This conversion accounts for two fusion surfaces along each seam weld. The weld was assumed to have an average width (or gap) of 1.61 in. for the PVRUF vessel and 1.52 in. for the Shoreham vessel.

Table 6.1 lists the flaw data and corresponding examined material volumes as reported by Jackson and Abramson (2000), which were used to calculate flaw densities. The parameter uncertainty for the Poisson distribution was calculated from a gamma distribution (see Appendix A) on the basis of the volume of material inspected and the number of flaws found. Each Monte Carlo trial of the flaw distribution algorithm samples from the gamma distribution to calculate a parameter for the six flaw densities of Table 6.1. Table 6.2 gives the values used to define the gamma distribution for sampling of the parameters of the Poisson distribution.

Table 6.3 lists the assumed through-thickness dimensions for weld beads that were used to identify small flaws versus large flaws. These same bead dimensions were used to normalize flaw dimensions in the development of statistical distributions to characterize the through-wall depths and lengths of flaws.

Vessel	Weld Type	Flaw Size	Number of Flaws	Examined Volume, m <sup>3</sup>	Flaw Density, Flaws per Cubic Meter			
					Mean	Median	25 <sup>th</sup> Quartile	75 <sup>th</sup> Quartile
PVRUF	SAW	Small	1419	0.180	7883	7881	7741	8023
PVRUF	SMAW	Small	197	0.014	14071	14047	13382	14734
PVRUF	Repair	Small	12	0.00123	9756	9486	7738	11480
PVRUF	SAW	Large	4	0.180	22.2	20.4	14.1	28.4
PVRUF	SMAW	Large	4	0.014	285	262	181	364
PVRUF	Repair	Large	7	0.00123	5671	5422	4132	6958
Shoreham	SAW	Small	3160	0.137	23065	(a)	(a)	(a)
Shoreham	SMAW	Small	741	0.0105	70571	“	“	“
Shoreham	Repair	Small	45	0.0030	15.0	“	“	“
Shoreham	SAW	Large	32	0.137	234	“	“	“
Shoreham	SMAW	Large	8	0.0105	761	“	“	“
Shoreham	Repair	Large	6	0.0030	2000	“	“	“

(a) Available data analyses did not provide these numbers.

Vessel	Weld Type	Flaw Size	Number of Flaws	Examined Volume, m <sup>3</sup>	Parameters for Gamma Distribution	
					$\alpha_1$	$\alpha_2$
PVRUF	SAW	Small	1419	0.180	0.180	1419
PVRUF	SMAW	Small	197	0.014	0.014	197
PVRUF	Repair	Small	12	0.00123	0.00123	12
PVRUF	SAW	Large	4	0.180	0.180	4
PVRUF	SMAW	Large	4	0.014	0.014	4
PVRUF	Repair	Large	7	0.001	0.001	4
Shoreham	SAW	Small	3160	0.137	0.137	3160
Shoreham	SMAW	Small	741	0.0105	0.0105	741
Shoreham	Repair	Small	45	0.0030	0.0030	45
Shoreham	SAW	Large	32	0.137	0.137	32
Shoreham	SMAW	Large	8	0.0105	0.0105	8
Shoreham	Repair	Large	6	0.0030	0.0030	6

Vessel	Weld Type	Weld Bead Thickness, mm
PVRUF	SAW	6.5
PVRUF	SMAW	3.5
PVRUF	Repair	3.5
Shoreham	SAW	5
Shoreham	SMAW	3.5
Shoreham	Repair	3.5

Figures 6.1 and 6.2 are plots of the calculated flaw densities as calculated from the parameters of Table 6.2, with the relative uncertainties in the calculated densities indicated by the relative slopes of the curves. The densities for small flaws are 2 to 3 orders of magnitude greater than the densities for large

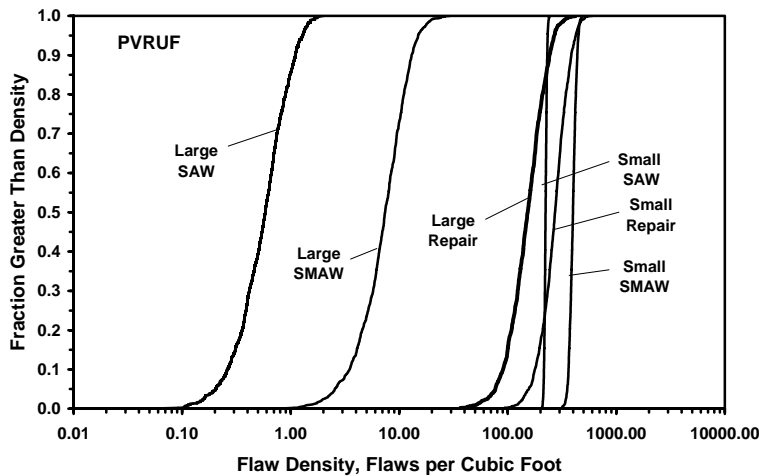


Figure 6.1. Uncertainty in Flaw Densities for Flaws in PVRUF Vessel

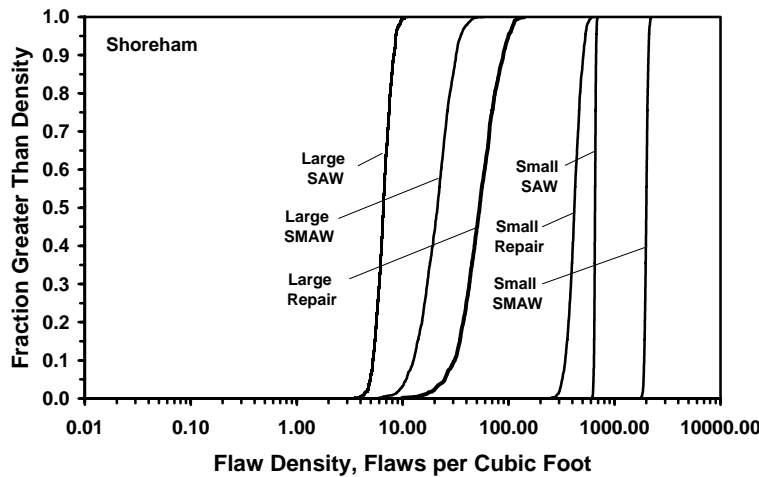


Figure 6.2. Uncertainty in Flaw Densities for Flaws in Shoreham Vessel

flaws. There are greater statistical uncertainties in the estimated densities for large flaws than for small flaws. Consistent with the relatively small number of observations, the uncertainties are greater for repair flaws than for the SAW and SMAW material.

### 6.2.2 Conditional Depth Distribution for Small Flaws

A single distribution was developed to describe the through-wall dimensions of small flaws. In this report, small flaws are defined as flaws having depths that are less than or equal to the weld bead size. One depth distribution was applied to small flaws for all three weld types (SAW, SMAW, and repair) and for the PVRUF and Shoreham vessels. The distribution was based on sets of flaw size data that were measured by radiography of 25-mm plate specimens cut from welds of the PVRUF vessel (Figure 6.3). These specimens had only a small fraction of the small flaws detected by SAFT-UT during the examinations of the PVRUF and Shoreham vessels. However, the sizing accuracy for these flaws by RT



**Figure 6.3. PVRUF Weld Metal Specimen Cut into 25-mm Plate**

was significantly better than the sizing accuracy possible with the SAFT-UT scans, which had an accuracy of no better than 2 mm. Limitations associated with the relatively small number of data points were addressed with the uncertainty analysis for parameters of the distribution function used for simulating flaw depth dimensions.

Randomly selected material from the PVRUF welds was prepared in the form of plate samples and examined by RT. A total of 43 small flaws were detected in the examined plates, with measured sizes (through-wall depth dimensions) ranging from 0.5 to 7.0 mm (see Table 6.4). The location of each flaw relative to the inner surface of the vessel was established. This location was used to determine if the weld metal at the flaw location was most likely SAW or SMAW. Most of the flaws were in SAW weld material. Flaws for both weld types were combined into one dataset. However, the size of the weld bead for each flaw was assigned according to the weld type. The estimated bead size ranged from 3.5 mm for SMAW welds to 6.0 mm for SAW welds. Because similar data from RT examinations were not available for the Shoreham vessel, the depths of flaws for the Shoreham vessel were assumed to be described by the same conditional distribution as the PVRUF vessel. Schuster et al. (1999, Figure 6.1) compare flaw depth distributions for the PVRUF and Shoreham welds. Whereas the Shoreham vessel has about three times the number of flaws per cubic meter more than the PVRUF vessel, the conditional depth distributions of the flaws for the two vessels were shown to follow similar trends.

Before a distribution function was developed, the data on flaw depths were normalized relative to the size of the weld bead for each flaw. A multinomial distribution (see Appendix A) described the complementary cumulative distribution of flaw depths. The uncertainties in the three parameters of this distribution were described by a Dirichlet distribution. The normalized flaw depths (bounded 0.1 and 1.0 for small flaws) were described as discrete sizes with three bins of width 0.3 of the bead thickness and centered at values of 0.25, 0.55, and 0.85. The three discrete flaw sizes described by the multinomial distribution had probabilities of occurrence given by a three-element vector  $\beta_i$ . The probability density function is defined as

$$f(a/\Delta) = \beta_i/0.3 \quad (6.1)$$

where  $a$  is the flaw through-wall depth dimension and  $\Delta$  is the bead thickness.

<b>ID Number</b>	<b>Plate</b>	<b>Bead Size, mm</b>	<b>Flaw Depth, mm</b>	<b>Flaw Depth Fraction of Bead</b>	<b>Fraction &gt; X</b>
20	5-1C-8	6.50	0.50	0.077	1.000
2	5-1AB-2	6.50	1.00	0.154	0.977
5	5-1AB-5	6.50	1.00	0.154	0.953
10	5-1AB-7	6.50	1.00	0.154	0.930
13	5-1AB-11	6.50	1.00	0.154	0.907
34	5-10B-10	6.50	1.00	0.154	0.884
37	5-12BA-2	6.50	1.00	0.154	0.860
17	5-1C-2	6.50	1.10	0.169	0.837
6	5-1AB-5	6.50	1.20	0.185	0.814
1	5-1AB-2	6.50	1.30	0.200	0.791
27	5-1C-14	6.50	1.30	0.200	0.767
3	5-1AB-3	6.50	1.50	0.231	0.744
14	5-1AB-12	6.50	1.50	0.231	0.721
15	5-1AB-12	6.50	1.50	0.231	0.698
19	5-1C-6	6.50	1.50	0.231	0.674
21	5-1C-8	6.50	1.50	0.231	0.651
22	5-1C-10	6.50	1.50	0.231	0.628
24	5-1C-12	6.50	1.50	0.231	0.605
32	5-10B-7	6.50	1.50	0.231	0.581
33	5-10B-8	6.50	1.50	0.231	0.558
35	5-12BA-1	6.50	1.50	0.231	0.535
36	5-12BA-1	6.50	1.50	0.231	0.512
42	5-12BA-11	6.50	1.75	0.269	0.488
4	5-1AB-5	6.50	1.80	0.277	0.465
25	5-1C-13	3.50	1.00	0.286	0.442
8	5-1AB-6	6.50	2.00	0.308	0.419
9	5-1AB-7	6.50	2.00	0.308	0.395
11	5-1AB-9	6.50	2.00	0.308	0.372
29	5-10B-4	6.50	2.00	0.308	0.349
39	5-12BA-4	6.50	2.00	0.308	0.326
30	5-10B-5	3.50	1.10	0.314	0.302
31	5-10B-5	6.50	2.20	0.338	0.279
41	5-12BA-8	6.50	2.20	0.338	0.256
43	5-12BA-13	6.50	2.50	0.385	0.233
18	5-1C-4	3.50	1.50	0.429	0.209
7	5-1AB-6	6.50	3.00	0.462	0.186
12	5-1AB-11	6.50	3.00	0.462	0.163
23	5-1C-11	6.50	3.00	0.462	0.140
38	5-12BA-3	6.50	3.00	0.462	0.116
28	5-10B-2	6.50	3.50	0.538	0.093
40	5-12BA-6	6.50	3.50	0.538	0.070
26	5-1C-13	6.50	4.00	0.615	0.047
16	5-1AB-14	3.50	4.50	1.286	0.023

From the data of Table 6.4, the mean, median, and quartiles of the distribution parameters of Table 6.5 were derived. The flaw distribution algorithm generates uncertainty distributions by sampling from the Dirichlet distribution using the parameters  $U_i$  listed as in Table 6.5. Figure 6.4 is a plot of curves based on the parameters from Table 6.5, which shows curves for various percentiles of the flaw depth distribution as obtained by sampling of the uncertainty distributions.

Table 6.5. Data and Parameters of the Uncertainty Distribution for Depth Distribution for Small Flaws							
Index i	Normalized Flaw Depth	Number of Flaws	U <sub>i</sub>	β <sub>i</sub> - Parameters of Multinomial Distribution			
				Mean β <sub>i</sub>	25 <sup>th</sup> Percentile β <sub>i</sub>	50 <sup>th</sup> Percentile β <sub>i</sub>	75 <sup>th</sup> Percentile β <sub>i</sub>
1	0.25	34	34	0.79	0.75	0.80	0.83
2	0.55	8	8	0.19	0.14	0.18	0.22
3	0.85	1	1	0.02	0.01	0.02	0.03

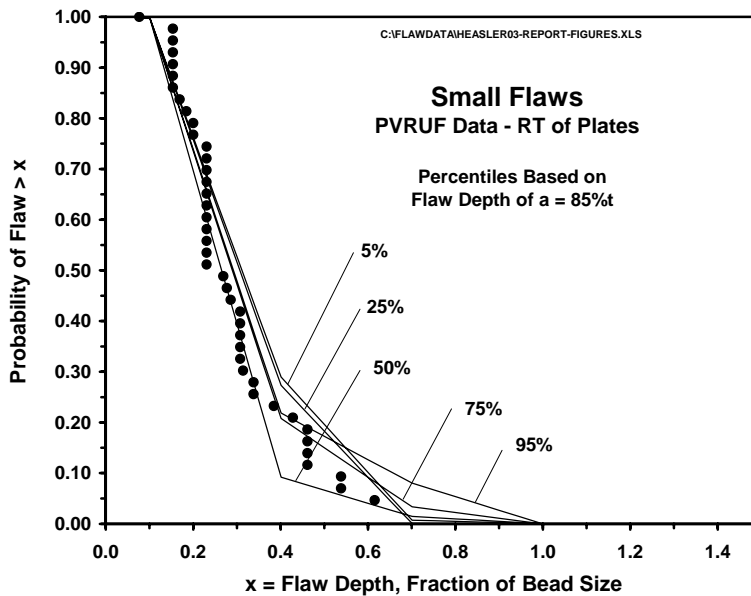


Figure 6.4. Depth Distribution for Small Flaws Including Uncertainty Analysis

### 6.2.3 Conditional Depth Distribution for Large SAW and SMAW Flaws

Two conditional distributions were developed to describe the through-wall dimensions of large flaws. Large flaws are defined as flaws having depths that are greater than the weld bead size. The data showed that the depth distribution for large repair flaws had a significantly different trend (larger sizes) than the large flaws in SAW and SMAW welds. Depth distribution for large repair flaws was addressed by a separate evaluation.

The depth distribution for large SAW and SMAW flaws was based on data from weld normal examinations of welds that had been sectioned from the intact vessel. The size measurements by SAFT-UT were of relatively high accuracy but not as accurate as the measurements performed later during the validation effort for repair flaws that employed a combination of SAFT-UT of small cubes, radiography, and destructive sectioning.

Table 6.6 presents a combined dataset for large SAW and SMAW flaws from both the PVRUF and Shoreham vessels. Because of the relatively small number of observed flaws, the data from the PVRUF and Shoreham vessels were combined to develop a distribution for flaw depths. A review of a sample of flaws from Schuster et al. (1999) indicated that about 81% of these flaws were in SAW material and the

**Table 6.6. Large SAW and SMAW Flaws in PVRUF and Shoreham Vessels**

<b>Index</b>	<b>ID No.</b>	<b>Bead Size, mm</b>	<b>Flaw Depth, mm</b>	<b>Depth Frac Bead</b>
1	10	6.0	5.50	1.00
2	11	6.0	5.50	1.00
3	20	5.0	5.00	1.00
4	22	5.0	5.00	1.00
5	24	5.0	5.00	1.00
6	26	5.0	5.00	1.00
7	28	5.0	5.00	1.00
8	30	5.0	5.00	1.00
9	32	5.0	5.00	1.00
10	34	5.0	5.00	1.00
11	1	3.5	4.00	1.14
12	2	3.5	4.00	1.14
13	12	6.5	7.50	1.15
14	13	6.5	7.50	1.15
15	14	6.5	7.50	1.15
16	15	6.5	7.50	1.15
17	36	5.0	6.00	1.20
18	38	5.0	6.00	1.20
19	40	5.0	6.00	1.20
20	42	5.0	6.00	1.20
21	44	5.0	6.00	1.20
22	46	5.0	6.00	1.20
23	16	6.0	7.50	1.25
24	17	6.0	7.50	1.25
25	49	5.0	7.00	1.40
26	50	5.0	7.00	1.40
27	52	5.0	7.00	1.40
28	3	3.5	5.00	1.43
29	4	3.5	5.00	1.43
30	21	3.5	5.00	1.43
31	23	3.5	5.00	1.43
32	25	3.5	5.00	1.43
33	27	3.5	5.00	1.43
34	29	3.5	5.00	1.43
35	31	3.5	5.00	1.43
36	33	3.5	5.00	1.43
37	53	5.0	8.00	1.60
38	56	5.0	8.00	1.60
39	35	3.5	6.00	1.71
40	37	3.5	6.00	1.71
41	39	3.5	6.00	1.71
42	41	3.5	6.00	1.71
43	43	3.5	6.00	1.71
44	45	3.5	6.00	1.71
45	57	5.0	9.00	1.80
46	58	5.0	9.00	1.80
47	59	5.0	9.00	1.80
48	51	3.5	7.00	2.00
49	62	5.0	10.00	2.00
50	54	3.5	8.00	2.29
51	55	3.5	8.00	2.29
52	60	3.5	9.00	2.57

remaining 19% in SMAW material. For developing complementary conditional depth distributions (CCDF), the approach of Jackson and Abramson (2000) combined the flaw size data for the two weld types. However, the flaw distribution algorithm did include separate treatments of flaw densities for SAW and SMAW welds as well as separate flaw densities for the PVRUF and Shoreham vessels.

Figure 6.5 presents flaw distribution curves that are based on the data of Table 6.6. An exponential distribution function was found to provide a relatively good description of the data. Flaw depth dimensions were normalized with respect to the weld bead thickness to develop the CCDF correlations indicated in Figure 6.5. An evaluation included the uncertainty in the parameter of the exponential distribution as indicated by the percentiles displayed on Figure 6.5. The distribution was calculated from

$$N(>d/\Delta) = \rho e^{-\beta(d/\Delta - 1)} \quad (6.2)$$

where  $N(>d/\Delta)$  is the number of flaws per cubic meter with the normalized depth dimensions greater than  $d/\Delta$  and  $\beta$  is the parameter of an exponential distribution assigned to provide a best fit of the data. Using equations from the Bayesian methodology as described in Appendix A, a gamma distribution function was established to describe the uncertainty in the value of  $\beta$ . The parameters of the gamma function are based on the data of Table 6.6. The values were established to be  $\alpha_1 = 21.68$  and  $\alpha_2 = 52$ , where (from Table 6.6) the parameter  $\alpha_1$  is calculated as the sum of the 52 values of the quantity  $(d/\Delta - 1)$  and  $\alpha_2$  corresponds to the number of data points in Table 6.6.

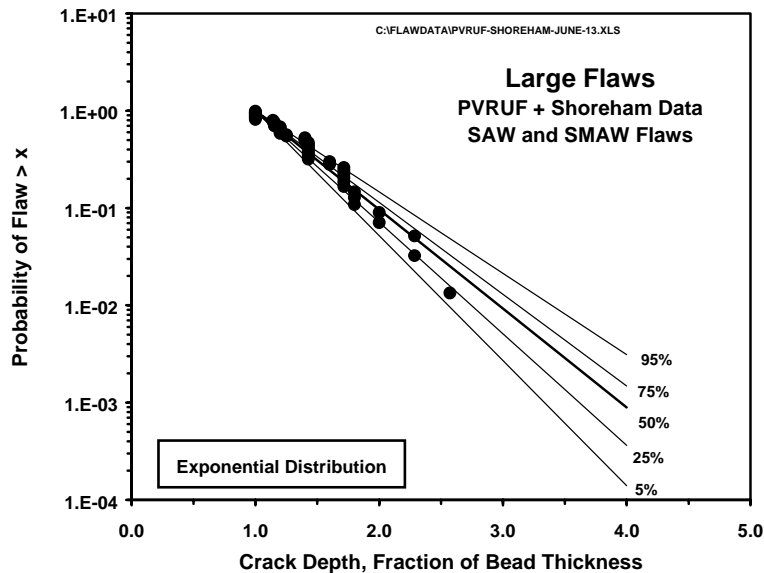


**Figure 6.5. Uncertainty Evaluation for Complementary Conditional Depth Distribution for Large SAW and SMAW Flaws**

### 6.2.4 Conditional Depth Distribution for Large Repair Flaws

A second conditional distribution was developed to describe the through-wall dimensions of large repair flaws, using the same approach as used for large flaws in SAW and SMAW welds. Because of the relatively small number of observed flaws, data from the PVRUF and Shoreham vessels were combined for developing a distribution for flaw depths. Large repair flaws had first been sized by weld normal

examinations. These measured dimensions were subsequently replaced by more accurate dimensions coming from the validation effort that used a combination of SAFT-UT of small cubes, radiography, and destructive examinations.

Table 6.7 presents the combined the dataset for repair flaws. Figure 6.6 presents flaw distribution curves based on the data of Table 6.7. An exponential distribution function was again found to provide a relatively good description of the data. The flaw depth dimensions were normalized with respect to the weld bead thickness as indicated in Figure 6.6. The evaluation addressed the uncertainty in the parameter of the exponential distribution as indicated by the percentiles displayed on Figure 6.6. The distribution was calculated from Equation (6.2) as described in Section 6.2.3.

Index	Bead Size, mm	Nominal Flaw Depth, mm	Measured Flaw Depth, mm	Measured Flaw Length, mm	No. Flaws > x
1	3.5	11.50	2.5	12.00	13
2	3.5	5.50	5.50	-	12
3	3.5	5.50	5.50	-	11
4	3.5	5.50	5.50	-	10
5	3.5	5.50	5.50	-	9
6	3.5	5.50	5.50	-	8
7	3.5	7.00	6.00	18.00	7
8	3.5	21.00	7.00	30.00	6
9	3.5	7.00	10.00	13.00	5
10	3.5	10.00	10.00	11.00	4
11	3.5	32.00	12.00	44.00	3
12	3.5	14.00	14.00	14.00	2
13	3.5	17.50	17.00	18.00	1

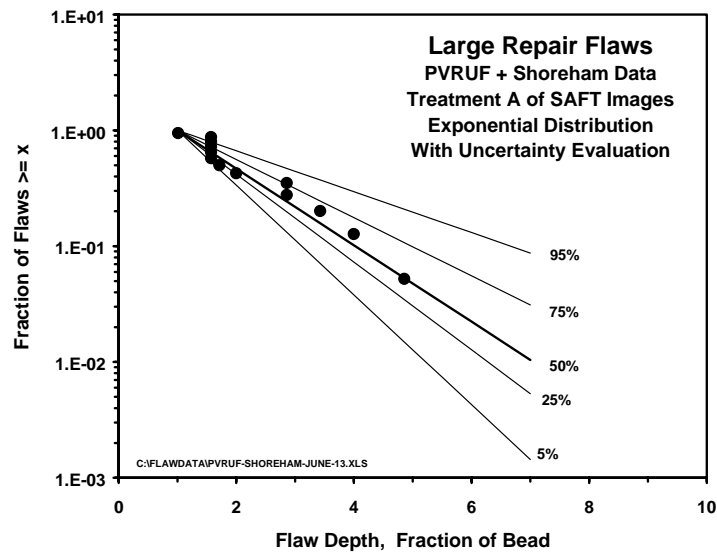


**Figure 6.6. Uncertainty Evaluation for Complementary Conditional Depth Distribution for Large Repair Flaws**

Parameters of the gamma function are based on the data of Table 6.7. The values were established to be  $\alpha_1 = 17.58$  and  $\alpha_2 = 13$  where (from Table 6.7) the parameter  $\alpha_1$  is calculated as the sum of the 17 values of the quantity  $(d/\Delta - 1)$  and  $\alpha_2$  corresponds to the number of data points in Table 6.7.

### 6.2.5 Length Distribution for Small SAW Flaws in PVRUF Vessel

Flaw aspect ratios (the ratio of flaw length to flaw depth) are an important input to the probabilistic fracture mechanics calculations of the FAVOR code. Considerable effort was applied to develop a method to define these flaw aspect ratios on the basis of the flaw lengths measured for the PVRUF and Shoreham vessels. PNNL adopted the approach of the PRODIGAL model (Chapman and Simonen 1998) for describing flaw aspect ratios, which assumed that the distribution of flaw lengths is independent of the depth dimension of the flaws. An evaluation of the length data from the PVRUF and Shoreham flaws showed that this was a reasonable assumption for the current work. The model established the statistical distributions for amounts by which normalized flaw lengths exceeded the normalized flaw depths.

The available data indicated different trends of flaw lengths for the PVRUF and Shoreham vessels and different trends for SAW versus SMAW welds. There appeared to be sufficient data for small flaws to address four flaw categories corresponding to the two vessels and two weld processes. Lacking sufficient data for small repair flaws, it was assumed that the lengths of small repair flaws can be described by the same distribution function as for flaws in SMAW welds.

This section addresses the lengths of small SAW flaws in the PVRUF vessel. The next three sections address small flaws in SMAW welds and the Shoreham vessel. The selected dataset included only those small SAW flaws in the PVRUF welds that were subjected to the most complete of the validation efforts (Schuster et al. 2000a, Table 9 and Figure 4). This selection excluded small flaws that were detected only by the examinations performed with the early SAFT-UT examinations at ORNL. Also excluded were the flaws that were validated only by the weld normal ultrasonic (UT) examinations but not further validated by RT and destructive evaluations. These restrictive requirements resulted in the most accurate measurements of flaw dimensions but meant that only 9 small flaws remained upon which to base a flaw length distribution.

Figures 6.7 and 6.8 show all of the length data for small and large flaws in the PVRUF vessel. The length distribution was characterized by the exponential distribution. The distribution was calculated from

$$P[>(\ell - a)/\Delta] = e^{-\beta(\ell - a)/\Delta} \quad (6.3)$$

where  $P[>(\ell - a)/\Delta]$  is the fraction of flaws with the normalized length dimensions greater than  $(\ell - a)/\Delta$  and  $\beta$  is the parameter of an exponential distribution assigned to provide a best fit of the data. Using equations from the Bayesian methodology as described in Appendix A, a gamma distribution function was established to describe the uncertainty in the value of  $\beta$ . The parameters of the gamma function were based on the data of Table 6.8. The values were established to be  $\alpha_1 = 0.53846$  and  $\alpha_2 = 9$ , where (from Table 6.8) the parameter  $\alpha_1$  is calculated as the sum of the nine values of the quantity  $(\ell - a)/\Delta$  and  $\alpha_2$  corresponds to the number of data points in Table 6.8. The resulting distribution function is shown in Figure 6.8 along with the data and results of the uncertainty evaluation.

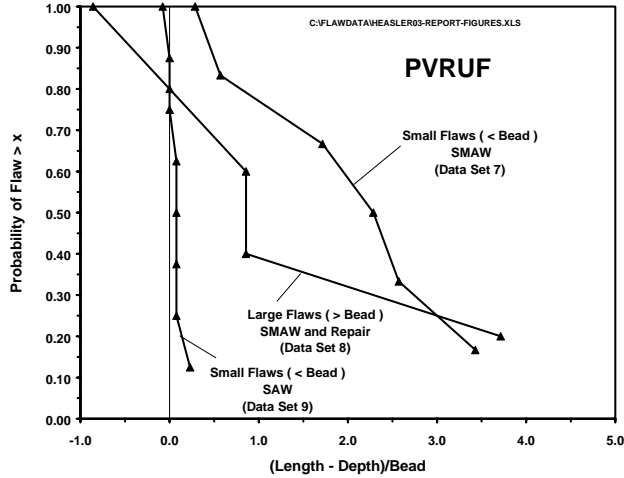


Figure 6.7. Lengths of Small Flaws in SAW and SMAW Welds of PVRUF Vessel

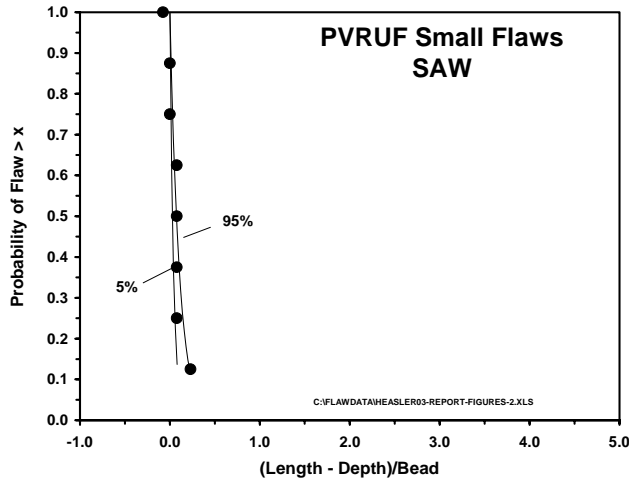


Figure 6.8. Lengths of Small Flaws in SAW Welds of PVRUF Vessel Showing Exponential Distribution Along with Uncertainties

Table 6.8. Lengths of Small Flaws in SAW Welds of PVRUF Vessel								
Label	Weld Type	Bead Size, mm	Flaw Depth, mm	Flaw Length, mm	Length Minus Depth, mm	Depth Frac Bead	Length Minus Depth Frac Bead	Fraction > x
5-1C-13	SAW	6.50	4.0	3.5	-0.50	0.615	-0.077	1.000
5-10B-2	SAW	6.50	3.5	3.5	0.00	0.538	0.000	0.875
5-12BA-1	SAW	6.50	3.5	3.5	0.00	0.538	0.000	0.750
5-1AB-6	SAW	6.50	3.0	3.5	0.50	0.462	0.077	0.625
5-1AB-11	SAW	6.50	3.0	3.5	0.50	0.462	0.077	0.500
5-1C-11	SAW	6.50	3.0	3.5	0.50	0.462	0.077	0.375
5-12BA-1	SAW	6.50	3.0	3.5	0.50	0.462	0.077	0.250
5-12BA-1	SAW	6.50	2.0	3.5	1.50	0.308	0.231	0.125

## 6.2.6 Length Distribution for Small SMAW and Repair Flaws in PVRUF Vessel

This section addresses the lengths of small SMAW flaws in the PVRUF vessel. Lacking sufficient data for small repair flaws, it was assumed that the lengths of small repair flaws could be described by the same distribution function as used for SMAW flaws. The length distribution was calculated from Equation (6.3) as described in Section 6.2.5. The parameters of the gamma function are based on the data of Table 6.9. The values were established to be  $\alpha_1 = 10.857$  and  $\alpha_2 = 6$ , where (from Table 6.9) the parameter  $\alpha_1$  is calculated as the sum of the six values of the quantity  $(\ell - a)/\Delta$  and  $\alpha_2$  corresponds to the number of data points in Table 6.9. The resulting distribution function is shown in Figure 6.9 along with the data and results of the uncertainty evaluation.

Label	Weld Type	Bead Size, mm	Flaw Depth, mm	Flaw Length, mm	Length Minus Depth, mm	Depth Frac Bead	Length Minus Depth, Frac Bead	Fraction > x
5-7H1iibiic	SMAW	3.50	3.0	4.0	1.00	0.857	0.286	1.000
5-4B1iidiie	SMAW	3.50	3.0	5.0	2.00	0.857	0.571	0.833
5-10B5ibic	SMAW	3.50	3.0	9.0	6.00	0.857	1.714	0.667
5-10EC1iibiic	SMAW	3.50	3.0	11.0	8.00	0.857	2.286	0.500
5-10EA1iibiic	SMAW	3.50	3.0	12.0	9.00	0.857	2.571	0.333
5-10ECiidiie	SMAW	3.50	3.0	15.0	12.00	0.857	3.429	0.167

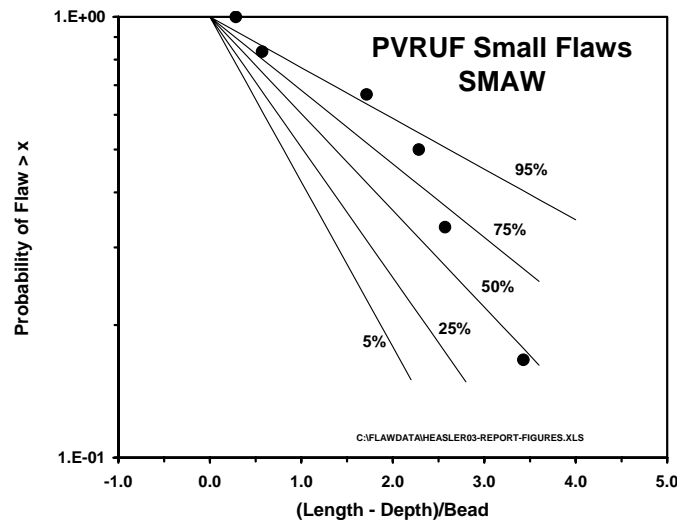


Figure 6.9. Lengths of Small Flaws in SMAW Welds of PVRUF Vessel Showing Exponential Distribution Along with Uncertainties

## 6.2.7 Length Distribution for Small SAW Flaws in Shoreham Vessel

This section addresses the lengths of small SAW flaws in the Shoreham vessel. The selected data set addressed only a sample of the small SAW flaws in the Shoreham welds (Schuster et al. 2000a). This selection included small flaws that were detected and sized by the examinations performed with the weld normal UT examinations but not further validated by SAFT-UT and destructive evaluations. These less

restrictive requirements for the data resulted in a relatively large number of measurements of flaw dimensions, which gave a total of 105 small flaws upon which to base a flaw length distribution.

Figure 6.10 shows the available length data for small and large flaws in the Shoreham vessel. Length distributions were calculated from Equation (6.3) as described in Section 6.2.5. Parameters of the gamma function for small flaws SAW welds of the Shoreham vessel were based on the data of Table 6.10. The values were established to be  $\alpha_1 = 286$  and  $\alpha_2 = 105$ , where (from Table 6.10) the parameter  $\alpha_1$  is calculated as the sum of the 105 values of the quantity  $(\ell - a)/\Delta$  and  $\alpha_2$  corresponds to the number of data points in Table 6.10. Figure 6.11 shows the length distribution along with the data used to establish the distribution function and the statistical uncertainty in the correlation.

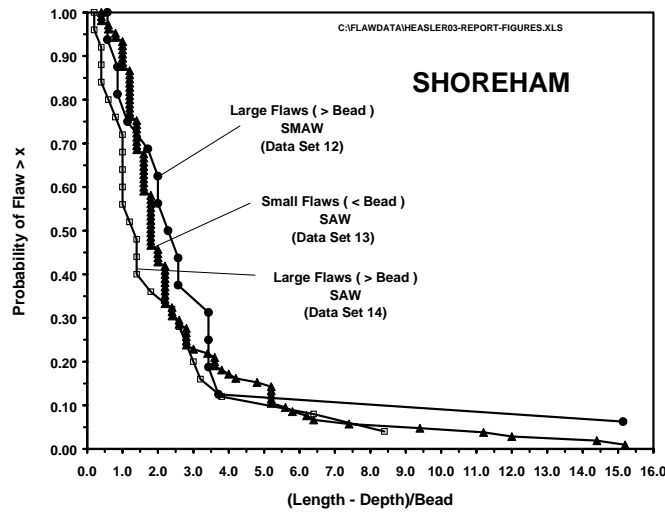


Figure 6.10. Lengths of Small Flaws in SAW and SMAW Welds of Shoreham Vessel

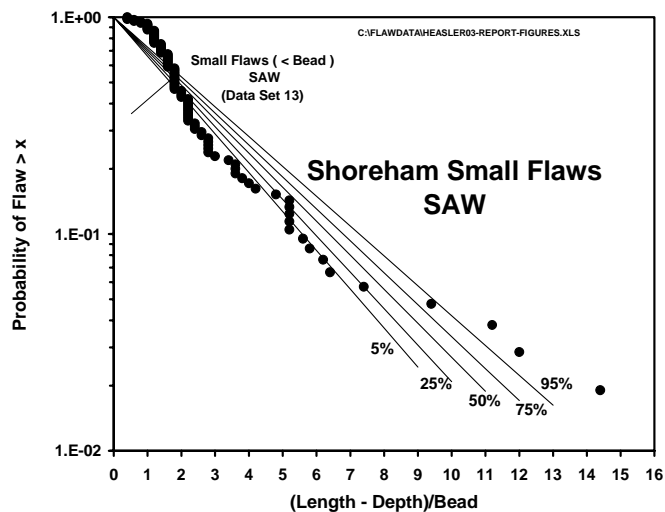


Figure 6.11. Lengths of Small Flaws in SAW Welds of Shoreham Vessel Showing Exponential Distribution Along with Uncertainties

**Table 6.10. Lengths of Small Flaws in SAW Welds of Shoreham Vessel**

<b>Label</b>	<b>Weld Type</b>	<b>Bead Size, mm</b>	<b>Flaw Depth, mm</b>	<b>Flaw Length, mm</b>	<b>Length Minus Depth, mm</b>	<b>Depth Frac Bead</b>	<b>Length Minus Depth Frac Bead</b>	<b>Fraction &gt; x</b>
208	SAW	5.0	5.0	7.0	2.0	1.000	0.400	1.000
144	SAW	5.0	5.0	7.0	2.0	1.000	0.400	0.990
11	SAW	5.0	5.0	7.0	2.0	1.000	0.400	0.981
68	SAW	5.0	5.0	8.0	3.0	1.000	0.600	0.971
153	SAW	5.0	5.0	8.0	3.0	1.000	0.600	0.962
132	SAW	5.0	5.0	9.0	4.0	1.000	0.800	0.952
124	SAW	5.0	5.0	9.0	4.0	1.000	0.800	0.943
64	SAW	5.0	4.0	9.0	5.0	0.800	1.000	0.933
30	SAW	5.0	4.0	9.0	5.0	0.800	1.000	0.924
177	SAW	5.0	4.0	9.0	5.0	0.800	1.000	0.914
8	SAW	5.0	5.0	10.0	5.0	1.000	1.000	0.905
184	SAW	5.0	5.0	10.0	5.0	1.000	1.000	0.895
2	SAW	5.0	5.0	10.0	5.0	1.000	1.000	0.886
37	SAW	5.0	5.0	10.0	5.0	1.000	1.000	0.876
262	SAW	5.0	4.0	10.0	6.0	0.800	1.200	0.867
258	SAW	5.0	4.0	10.0	6.0	0.800	1.200	0.857
100	SAW	5.0	4.0	10.0	6.0	0.800	1.200	0.848
48	SAW	5.0	4.0	10.0	6.0	0.800	1.200	0.838
98	SAW	5.0	4.0	10.0	6.0	0.800	1.200	0.829
23	SAW	5.0	4.0	10.0	6.0	0.800	1.200	0.819
160	SAW	5.0	4.0	10.0	6.0	0.800	1.200	0.810
233	SAW	5.0	4.0	10.0	6.0	0.800	1.200	0.800
180	SAW	5.0	4.0	10.0	6.0	0.800	1.200	0.790
231	SAW	5.0	4.0	10.0	6.0	0.800	1.200	0.781
123	SAW	5.0	4.0	10.0	6.0	0.800	1.200	0.771
38	SAW	5.0	4.0	10.0	6.0	0.800	1.200	0.762
67	SAW	5.0	4.0	11.0	7.0	0.800	1.400	0.752
42	SAW	5.0	4.0	11.0	7.0	0.800	1.400	0.743
112	SAW	5.0	4.0	11.0	7.0	0.800	1.400	0.733
158	SAW	5.0	4.0	11.0	7.0	0.800	1.400	0.724
52	SAW	5.0	4.0	11.0	7.0	0.800	1.400	0.714
16	SAW	5.0	4.0	11.0	7.0	0.800	1.400	0.705
18	SAW	5.0	4.0	11.0	7.0	0.800	1.400	0.695
107	SAW	5.0	5.0	12.0	7.0	1.000	1.400	0.686
34	SAW	5.0	4.0	12.0	8.0	0.800	1.600	0.676
105	SAW	5.0	4.0	12.0	8.0	0.800	1.600	0.667
12	SAW	5.0	4.0	12.0	8.0	0.800	1.600	0.657
293	SAW	5.0	4.0	12.0	8.0	0.800	1.600	0.648
317	SAW	5.0	4.0	12.0	8.0	0.800	1.600	0.638
338	SAW	5.0	4.0	12.0	8.0	0.800	1.600	0.629
256	SAW	5.0	5.0	13.0	8.0	1.000	1.600	0.619
74	SAW	5.0	5.0	13.0	8.0	1.000	1.600	0.610
126	SAW	5.0	5.0	13.0	8.0	1.000	1.600	0.600
111	SAW	5.0	5.0	13.0	8.0	1.000	1.600	0.590
38	SAW	5.0	4.0	13.0	9.0	0.800	1.800	0.581
47	SAW	5.0	4.0	13.0	9.0	0.800	1.800	0.571
65	SAW	5.0	4.0	13.0	9.0	0.800	1.800	0.562
222	SAW	5.0	4.0	13.0	9.0	0.800	1.800	0.552

Table 6.10. Lengths of Small Flaws in SAW Welds of Shoreham Vessel (contd)								
Label	Weld Type	Bead Size, mm	Flaw Depth, mm	Flaw Length, mm	Length Minus Depth, mm	Depth Frac Bead	Length Minus Depth Frac Bead	Fraction > x
125	SAW	5.0	4.0	13.0	9.0	0.800	1.800	0.533
94	SAW	5.0	4.0	13.0	9.0	0.800	1.800	0.524
17	SAW	5.0	4.0	13.0	9.0	0.800	1.800	0.514
26	SAW	5.0	4.0	13.0	9.0	0.800	1.800	0.505
51	SAW	5.0	4.0	13.0	9.0	0.800	1.800	0.495
51	SAW	5.0	5.0	14.0	9.0	1.000	1.800	0.486
39	SAW	5.0	5.0	14.0	9.0	1.000	1.800	0.476
47	SAW	5.0	5.0	14.0	9.0	1.000	1.800	0.467
21	SAW	5.0	4.0	14.0	10.0	0.800	2.000	0.457
274	SAW	5.0	4.0	14.0	10.0	0.800	2.000	0.448
196	SAW	5.0	5.0	15.0	10.0	1.000	2.000	0.438
58	SAW	5.0	5.0	15.0	10.0	1.000	2.000	0.429
73	SAW	5.0	4.0	15.0	11.0	0.800	2.200	0.419
45	SAW	5.0	4.0	15.0	11.0	0.800	2.200	0.410
49	SAW	5.0	4.0	15.0	11.0	0.800	2.200	0.400
299	SAW	5.0	4.0	15.0	11.0	0.800	2.200	0.390
124	SAW	5.0	4.0	15.0	11.0	0.800	2.200	0.381
310	SAW	5.0	4.0	15.0	11.0	0.800	2.200	0.371
334	SAW	5.0	4.0	15.0	11.0	0.800	2.200	0.362
98	SAW	5.0	4.0	15.0	11.0	0.800	2.200	0.352
284	SAW	5.0	5.0	16.0	11.0	1.000	2.200	0.343
119	SAW	5.0	5.0	16.0	11.0	1.000	2.200	0.333
39	SAW	5.0	4.0	16.0	12.0	0.800	2.400	0.324
4	SAW	5.0	4.0	16.0	12.0	0.800	2.400	0.314
22	SAW	5.0	4.0	16.0	12.0	0.800	2.400	0.305
17	SAW	5.0	5.0	18.0	13.0	1.000	2.600	0.295
206	SAW	5.0	5.0	18.0	13.0	1.000	2.600	0.286
32	SAW	5.0	4.0	18.0	14.0	0.800	2.800	0.276
151	SAW	5.0	4.0	18.0	14.0	0.800	2.800	0.267
95	SAW	5.0	4.0	18.0	14.0	0.800	2.800	0.257
29	SAW	5.0	4.0	18.0	14.0	0.800	2.800	0.248
173	SAW	5.0	4.0	18.0	14.0	0.800	2.800	0.238
55	SAW	5.0	4.0	19.0	15.0	0.800	3.000	0.229
24	SAW	5.0	5.0	22.0	17.0	1.000	3.400	0.219
17	SAW	5.0	4.0	22.0	18.0	0.800	3.600	0.210
286	SAW	5.0	4.0	22.0	18.0	0.800	3.600	0.200
83	SAW	5.0	5.0	23.0	18.0	1.000	3.600	0.190
22	SAW	5.0	4.0	23.0	19.0	0.800	3.800	0.181
79	SAW	5.0	5.0	25.0	20.0	1.000	4.000	0.171
65	SAW	5.0	4.0	25.0	21.0	0.800	4.200	0.162
153	SAW	5.0	4.0	28.0	24.0	0.800	4.800	0.152
239	SAW	5.0	4.0	30.0	26.0	0.800	5.200	0.143
164	SAW	5.0	4.0	30.0	26.0	0.800	5.200	0.133
102	SAW	5.0	4.0	30.0	26.0	0.800	5.200	0.124
318	SAW	5.0	4.0	30.0	26.0	0.800	5.200	0.114
345	SAW	5.0	4.0	30.0	26.0	0.800	5.200	0.105
112	SAW	5.0	5.0	33.0	28.0	1.000	5.600	0.095
18	SAW	5.0	4.0	33.0	29.0	0.800	5.800	0.086

<b>Label</b>	<b>Weld Type</b>	<b>Bead Size, mm</b>	<b>Flaw Depth, mm</b>	<b>Flaw Length, mm</b>	<b>Length Minus Depth, mm</b>	<b>Depth Frac Bead</b>	<b>Length Minus Depth Frac Bead</b>	<b>Fraction &gt; x</b>
139	SAW	5.0	5.0	36.0	31.0	1.000	6.200	0.076
22	SAW	5.0	4.0	36.0	32.0	0.800	6.400	0.067
113	SAW	5.0	4.0	41.0	37.0	0.800	7.400	0.057
81	SAW	5.0	4.0	51.0	47.0	0.800	9.400	0.048
40	SAW	5.0	5.0	61.0	56.0	1.000	11.200	0.038
28	SAW	5.0	4.0	64.0	60.0	0.800	12.000	0.029
149	SAW	5.0	4.0	76.0	72.0	0.800	14.400	0.019
78	SAW	5.0	5.0	81.0	76.0	1.000	15.200	0.010

### 6.2.8 Length Distribution for Small SMAW and Repair Flaws in Shoreham Vessel

This section addresses the lengths of small SMAW flaws in the Shoreham vessel. A review of the available data (Schuster et al. 1999) indicated that length measurements for small flaws were insufficient to support a length distribution, whereas a combined dataset covering both small and large SMAW and repair flaws provided an adequate database. The dataset included only larger flaws for which the length measurements were made with a reasonable level of accuracy. These flaws were detected and sized by the weld normal UT examinations. None of these measurements had been further validated by SAFT-UT and destructive evaluation. The acceptance requirements for the data resulted in a total of 16 small flaws upon which to base a distribution function for flaw lengths.

The flaw lengths were calculated from Equation (6.3) as described in Section 6.2.5. The parameters of the gamma function for small SAW in the Shoreham vessel were based on the data of Table 6.11. The values were established to be  $\alpha_1 = 46.3$  and  $\alpha_2 = 16$ , where (from Table 6.11) the parameter  $\alpha_1$  was calculated as the sum of the 25 values of the quantity  $(\ell - a)/\Delta$  and  $\alpha_2$  corresponds to the number of data

<b>ID</b>	<b>Table</b>	<b>Specimen</b>	<b>Length</b>	<b>Figure</b>	<b>TW-Size, mm</b>	<b>Length, mm</b>	<b>Length-TW</b>	<b>Bead Size, mm</b>	<b>Depth Frac Bead</b>	<b>Length-TW Frac Bead</b>
13	I.1	C0G	58.4	I.6	7.0	9.0	2.0	3.5	2.0	0.6
14	D.1	B180C-2	41.5	D.3	7.0	9.0	2.0	3.5	2.0	0.6
47	T.1	C270D	117.4	T.9	8.0	11.0	3.0	3.5	2.3	0.9
59	D.1	B180C-2	41.5	D.4	9.0	12.0	3.0	3.5	2.6	0.9
32	G.1	C0E	55.2	G.1	6.0	10.0	4.0	3.5	1.7	1.1
15	T.1	C270D	117.4	T.3	4.0	10.0	6.0	3.5	1.1	1.7
36	F.1	C0D	19.4	F.1	4.0	11.0	7.0	3.5	1.1	2.0
37	G.1	C0E	55.2	G.5	4.0	11.0	7.0	3.5	1.1	2.0
50	G.1	C0E	55.2	G.4	4.0	12.0	8.0	3.5	1.1	2.3
60	T.1	C270D	117.4	T.11	4.0	13.0	9.0	3.5	1.1	2.6
80	I.1	C0G	58.4	I.1	5.0	14.0	9.0	3.5	1.4	2.6
96	T.1	C270D	117.4	T.8	4.0	16.0	12.0	3.5	1.1	3.4
97	T.1	C270D	117.4	T.13	4.0	16.0	12.0	3.5	1.1	3.4
98	T.1	C270D	117.4	T.12	4.0	16.0	12.0	3.5	1.1	3.4
114	M.1	C120E	53.6	M.9	7.0	20.0	13.0	3.5	2.0	3.7
142	P.1	C180B	71.7	P.7	4.0	57.0	53.0	3.5	1.1	15.1

points in Table 6.11. The resulting distribution function is shown in Figure 6.12 along with the data and results of the uncertainty evaluation.

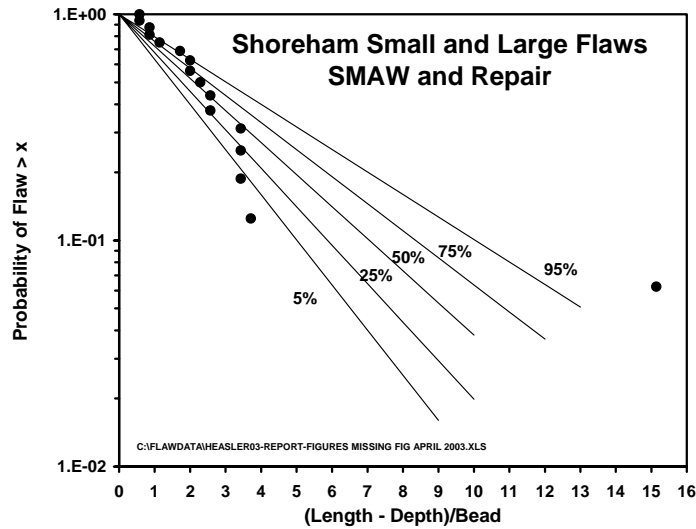


**Figure 6.12. Lengths of Small and Large Flaws in SMAW and Repair Welds of Shoreham Vessel Showing Exponential Distribution Along with Uncertainties**

### 6.2.9 Length Distribution for Large SAW Flaws in PVRUF Vessel

This section addresses the lengths of large flaws in SAW welds of the PVRUF vessel. The selected dataset addressed only those flaws in the PVRUF welds that were subjected to the most thorough of the validation efforts (Schuster et al. 2000a, Table 9 and Figure 4). The selection excluded small flaws that were detected only by the examinations performed with the early SAFT-UT examinations at ORNL. The selection also excluded flaws that were validated by the weld normal UT examinations but not further validated by RT and destructive evaluations. These restrictive requirements for validation resulted in the most accurate measurements of flaw dimensions but meant that only 9 small flaws remained upon which to base a flaw length distribution. The relatively small number of flaws with high-accuracy length measurements was judged to be insufficient to develop separate length distributions for large versus small flaws. Therefore, a single depth distribution was used to describe the lengths of both small and large flaws in SAW welds of the Shoreham vessel.

Figure 6.7 showed the length data for small and large SAW flaws in the PVRUF vessel. The length distribution was calculated from Equation (6.3) as described in Section 6.2.5. The parameters of the gamma function are based on the data of Table 6.6. The values were established to be  $\alpha_1 = 0.53846$  and  $\alpha_2 = 9$ , where (from Table 6.8) the parameter  $\alpha_1$  is calculated as the sum of the nine values of the quantity  $(\ell - a)/\Delta$  and  $\alpha_2$  corresponds to the number of data points in Table 6.8.

### 6.2.10 Length Distribution for Large SMAW and Repair Flaws in PVRUF Vessel

This section addresses the lengths of large flaws in SMAW and repair welds of the PVRUF vessel. The selected dataset addressed only those large SMAW and repair flaws in the PVRUF welds (Schuster et al. 1999). This selection excluded large flaws that were detected and sized by the examinations performed

with the weld normal UT examinations but not further validated by SAFT-UT and destructive evaluations after being removed as cube samples. The dataset resulted in a relatively small number of measurements of flaw lengths, which gave a total of 5 large flaws upon which to base a flaw length distribution.

The length distributions were calculated from Equation (6.3) as described in Section 6.2.5. The parameters of the gamma function were based on the data of Table 6.12. The values were established to be  $\alpha_1 = 5.428$  and  $\alpha_2 = 5$ , where (from Table 6.12) the parameter  $\alpha_1$  is calculated as the sum of the five values of the quantity  $(l - a)/\Delta$  and  $\alpha_2$  corresponds to the number of data points in Table 6.12. The resulting distribution function is shown in Figure 6.13 along with the data and results of the uncertainty evaluation.

Label		Bead Size, mm	TW-Size, mm	Length, mm	Aspect Ratio	L-TW, mm	TW Frac Bead	Large=2 Small=1	L-TW Frac Bead	Frac > L-TW Frac Bead
5-12AC5&6	REPAIR	3.50	17.0	14.0	0.8235	-3.00	4.8571	2	-0.8571	1.0000
5-12AC3	REPAIR	3.50	5.0	5.0	1.0000	0.00	1.4286	2	0.0000	0.8000
5-1AB14ibic	SMAW	3.50	5.0	8.0	1.6000	3.00	1.4286	2	0.8571	0.6000
5-12AC2	REPAIR	3.50	12.0	15.0	1.2500	3.00	3.4286	2	0.8571	0.4000
5-10EBiibiic	SMAW	3.50	4.0	17.0	4.2500	13.00	1.1429	2	3.7143	0.2000

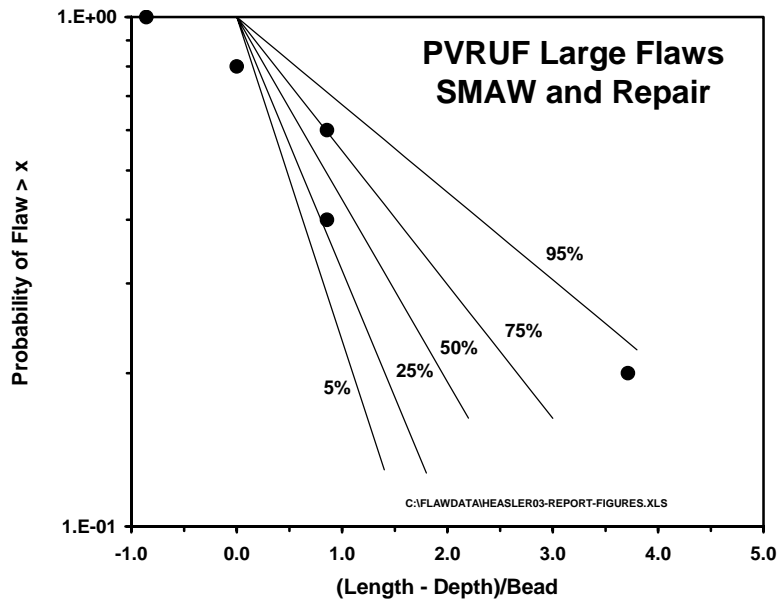


**Figure 6.13. Lengths of Large Flaws in SMAW and Repair Welds of PVRUF Vessel Showing Exponential Distribution Along with Uncertainties**

### 6.2.11 Length Distribution for Large SAW Flaws in Shoreham Vessel

This section addresses the lengths of large flaws in SAW welds in the Shoreham vessel. The selected data are reported in Schuster et al. (1999). These large flaws were detected and sized by the

examinations performed with the weld normal UT examinations but not further validated by SAFT-UT and destructive evaluations. The dataset gave a total of 25 large flaws upon which to base a flaw length distribution.

The length distributions was calculated from Equation (6.3) as described in Section 6.2.5. The parameters of the gamma function for small SAW in the Shoreham vessel were based on the data of Table 6.13. The values were established to be  $\alpha_1 = 47.80$  and  $\alpha_2 = 25$ , where (from Table 6.13) the parameter  $\alpha_1$  is calculated as the sum of the 25 values of the quantity  $(\ell - a)/\Delta$  and  $\alpha_2$  corresponds to the number of data points in Table 6.13. The resulting distribution function is shown in Figure 6.14 along with the data and results of the uncertainty evaluation.

<b>Table 6.13. Lengths of Small Flaws in SAW Welds of Shoreham Vessel</b>								
<b>Label</b>	<b>Weld Type</b>	<b>Bead Size, mm</b>	<b>Flaw Depth, mm</b>	<b>Flaw Length, mm</b>	<b>Length Minus Depth, mm</b>	<b>Depth Frac Bead</b>	<b>Length Minus Depth Frac Bead</b>	<b>Fraction &gt; x</b>
200	SAW	5.0	7.0	8.0	1.0	1.400	0.200	1.000
39	SAW	5.0	9.0	10.0	1.0	1.800	0.200	0.960
197	SAW	5.0	8.0	10.0	2.0	1.600	0.400	0.920
123	SAW	5.0	9.0	11.0	2.0	1.800	0.400	0.880
42	SAW	5.0	9.0	11.0	2.0	1.800	0.400	0.840
116	SAW	5.0	6.0	9.0	3.0	1.200	0.600	0.800
272	SAW	5.0	6.0	10.0	4.0	1.200	0.800	0.760
207	SAW	5.0	6.0	11.0	5.0	1.200	1.000	0.720
65	SAW	5.0	6.0	11.0	5.0	1.200	1.000	0.680
7	SAW	5.0	7.0	12.0	5.0	1.400	1.000	0.640
31	SAW	5.0	8.0	13.0	5.0	1.600	1.000	0.600
2	SAW	5.0	10.0	15.0	5.0	2.000	1.000	0.560
5	SAW	5.0	32.0	38.0	6.0	6.400	1.200	0.520
6	SAW	5.0	6.0	13.0	7.0	1.200	1.400	0.480
112	SAW	5.0	6.0	13.0	7.0	1.200	1.400	0.440
13	SAW	5.0	21.0	28.0	7.0	4.200	1.400	0.400
32	SAW	5.0	6.0	15.0	9.0	1.200	1.800	0.360
8	SAW	5.0	6.0	18.0	12.0	1.200	2.400	0.320
148	SAW	5.0	7.0	20.0	13.0	1.400	2.600	0.280
214	SAW	5.0	6.0	20.0	14.0	1.200	2.800	0.240
186	SAW	5.0	10.0	25.0	15.0	2.000	3.000	0.200
103	SAW	5.0	14.0	30.0	16.0	2.800	3.200	0.160
101	SAW	5.0	6.0	25.0	19.0	1.200	3.800	0.120
157	SAW	5.0	6.0	38.0	32.0	1.200	6.400	0.080
111	SAW	5.0	6.0	48.0	42.0	1.200	8.400	0.040

### 6.2.12 Length Distribution for Large SMAW and Repair Flaws in Shoreham Vessel

The available length measurements for small and large SMAW and repair flaws were combined into a single dataset. The resulting distribution including uncertainties is described in Section 6.2.8.

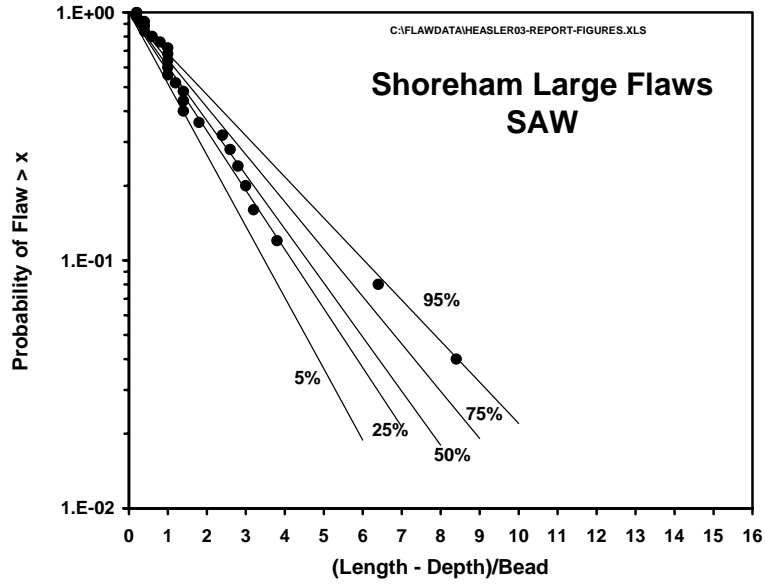


**Figure 6.14. Lengths of Large Flaws in SAW Welds of Shoreham Vessel Showing Exponential Distribution Along with Uncertainties**

## 7 BASE METAL FLAWS - DATA AND STATISTICAL CORRELATIONS

The flaw distribution model provides a total of three input files for the FAVOR code, with one of these files describing flaws in base metal regions. The treatment of base metal flaws is documented in this section along with a discussion of the available flaw data and other sources of information that support the model.

### 7.1 Approach and Assumptions

Basic considerations and assumptions related to the development of the flaw distributions for base metal regions are described in this section.

**Scope of Generalized Distribution** - Available data to PNNL for base metal flaws were obtained from plate material from four specific vessels (PVRUF, Shoreham, River Bend II, and Hope Creek II). The flaw distribution model, however, was developed to be applied on a generic basis for any vessel constructed with rolled plates. The model was not intended to apply to vessels constructed with forged rings. Flaw distributions as predicted by the model were intended to apply to the material of the surface regions of plates down to a depth of about 1 in. because this material region is of primary concern to vessel integrity for conditions of pressurized thermal shock.

The FAVOR code addresses three categories of flaws that have the potential to impact the integrity vessels that have low-toughness base metal:

1. flaws distributed within the volume of the base metal with their origins from the production processes for the plates or forgings—These flaws are addressed here in this section.
2. weld flaws located along the fusion zone, which can propagate into embrittled base metal—These flaws were addressed in Section 6 on distributions of weld flaws.
3. flaws within cladding material, which can extend to the clad-to-base metal interface such to have a potential to propagate into the base metal—These flaws are addressed in Section 8 as clad flaws.

The present methodology does not address under-clad cracks in the base metal that originate during the cladding process.

**Flaws per Unit Volume Versus Flaws per Unit Area** - The FAVOR code describes flaw densities for base metal in terms of flaws per unit volume. This approach is consistent with PNNL's treatment of flaws in base metal regions. The input files for FAVOR are based on flaws per unit volume.

**Use of Data Versus Models and Expert Elicitation** - The approach taken in developing base metal flaw distributions was to use measured data to the maximum extent possible and to use results of the expert judgment elicitation only when data are inadequate. For base metal flaws, there were only a limited amount of data on observed flaws. The quantity of data was limited because PNNL could examine only a small volume of base metal relative to the volume of such material in the beltline of a typical vessel. In addition, there were relatively few flaws in the volumes of the examined base metal. Lacking an adequate

body of data, the expert elicitation (Jackson and Abramson 2000) was an important element that was used to estimate flaw densities and size distributions. In this regard, the measured data were used mainly as a benchmark against which the inputs derived from the expert judgment elicitation could be compared.

**Vessel-to-Vessel Variability** - Examinations of plate material from the four vessels showed significant vessel-to-vessel variations in flaw densities. However, flaw depth distributions in the four vessels were found to follow a common trend. The approach was to develop a single flaw distribution that was consistent with both the inputs from the expert elicitation and trends of the available data. The objective was to describe the flaws in the plate material of a so-called average vessel.

**Locations of Flaws Relative to Vessel Inner Surface** - Flaws in welds were assumed to be buried within the thickness of the vessel wall. The locations of the flaw inner tips relative to the vessel inner surface were assigned in a random manner. As a limiting case, a weld flaw could have its inner tip at the clad-to-base metal interface, a condition that would have a statistically zero probability of occurrence.

For base metal, the information from the expert elicitation clearly indicated that the midsections of rolled plates consistently have larger flaw densities and larger flaw sizes than near-surface regions. The plate flaw distribution was therefore developed to address only the near-surface region because of the concerns for this region from the standpoint of pressurized thermal shock. It was assumed that flaws in the plate mid-section, even with their greater densities and sizes, are relatively unimportant to vessel integrity.

**Flaw Orientation** - The base metal flaw distribution was intended to address only flaws with significant through-wall dimensions. The approach was to neglect flaws of no structural significance, which have orientations parallel to the vessel surfaces. The PNNL inspections of plate materials selected techniques for the SAFT-UT examinations that were optimized to detect and size small flaws with through-wall dimensions rather than larger flaws that are parallel to the vessel surface.

**Crack Shape** - All plate flaws were assumed to be crack-like flaws without detailed consideration of the sharp or blunted nature of flaw tips. It was recognized that the treatment of flaws by FAVOR assumes planar flaws of ideal elliptical shape. In FAVOR, the plane of the cracks and the major and minor axes of the flaws are aligned with the radial and axial coordinates of the vessel. The PNNL measurements of plate flaws by SAFT-UT provided dimensions of flaws in terms of an enclosing box that would contain the flaw.

A typical plate flaw is shown in Figure 7.1. As in the case of weld flaws, the dimensions of the enclosing box provide a realistic representation of the overall flaw dimensions. However, the FAVOR assumption of idealized elliptical cracks is a conservative treatment of flaws, as shown by Figure 7.1. The flaw of Figure 7.1 is a cluster of crack-like flaws with complex interactions between the individual features of the flaw. Current fracture mechanics models do not permit treatment of detailed geometries of the complex flaws such as shown in Figure 7.1; consequently, the use of simplified fracture mechanics models is believed to be necessary and reasonable. Other, less conservative fracture mechanics models could be developed in the future, particularly if the flaws within base metal are shown to be the most limiting type of flaw to the integrity of vessels with an embrittled plate material.



**Figure 7.1. A Flaw Detected in Plate Material**

**Flaw Orientation** - Flaws in base metal were assumed to have both axial and circumferential orientations. FAVOR assigns an axial orientation to 50% of the base metal flaws and a circumferential orientation to the remaining 50% of the flaws.

**Truncation of Flaw Distributions** - Inputs for flaw depth dimensions for use with the FAVOR code were truncated to avoid excessive extrapolations of the statistically based depth distributions. The truncations for base metal flaws were such to preclude flaws that were greater than about two times the depth dimensions of any of the flaws observed in PNNL's examinations of base metal. This truncation value has been assigned as 11 mm.

**Service-Related Flaws** - The flaw distribution methodology for base metal flaws addresses only fabrication flaws, with no consideration of service-initiated cracks or service-induced growth of fabrication flaws (by fatigue or stress corrosion cracking). In this regard, all the material examined by PNNL was from vessels that had never been placed into operation. However, inservice inspections of PWR vessels and fracture mechanics calculations of fatigue crack growth provide no reason to believe that crack initiation or growth for flaws in the vessel beltline region are likely.

## 7.2 Inputs from Expert Elicitation

The expert elicitation (Jackson and Abramson 2000) addressed the subject of flaws in base metal regions, including both plate and forging materials. Many of the questions covered qualitative factors such as details regarding processes used to manufacture plates and forgings. Other questions related to mechanisms that are most likely to cause flaws in base metal and the most likely locations of flaws relative to the inner surface of the vessel.

The experts also were requested to make quantitative estimates of flaw occurrence rates. These questions were posed in terms of relative estimates. During the expert elicitation process, PNNL described the examination methods and flaws observed for the PVRUF vessel. It was therefore convenient to make the relative estimates in terms of the PVRUF vessel. Estimates provided by the experts for the numbers and sizes of flaws in plates and forging relative to the flaws observed in the welds of the PVRUF vessel are shown earlier in Figure 4.1. Large base metal flaws were defined as flaws with through-wall depth dimensions greater than a typical bead dimension (6 mm for SAW welds).

The chart of Figure 4.1 indicates the rather large range of individual estimates provided by members of the expert panel. Using standard practices to evaluate the variability in data from the elicitation processes, the data were evaluated in terms of minimum and maximum values, median values, and quartiles (which indicate the range of values that cover estimates from 50% of the experts). Experience has shown that, even with a wide range of estimates from experts on a panel, the median values of estimates tend to provide a reasonable and consistent basis for decision-making.

The flaw distribution model used the median values of relative flaw densities from Figure 4.1. The density of small flaws (<6 mm) in plate material was a factor of 10 less than the flaw density for the PVRUF welds. The density of large flaws (>6 mm) in plate material was a factor of 40 less than the flaw density for the PVRUF welds. These estimates were compared for consistency with the data for plate flaws from the PNNL examinations of plate materials from various vessels.

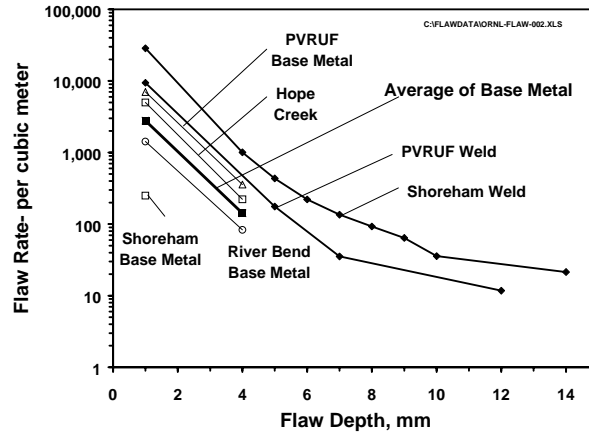
### 7.3 Flaw Data from PNNL Base Metal Examinations

Table 7.1 presents data from PNNL’s examinations of plate materials from the PVRUF, Shoreham, Hope Creek II, and River Bend II vessels. These examinations detected a total of 175 flaws in 0.063 m<sup>3</sup> (2.2 ft<sup>3</sup>) of examined material. Only 9 flaws had through-wall depth dimensions as large as 4 mm. No observed flaws had depth dimensions as large as 6 mm.

<b>Flaw Depth, mm</b>	<b>Shoreham Cum Indication Rate, per m<sup>3</sup></b>	<b>Hope Creek Cum Indication Rate, per m<sup>3</sup></b>	<b>River Bend Cum Indication Rate, per m<sup>3</sup></b>	<b>PVRUF Cum Indication Rate, per m<sup>3</sup></b>	<b>Combined Data Cum Indication Rate, per m<sup>3</sup></b>
1.0	250	5000	1420	7000	2783
4.0	0.0	222	83	357	142
6.0	0.0	0.0	0.0	0.0	0.0
<b>Volume Examined, m<sup>3</sup></b>	0.016	0.009	0.024	0.014	0.063

Figure 7.2 is a plot of the base metal flaw rates as a function of the measured through-wall depth dimensions. Also shown are the flaw rates for welds from the examinations of the PVRUF and Shoreham vessel. The flaw rates for all the plate materials were less than the flaw rates for welds. There was a wide range of flaw rates for the plate materials with a factor of 30 difference between the highest rate (PVRUF plate material) and the lowest rate (Shoreham plate material). The average rate indicated in Figure 7.2 was obtained by combining the data from all four vessels. This rate was a factor of about 5 less than the flaw rate for the PVRUF welds.

The average flaw rate from the plate examinations is generally consistent with the factor of 10 ratio of flaw rates from the median of the estimates from the expert elicitation. It is also noted from Figure 7.2 that the slopes of the curves for plate materials are nearly the same as for the weld metal of the PVRUF and Shoreham vessels. It was therefore concluded that the 10:1 ratio of flaw rates of welds versus plates, as provided by the expert elicitation, is consistent with the limited amount of data. This 10:1 ratio was used to generate flaw distributions for use as inputs to the FAVOR code.



**Figure 7.2. Flaw Frequencies for Plate Materials with Comparisons to Data for Weld Flaws**

There were no observed flaws greater than 6 mm from the PNNL examinations of plate material. Extrapolation of the flaw rate curves of Figure 7.2 would predict that no flaws would be expected from the examination of  $0.063 \text{ m}^3$  of plate material. Therefore, the 40:1 ratio from the expert elicitation for densities of large flaws in welds versus plate material is not inconsistent with the available data. However, the data do not allow a quantitative evaluation of the 40:1 ratio from the expert elicitation.

## 7.4 Flaw Estimation Procedure for Plate Materials

Flaw frequencies for use as inputs to the FAVOR code were generated using simple adjustments to the flaw rates that were estimated on the basis of the data for flaws in the PVRUF vessels. In these calculations, it was assumed that the welds consisted of SAW, SMAW, and repair weld material in the percentages of 93, 5 and 2, respectively. The weld bead dimensions were assigned as 6 mm, 3.5 mm, and 3.5 mm, respectively, for the SAW, SMAW, and repair welds. Flaw densities for small and large flaws were reduced by factors of 10 and 40. Flaw depth distributions were assigned using the same distribution functions developed for the PVRUF vessel welds. A truncation was made for large flaws by assigning a zero flaw rate for all flaws with depth dimensions greater than 11 mm in through-wall depth dimension.

Aspect ratios for base metal flaws were assigned to be the same aspect ratios that were established on the basis of the PVRUF data. The rates for small weld flaws are dominated by the contribution from SAW materials, for which the PVRUF data indicated flaws of relatively small aspect ratios (a distribution with most flaws having aspect ratios of about 1:1). This 1:1 aspect ratio turns out to be generally consistent with the observed aspect ratios for flaws in plate material, as shown by Figure 7.1. In the case of large flaws, the aspect ratio distributions based on the PVRUF data predicted flaws with greater aspect ratios than the 1:1 trend of the small flaw data. The PNNL examinations did not detect any large flaws (>6 mm) in plate material. There is, therefore, no empirical basis to evaluate the extent to which the assignment of aspect ratios >1:1 is conservative for large flaws.

The treatment of uncertainties in flaw distribution inputs to FAVOR for base metal regions is the same as that for the weld regions as established for the PVRUF flaw regions. The development of an uncertainty treatment based on evaluations of data for base metal flaws could be performed in the future. This evaluation is recommended, once examinations of base metal materials and the validations of the observed flaws are sufficient.

## 8 CLAD FLAWS - DATA AND STATISTICAL CORRELATIONS

The flaw distribution model provides three input files for the FAVOR code; one of these files describes surface-breaking flaws—the flaws in the clad metal of the vessel. The treatment of clad flaws is documented in this section, as are the available flaw data and other sources of information that support the model.

### 8.1 Approach and Assumptions

The objective was to estimate the expected number and sizes of fabrication flaws in the beltline cladding of a PWR vessel. Consistent with the assumptions of the FAVOR code, the clad material was assumed to have sufficient toughness to preclude fracture for flaws located entirely within the clad. Attention was therefore directed to (1) surface-breaking flaws that penetrate the full thickness of the clad and extend up to the underlying embrittled weld metal or base metal and (2) large buried flaws in the cladding that extend up to the clad/base metal interface but do not entirely penetrate the thickness of the clad. An example of the second category of clad flaw is shown in Figure 8.1 as seen in a cross section of clad from the PVRUF vessel.

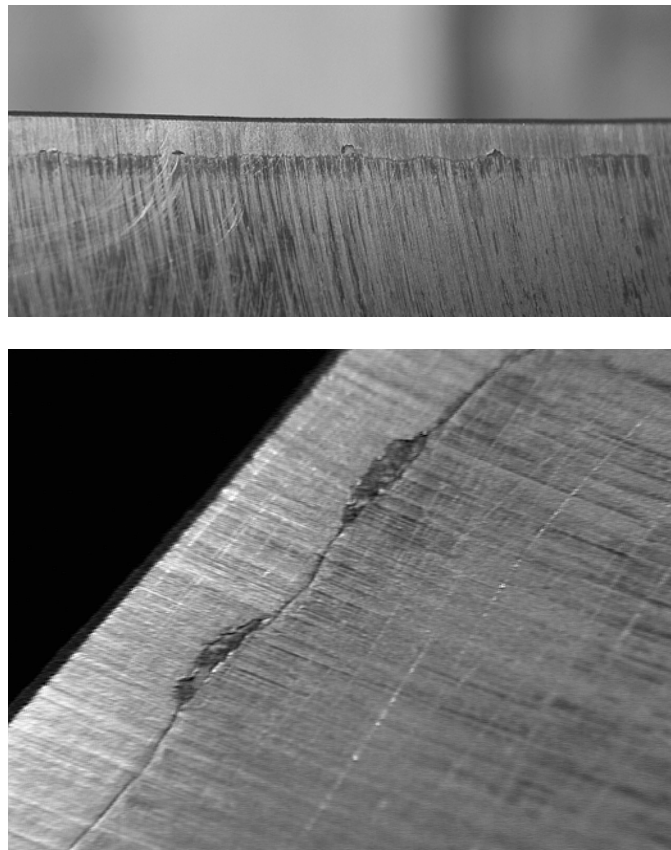


**Figure 8.1. Examples of Flaws in Cladding of PVRUF Vessel**

## 8.2 Sources of Information Cladding Flaws

The estimates for flaws in cladding were based on four sources of information:

1. data on observed flaws from destructive and nondestructive examinations of the PVRUF vessel (Schuster et al. 1998, 1999, 2000a)
2. simulations of clad flaws with the PRODIGAL computer code (Chapman and Simonen 1998)
3. examinations of cladding material performed at Bettis Laboratory (Li and Mabe 1998)
4. an NRC expert judgment elicitation on vessel flaws (Jackson and Abramson 2000).

The measured data and/or estimated occurrence frequencies of clad flaws are summarized in Figure 8.2. The data in Figure 8.2 were normalized to compare information from various sources on a common basis. Flaw depths were expressed as a fraction of the through-wall dimensions of weld beads of the cladding. The numbers of flaws were expressed as flaws per meter of weld bead length. This approach followed the methodology of the PRODIGAL flaw simulation model. Significant variability is seen in the curves of Figure 8.2, which reflects the uncertainties in flaw occurrence rates.

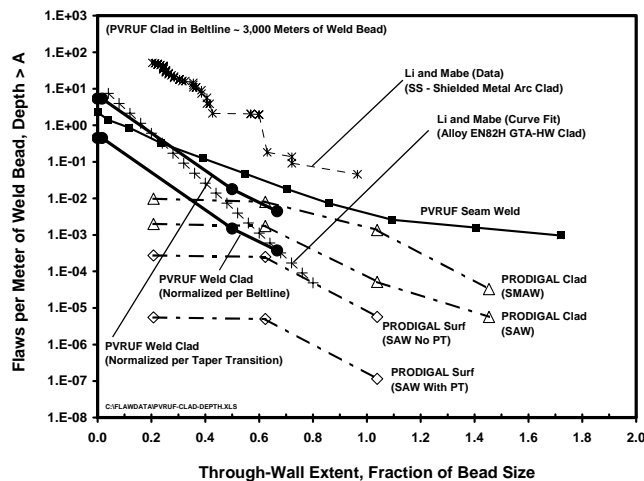


Figure 8.2. Summary of Data on Flaws in Vessel Cladding

### 8.2.1 PVRUF Data

Data in Figure 8.2 for the PVRUF vessel were reported in Schuster et al. (1998). For comparison purposes, flaw data for the seam welds of the PVRUF vessel also are displayed in Figure 8.2. The volume of examined PVRUF clad was 0.027 m<sup>3</sup>. The clad consisted of submerged arc strip clad, manual metal arc clad, and multi-wire clad. Table 8.1 presents the flaw data for the PVRUF clad material. Two PVRUF data points in Figure 8.2 at larger flaw depths corresponded to the two largest flaws observed in the PVRUF clad. The single data point at zero flaw depth represents the large number of small flaw indications that were observed but were too small for accurate size measurements. The PVRUF data included a large number of flaws less than 2 mm in depth, for which it was not possible to measure flaw sizes with any degree of accuracy by nondestructive methods.

<b>Table 8.1. Flaws in Cladding of PVRUF Vessel</b>					
<b>Flaw Depth, mm</b>	<b>Flaw Depth Fraction of Bead</b>	<b>Number of Flaws</b>	<b>Number of Flaws with Depth &gt; a</b>	<b>Number of Flaws Depth &gt; a, per Meter of Examined Weld Bead</b>	<b>Number of Flaws Depth &gt; a, per Meter of Beltline Weld Bead</b>
0.00	0.000	0	1204	5.35	0.447
0.10	0.017	1200	1204	5.35	0.447
3.00	0.500	3	4	0.0177	0.00148
4.00	0.667	1	1	0.0044	0.00037
Data from NUREG/CR-6471 Vol. 3 Clad Thickness = 6 mm Width of Strip Clad Bead = 20 mm			Length of Examined Clad Bead = 222 m Length of Beltline Clad Bead = 2690 m		

Although a large number of flaws were detected in the PVRUF cladding, none of these flaws was of the surface-breaking category. The occurrence frequency of surface-breaking flaws is clearly much lower than the frequency for buried clad flaws. It was not possible, however, to assign an occurrence frequency of zero for surface flaws because of the limited amount of examined vessel cladding.

Two bounding approaches were used to estimate flaw frequencies for the PVRUF cladding, which gave bounding estimates of flaw densities that differed by a factor of about 10. The first approach assumed that all of the clad was deposited by manual metal arc welding. The total length of weld bead was calculated accordingly to establish the lower curve of Figure 8.2. The second approach was based on the observation that the majority of flaws, including all of the flaws having depths greater than 2 mm, were found within a relatively small region where the PVRUF clad was applied by the multi-wire process. This region was at a thickness transition between the component rings of the vessel. Local areas of changing diameter evidently presented difficulties to the automatic welding procedure, which resulted in lack-of-fusion flaws between adjacent weld runs. Such flaws were not observed in cladding deposited over vessel regions of uniform diameter.

### 8.2.2 Data from Bettis Laboratory

Li and Mabe (1998) performed tests on two types of weld-deposited cladding. The examined cladding was not from actual vessels but was fabricated to simulate a range of cladding qualities that might occur in practice. The examinations were performed destructively on relatively small samples of material (9.5 cm<sup>3</sup>). In one case, the cladding was deposited by shielded metal arc welding. This material was intended to represent a bounding case of poor quality cladding, with steps being taken (e.g., no special grinding at the locations of weld stop/starts) to increase the potential for flaws. In the other case, the cladding was deposited by a gas tungsten arc process (GTA-HW) that was intended to decrease the potential for flaws.

Figure 8.2 shows data points and data correlations from the Li and Mabe work. Very few flaws were found in the higher quality GTA-HW welds. The curve for this clad material as shown in Figure 8.2 was a correlation based on the data for the very small flaws that were detected. An extrapolation of this curve falls between the two curves for the PVRUF cladding. In contrast, the data gave a flaw occurrence rate for the shielded metal arc cladding that was more than a factor of 10 above the observed flaw rate in the PVRUF cladding.

### 8.2.3 Expert Judgment Elicitation

As part of the NRC expert judgment elicitation (Jackson and Abramson 2000), the members of the expert panel were asked to estimate the number and sizes of flaws in cladding relative to the flaws in the main seam welds of a vessel. Although the experts provided a wide range of estimates, a significant subset of the experts provided estimates in a mid range between the extreme values. The data were treated in a statistical manner to establish median values, which served as the basis for establishing best-estimate distributions of flaw occurrence rates. The scatter in the data provided an indication of the uncertainty in the estimates. The rationale for the best-estimate values as expressed by the experts were as follows:

1. Cladding should have fewer flaws than the corresponding amount of seam weld material by a factor of about 2. The experts explained that welding of cladding to a vessel surface is performed under relatively favorable conditions of good access, compared to the more difficult access for the narrow gaps of the weld geometries for seam welds.
2. The cladding should have essentially no flaws greater than the dimension of a single weld bead. Therefore, the decrease in slope of the flaw depth distribution curve for the seam welds (as seen in Figure 8.2) should be absent for clad flaws.

Although Figure 8.2 does not present a specific curve from the expert judgment process, such a curve could be constructed by adjusting the curve labeled “PVRUF seam weld.” This curve would be a straight line with a constant slope, equal to the slope of the seam weld curve for the flaw depths ranging from 0 to 0.5 of the weld bead size. In addition, the curve for clad flaws would be shifted downward by a factor of 2 relative to the PVRUF curve for seam welds. A curve from the expert judgment process would fall between of the two bounding curves of Figure 8.2 based on the PVRUF data for clad flaws.

### 8.2.4 PRODIGAL Predictions

Calculations were performed with the PRODIGAL code (Chapman and Simonen 1998) to estimate flaw sizes and densities for cladding material. The model of this code includes predictions that specifically address flaws in cladding. The development of a clad model was a significant part of building the PRODIGAL code (Chapman and Simonen 1998). Parameters used to quantify the frequencies for flaws in cladding were established through detailed discussions with a panel of U.S. experts on welding and vessel fabrication.

#### 8.2.4.1 Scope of Calculations

The PRODIGAL calculations reported here addressed both manual metal arc cladding and submerged arc (strip) cladding. Table 8.2 lists parameters for the PWR vessel addressed by the PRODIGAL calculations. Calculations were first performed by assuming no dye penetrant examination of the clad surface and then by simulating a dye penetrant examination (assuming repairs of the detected surface-breaking defects).

All calculations assumed a total clad thickness of 11 mm, consisting of two weld layers. The modeled region of the clad surface was assumed to be 52 mm wide. This region of clad included 7 weld beads for each weld layer. For the manual metal arc weld, there were 26 start/stops during the cladding of the modeled region that had a width of 52 mm and length of 1 m (surface area of 0.05208 m<sup>2</sup>), giving a total weld bead length of 14 m.

<b>Parameter</b>	<b>Value</b>
Vessel Inner Diameter	4.4 m
Beltline Height	4.4 m
Number of Axial Welds in Beltline	3
Number of Circumferential Welds in Beltline	1
Width of Weld at Vessel Inner Surface	5 cm
Total Beltline Surface Area	60.8 m <sup>2</sup>
Length of Circumferential Welds in Beltline	13.8 m
Surface Area of Circumferential Welds in Beltline	0.69 m <sup>2</sup>
Length of Axial Welds in Beltline	13.2 m
Surface Area of Axial Welds in Beltline	0.66 m <sup>2</sup>
Total Clad Thickness	11 mm
Number of Clad Layers	2
Number of Runs per Layer Over Weld	7
Number of Clad Start/Stops per Meter of Weld (manual clad)	26

The number and sizes of weld beads for the PRODIGAL calculations were based on dimensions as observed on cross-sectioned welds from the PVRUF vessel. The exact configuration of weld beads is not critical to the present evaluations because the results were normalized such that flaw depths were expressed as fractions of the weld bead thickness. Flaw frequencies were expressed in terms of flaws per unit length of weld bead. This allowed combinations of clad thickness and weld bead dimensions as they exist in other vessels to be addressed.

#### **8.2.4.2 Results for PRODIGAL Runs**

Results from the PRODIGAL calculations for the selected region of cladding are given in Tables 8.3 and 8.4. These calculations addressed both submerged arc and manual metal arc clad along with the benefits of dye penetrant (PT) examinations of the clad inner surface. The PT examinations were predicted to reduce the number of surface-breaking flaws by a factor approaching 100. The predicted densities of buried flaws were much higher than the densities for surface-breaking flaws (Table 8.3 versus Table 8.4), which is consistent with the data from examinations of clad in the PVRUF vessel.

<b>N</b>	<b>Flaw Depth, mm</b>	<b>Depth, Fraction of Bead</b>	<b>No PT Inner Surface, Flaws per Meter of Bead Depth &gt; a</b>	<b>With PT Inner Surface, Flaws per Meter of Bead with Depth &gt; a</b>
1	1.1	0.208	2.743E-04	5.486E-06
2	3.4	0.623	2.486E-04	4.971E-06
3	5.7	1.038	5.714E-06	1.143E-07
4	8.0	1.453	0.000E+00	0.000E+00
5	10.3	1.869	0.000E+00	0.000E+00
6	12.6	2.284	0.000E+00	0.000E+00
7	14.8	2.699	0.000E+00	0.000E+00
8	17.1	3.114	0.000E+00	0.000E+00
9	19.4	3.530	0.000E+00	0.000E+00
10	21.7	3.945	0.000E+00	0.000E+00

<b>N</b>	<b>Depth, mm</b>	<b>Depth, Fraction of Bead</b>	<b>Submerged Arc Buried Flaw, Flaws per Meter of Bead Depth &gt; a</b>	<b>Shielded Metal Arc Buried Flaw, Flaws per Meter of Bead with Depth &gt; a</b>
1	1.1	0.208	1.999E-03	9.736E-03
2	3.4	0.623	1.760E-03	8.074E-03
3	5.7	1.038	5.143E-05	1.369E-03
4	8.0	1.453	5.714E-06	3.286E-05
5	10.3	1.869	0.000E+00	0.000E+00
6	12.6	2.284	0.000E+00	0.000E+00
7	14.8	2.699	0.000E+00	0.000E+00
8	17.1	3.114	0.000E+00	0.000E+00
9	19.4	3.530	0.000E+00	0.000E+00
10	21.7	3.945	0.000E+00	0.000E+00

### 8.2.4.3 Comparison of Observed Flaw Data with PRODIGAL Predictions

Figure 8.2 shows comparisons of flaw frequencies as predicted by PRODIGAL with data from experimental studies. All comparisons were made on the basis of flaw depths expressed as a fraction of the weld bead thickness. Flaw occurrence rates were expressed in terms of flaws per linear meter of weld bead. For flaw depths greater than about half a weld bead thickness, the data are seen to generally agree with the PRODIGAL predictions. It was not appropriate to make comparisons for flaws having depths less than about half a weld bead because the PRODIGAL methodology was not intended to address these very small flaws. Figure 8.2 shows (for flaw depths greater than about 50% of the clad thickness) that PRODIGAL predicts flaw frequencies that are consistent with the range based on the PVRUF data.

### 8.2.5 Vessel-Specific Considerations

The data in Figure 8.2 indicate considerable variability and uncertainty associated with estimates of cladding flaws. Some of the variability is due to effects of the different processes used to apply clad to vessel surfaces. Because cladding is considered in design to make no contribution to vessel integrity, more variations in the quality of clad welding may occur than for other welds.

The data from the PVRUF vessel show significant variability in clad quality, even within a given vessel. The PRODIGAL model (based on an elicitation of welding experts) indicates that machine-welded strip clad should have fewer welding defects than manual cladding. It has been observed that one region of the PVRUF vessel (thickness transition) had an unusually large number of flaws. The greater number of flaws in this region is not considered to be particularly significant because the embrittled region of the PVRUF vessel beltline would be outside the thickness transition region.

An important consideration is that of flaw orientation. For machine-deposited strip clad, the significant flaws (as evidenced by the PVRUF data) are circumferential in orientation. Such flaws should have a minimal impact on the integrity of axial welds (and also the plate regions) of a vessel. Manual cladding applied to circumferential welds also will have circumferential flaws as the expected orientation.

Manually applied cladding can have a large number of small axial flaws associated with start/stops of the stick-welding process, while machine-deposited cladding is likely to produce fewer flaws because such cladding usually consists of only one weld layer. On the other hand, there is a much greater likelihood of through-clad flaws for single-layer clad than for clad with two or more layers. Manual cladding inevitably has more than one layer, which reduces the likelihood of through-clad flaws in manual clad. However, as indicated by the PVRUF data, manual clad often had a greater thickness than the machine cladding. As such, a through-clad flaw in the manual clad would have a greater impact on structural integrity than a through-clad flaw in a single-layer machine-deposited clad.

### 8.3 Flaw Length Distribution for Clad Flaws

It was initially assumed that all clad flaws had large aspect ratios (infinity) because observed clad flaws tended to be relatively long. Later work<sup>1</sup> compiled data on more exact measurements for the lengths of clad flaws because the FAVOR code can address surface flaws with aspect ratios other than infinity (i.e., discrete aspect ratios of 2, 6, 10, and infinity).

Tables 8.5 through 8.11 were reproduced from Schuster<sup>a</sup> to document the data on measured lengths of clad flaws for the PVRUF and Hope Creek Unit II vessels. Most of the inspected cladding was deposited as strip clad to the PVRUF vessel in a single pass using a welding machine giving a thickness of 3/16 in. Manual cladding was deposited over circumferential welds, over areas that were difficult to weld with the cladding machine, and for repairs to the clad surface.

Table 8.5 lists the amount of clad and product forms, along with a summary of the early unvalidated inspection results for the PVRUF vessel (Schuster et al. 1998). Table 8.6 gives dimensions of 10 of the larger PVRUF cladding flaws reported in Appendix A of Schuster et al. (1998). Table 8.7 gives the validated dimensions of one of the flaws as obtained by sectioning of the vessel material. Table 8.8 describes the cladding examined for the Hope Creek Unit II vessel. In this case the clad was deposited as 1-in. strips by a multi-wire process. The measured lengths of the Hope Creek II flaws are given in Table 8.9. Other measurements of clad flaws for the PVRUF vessel are indicated by Tables 8.10 and 8.11.

The data from the PVRUF and Hope Creek II vessels were combined into one dataset to establish a statistical distribution of flaw lengths (Table 8.12). These evaluations did not include any uncertainty analyses. It was recognized that the examined material was from a small sample of cladding from only two vessels. The flaws selected for size measurements were clad flaws with larger flaw depth dimensions. No attempt was made to normalize the flaw length dimensions to the thicknesses of the clad layers or to develop separate distributions for the PVRUF and Hope Creek II vessels.

Figure 8.3 is a plot of the length data of Table 8.12 along with exponential fitting of the data. There were two separate trends in the data. One trend applied to flaws with lengths less than about 20 mm, and another trend applied to flaws with greater lengths. There was no apparent trend to suggest a separation of the PVRUF data from the Hope Creek II data. Figure 8.3 shows two data fits (smaller than 30 mm and greater than 30 mm). The smallest flaw length was 4 mm.

---

<sup>1</sup> Schuster GJ. 2001. *Length of Flaws in Cladding with Recommendations for Treatment of Aspect Ratio*, Letter Report prepared by Pacific Northwest National Laboratory, Richland, Washington, for U.S. Nuclear Regulatory Commission, JCN W6275, August 6, 2001.

<b>Product Form</b>	<b>Bead Size, mm</b>	<b>No. of Clad Passes</b>	<b>Volume, m<sup>3</sup></b>	<b>Area, m<sup>2</sup></b>	<b>No. of Small Flaws</b>	<b>No. of Large Flaws</b>
4 in. Strip Clad	6	1	0.016	2.6	180	0
Manual Clad	4	2	0.012	1.4	80	0
1 in. Strip Clad	6	1	0.0028	0.46	700	0

<b>Name</b>	<b>Product</b>	<b>Depth, mm</b>	<b>Length, mm</b>	<b>Width, mm</b>
P1	SMAW	<1.5	14	-
P2	Strip, 4 in.	<1.5	-	7
P3	SMAW	<1.5	8	-
P4	SMAW	<1.5	-	16
V1	Strip, 4 in.	3	12	10
V2	SMAW	3	11	12
V3	SMAW	2	6	18
V4	Strip, 1 in.	2	16	8
V5	SMAW	<1.5	12	11
V6	Strip, 1 in.	<1.5	20	-

<b>Name</b>	<b>Product</b>	<b>Depth, mm</b>	<b>Length, mm</b>	<b>Width, mm</b>
4-5DBAC-Z5	Strip, 1 in.	4	80	10

<b>Area of Clad, cm<sup>2</sup></b>	<b>Length of Clad Pass, cm</b>
412	162

<b>Indication</b>	<b>Length (mm)</b>
1	7
2	6
3	9
4	17
5	12
6	18
7	6
8	8
9	9
10	14
11	11
12	18
13	5
14	6
15	97
16	19

<b>Table 8.9 (contd)</b>	
<b>Indication</b>	<b>Length (mm)</b>
17	13
18	18
19	48
20	4
21	7
22	12
23	16
24	7
25	6
26	103
27	11
28	31

<b>Table 8.10. Amount of 4-in. Strip Clad in Specimen 5-10D</b>	
<b>Area of Clad, cm<sup>2</sup></b>	<b>Length of Clad Pass, cm</b>
206	20

<b>Table 8.11. Length of Flaws in Cladding for Specimen 5-10D</b>	
<b>Indication</b>	<b>Length, mm</b>
1	15
2	6
3	9
4	53
5	7
6	11
7	9
8	7
9	11
10	6
11	9
12	13

<b>Table 8.12. Data Used to Develop Length Distribution for Clad Flaws</b>	
<b>Source Table</b>	<b>Length, mm</b>
2	14.0
2	8.0
2	12.0
2	11.0
2	6.0
2	16.0
2	12.0
2	20.0
3	80.0
5	7.0
5	6.0
5	9.0
5	17.0
5	12.0
5	18.0
5	6.0
5	8.0
5	9.0
5	14.0
5	11.0
5	18.0
5	5.0
5	6.0
5	97.0
5	19.0
5	13.0
5	18.0
5	48.0
5	4.0
5	7.0
5	12.0
5	16.0
5	7.0
5	6.0
5	103.0
5	11.0
5	31.0
7	15.0
7	6.0
7	9.0
7	53.0
7	7.0
7	11.0
7	9.0
7	7.0
7	11.0
7	6.0
7	9.0
7	13.0

The two exponential functions forms indicated on Figure 8.3 are

$$P(>L) = 1.876e^{-0.1225L}$$

$$P(>L) = 0.2676e^{-0.0215L}$$
(8.1)

where  $P(>L)$  is the probability that the flaw length is greater than the length  $L$ , with  $P(>L)$  calculated from Equation (8.1) that gives the larger conditional probability. If the calculated value of  $P(>L)$  is greater than 1.0, then  $P(>L)$  is set equal to 1.0.

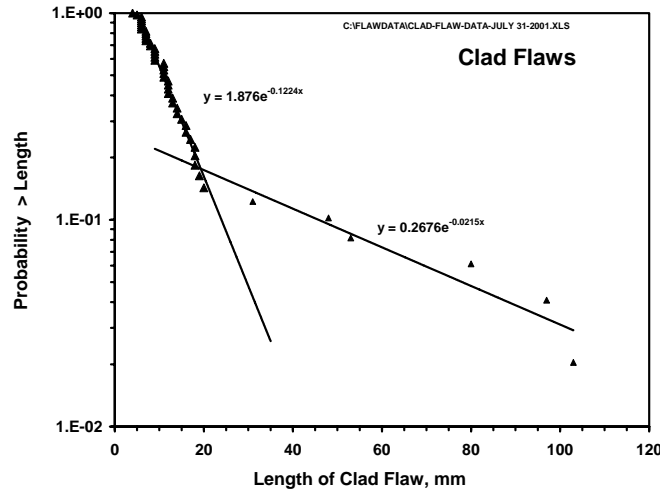


**Figure 8.3. Lengths of Clad Flaws in PVRUF and Hope Creek II Vessels**

The flaw distribution algorithm for the FAVOR code generates a distribution of flaw aspect ratios rather than a distribution of flaw lengths. Flaw depths for the clad/surface flaws were set equal to the clad thickness in accordance with the through-clad surface flaw assumption of the FAVOR code. The FAVOR code required a distribution of aspect ratios binned into discrete categories of four ratios of 2:1, 6:1, 10:1, and infinity. These aspect ratio bins are assigned the portions of the probability distributions corresponding to the aspect ratio ranges of 1 to 3, 3 to 8, 8 to 12, and 12 to 1000.

## 8.4 Flaw Inputs to Fracture Mechanics

An estimate of the number and sizes of surface-breaking and buried flaws in cladding was developed for use in the fracture mechanics calculations as described below. Figure 8.4 shows a plot of these distributions along with the data of Figure 8.2 used to support the estimates.

The number of buried flaws per meter of weld bead is given by the exponential distribution function (corresponding to a straight line on the semi log scale of Figure 8.2) as follows

$$N_{\text{BURIED}}(>a) = 1.0 \times \exp(-5.0 \times a)$$
(8.2)

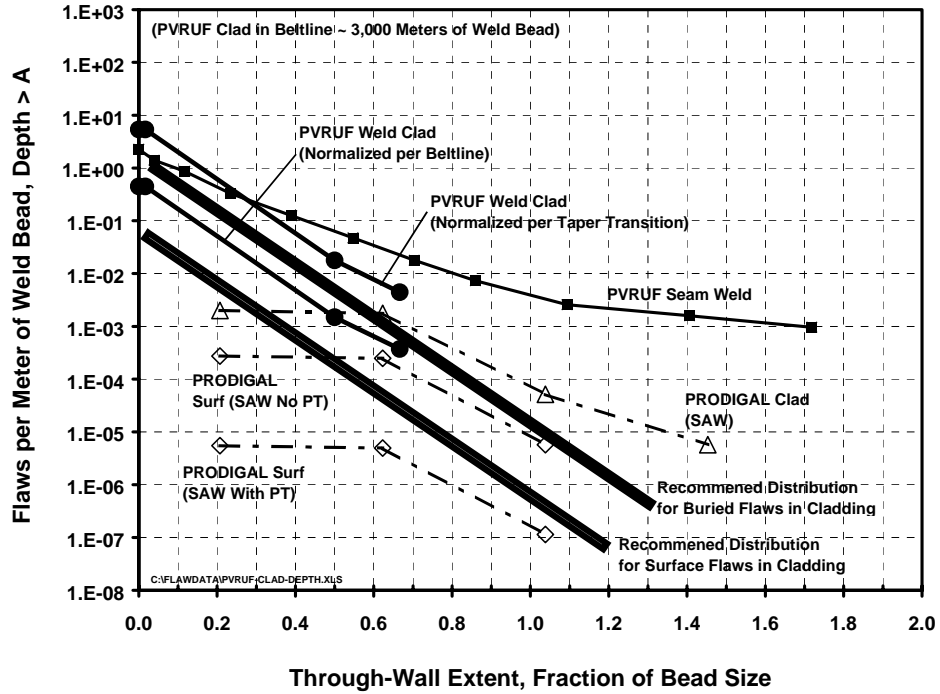


**Figure 8.4. Proposed Curves for Estimating Number and Sizes of Flaws in Vessel Cladding**

where

$$N_{\text{BURIED}}(>a) = \text{number of buried flaws per meter of weld bead with depth greater than } a$$

$$a = \text{depth of buried flaw as fraction of weld bead thickness}$$

The best estimate of the number of surface flaws per meter of weld bead is given by

$$N_{\text{SURFACE}}(>a) = 0.1 \times \exp(-5.0 \times a) \tag{8.3}$$

$$N_{\text{SURFACE}}(>a) = \text{number of surface flaws per meter of weld bead with depth greater than } a$$

$$a = \text{depth of surface flaw as fraction of weld bead thickness}$$

Equation (8.2) for buried flaws (as plotted in Figure 8.4) is intended to describe submerged arc cladding. The slope of the curve is based on the PVRUF data for clad flaws, which is consistent with the slope of the curve from the PRODIGAL calculations. The selected intercept falls between the two normalizations of the PVRUF data. This intercept provides a good correlation with the PRODIGAL predictions for flaw depths greater than 50% of the clad thickness.

The curve for surface flaws was assumed to be a factor of 10 below the corresponding curve for buried flaws. This estimate of surface flaw density may be conservative by perhaps an order of magnitude. Because no surface-breaking flaws were observed in the PVRUF examinations, the approach was to recommend conservative inputs for fracture mechanics calculations. Refined inputs can be developed

later if surface-breaking flaws were found to make significant contributions to calculated vessel failure probabilities.

The treatment and implementation of clad flaws for the generation of flaw input files for the FAVOR code has been based on the following considerations:

1. The recommended orientation of the flaws is circumferential to be consistent with the flaws observed in the PVRUF and other vessels; the circumferential orientation is consistent with information from the expert elicitation and with the treatment of clad flaws in the PRODIGAL model.
2. The number of surface-breaking flaws accounts for (1) flaws that are truly surface-breaking and extending into the base metal of the vessel and (2) a small fraction of buried clad flaws at the clad-to-base metal interface that have sufficiently large through-wall dimensions to contribute to vessel failure. The fraction of flaws of Type 2 has been estimated using probabilistic fracture mechanics calculations.
3. The flaw input files for surface flaws as generated by the PNNL algorithm do not account for statistical uncertainty; the flaw input file has 1000 datasets that are identical to maintain a format for the input file to allow for future work to include a treatment of statistical uncertainties.
4. The flaw density for buried clad flaws has been assigned to be one flaw per meter of clad weld bead.
5. The PNNL flaw distribution algorithm includes inputs for the number of clad layers, the thickness of each clad layer and the width of the clad weld bead; this permits calculations of the total length of weld bead per unit area of vessel surface and thereby the number of clad flaws per unit area.
6. Based on probabilistic fracture mechanics calculations (described below), the density for buried surface flaws is reduced by a factor of  $1.0E-3$  for a single-layer clad and a factor of  $1.0E-6$  for clad consisting of two or more layers.
7. Flaws from the input file are treated by FAVOR as surface-breaking flaws with a depth equal to the clad thickness; the flaws are assigned to the particular depth bin (percentage of vessel wall thickness in steps of 1% of the wall thickness) that includes the clad-to-base metal interface; the FAVOR code assigns a flaw depth equal to the coordinate of the outer extent of the depth bin.
8. The PNNL flaw distribution algorithm assigns a distribution of flaw aspect ratios as described by the discussion of flaw aspect ratios as given above.
9. The PNNL flaw distribution algorithm first generates the flaw data in terms of flaws per unit area of vessel surface; these data can then if requested be expressed in terms of flaws per unit volume following the definitions used in the FAVOR fracture mechanics model by dividing the number of flaws per unit area by the vessel wall thickness.

## **8.5 Probabilistic Fracture Mechanics Calculations**

Probabilistic fracture mechanics calculations were performed with the VISA-II computer code (Simonen et al. 1986) to study the implications to vessel integrity of the distributions in Figure 8.4. These calculations had several objectives:

1. Evaluate the potential contributions of clad flaws to vessel failure probabilities relative to the contributions from flaws in the underlying seam welds and base metal of the vessel wall.
2. Evaluate the relative importance of clad flaws buried in the cladding versus surface-breaking flaws in the cladding.
3. Establish the relative importance of clad flaws at seam welds compared to flaws in the clad applied over plate regions of a vessel.
4. Establish priorities for collecting data needed to make refined estimates of clad flaws. The methodology and results of the calculations are presented below. More details can be found in Simonen et al. (2001).

### **8.5.1 Fracture Mechanics Methodology**

The primary objective of the probabilistic fracture mechanics calculations was to perform sensitivity calculations to estimate the relative contributions to failure probabilities from the different categories of flaws and the different material regions of the vessel:

1. buried clad flaws located such that the outer flaw tip was at the clad/base metal interface with the through-wall dimension of this flaw sampled from the distribution of flaw depths in Figure 8.4
2. surface flaws that penetrate the full thickness of the clad such that the crack tip is at the clad/base metal interface
3. buried flaws randomly located within the thickness of the seam welds (or plate material) with the flaw depths simulated from the curve in Figure 8.2 for “PVRUF seam weld.”

Consistent with the FAVOR code (Dickson and Simonen 1997), the present calculations assumed that vessel failure does not occur if a clad flaw has both flaw tips entirely within clad material. This assumption is consistent with the high toughness of cladding materials relative to the embrittled ferritic steels.

Computer calculations were performed for a single flaw with these failure probabilities adjusted outside the VISA-II code to account for the actual number of flaws in the material regions of interest. Four levels of neutron fluence ( $2.0 \times 10^{19}$ ,  $1.0 \times 10^{19}$ ,  $0.5 \times 10^{19}$ , and  $0.25 \times 10^{19}$  neutrons/cm<sup>2</sup>) were evaluated to cover a range of vessel embrittlement.

The current calculations used the exponential thermal transient with a constant pressure of 1000 psi that was used in the 1993 benchmarking study. The copper and nickel compositions were 0.30 and 0.75 wt%, respectively, with an initial value of  $RT_{NDT}$  of 20°F.

The probabilistic fracture mechanics model of the existing VISA-II code could not address the case of a buried flaw in the cladding. An enhancement of the code capabilities was therefore required. The revised model followed the approach described by Simonen and Johnson (1993) to treat a buried flaw that has its inner tip located very close to the inner surface of the vessel. The trend is that large buried clad flaws can have stress intensity factors that approach those for surface-breaking flaws.

Additional inputs and assumptions used for the calculations were as follows:

1. Flaw lengths were assumed to be long (two-dimensional solutions for stress intensity factors).
2. The stress-free temperature for the cladding was consistent with recent ORNL publications (468°F).
3. All buried flaws in the cladding had their outer crack tip at the clad to base metal interface, which gave a flaw configuration that could initiate vessel fracture in accordance with the toughness for the embrittled material of the vessel wall.
4. All flaws in the cladding were assumed to have a circumferential orientation.
5. There were no fabrication flaws in the ferritic steel that linked with the clad flaws, based on the fact that dye penetrant and/or magnetic particle examinations of the base metal are performed prior to cladding of the vessel surface to ensure a relatively flaw-free surface.
6. Flaws in seam welds and base metal were at random locations through the thickness of the vessel; inner tips of these flaws could, in the limit, randomly occur at the clad-base metal interface but never extend into the clad.
7. The failures caused by embrittled plate material were governed by flaws along the fusion lines along axial welds, with contributions of flaws within the volume of the plate material being neglected.

### **8.5.2 Description of Reference Vessel**

All calculations were for the vessel dimensions used for the joint NRC/industry calculations that benchmarked probabilistic fracture mechanics codes (Bishop 1993), as indicated in Table 8.1. The inner diameter and wall thickness (180.0 and 9.0 in., respectively) were typical for a PWR vessel. The height of the irradiated/embrittled beltline region was assumed to be nominally equal to the vessel inner diameter (4.4 m). Where additional details were needed to define clad inputs, the current evaluations based these inputs on available information from the PVRUF vessel.

The number and sizes of clad flaws were estimated for the beltline region of the selected vessel. The surface area of the weld metal at the inner surface of the vessel and subsequently clad was estimated from cross sections of welds shown in Chapman and Simonen (1998). The evaluations addressed failures of both axial welds and of base metal regions. These parts of the vessel surface were assumed to be clad by submerged arc welding using a strip clad process. Circumferential welds were assumed to be clad with a manual metal arc process. The fracture mechanics calculations, however, indicated that circumferential welds contribute little to vessel failure probabilities.

### **8.5.3 Results of Probabilistic Fracture Mechanics Calculations**

Figures 8.5 and 8.6 are plots of the calculated probabilities as a function of the fluence at the inner surface of the vessel. The initiation of flaw growth from clad flaws for embrittled seam welds (Figure 8.5) and plate materials (Figure 8.6) are addressed. In all cases, the crack initiation is due to a circumferential crack, consistent with the orientation of the clad flaw. Figure 8.5 shows that clad flaws make only small

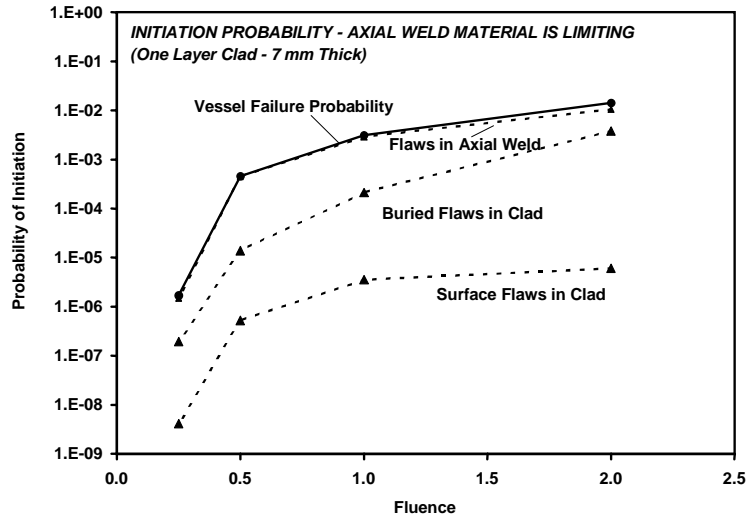


Figure 8.5. Probability of Flaw Initiation in Vessel with Axial Welds as Limiting Material

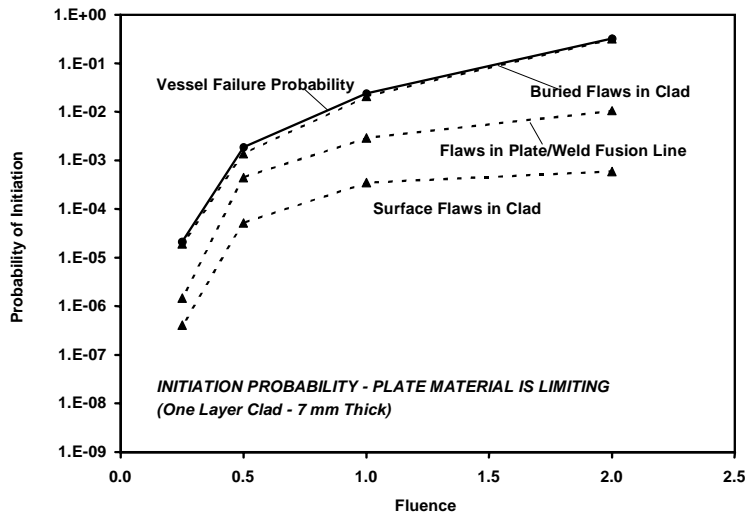


Figure 8.6. Probability of Flaw Initiation in Vessel with Plates as Limiting Material

contributions to crack initiation in axial welds themselves compared to the contribution of the flaws in the seam welds themselves. Surface-breaking flaws make only a negligible contribution (less than 0.1% of the total) and buried flaws contribute about 10% of the total failure probability for seam welds.

In contrast, Figure 8.6 shows that clad flaws make a dominant contribution to crack initiation for vessels that have plate material as the limiting material. Surface flaws again make negligible contributions. Buried flaws in the clad make a larger contribution (by a factor of 10 or more) to vessel failure probability than flaws in the plate material itself.

These calculations for through-wall crack probabilities were performed as a sensitivity study. There appears to be a basis for neglecting clad flaws if the material of the axial or circumferential welds governs

vessel embrittlement. The clad for circumferential welds of a typical vessel is a multi-layer manual weld type for which the calculations show only small contributions of clad flaws to vessel failure. The current study, therefore, focused on axial welds and base metal regions. In the case of axial welds, the fracture mechanics calculations (Figure 8.5) also show small contributions of clad flaws relative to flaws in the seam welds. Plate materials appear to be the main concern.

#### **8.5.4 Concluding Discussion**

In summary, probabilistic fracture mechanics calculations using the VISA-II computer code were performed to explore the implications of the estimated number and sizes of clad flaws. The calculations have indicated that clad flaws contribute only negligibly to the failure of embrittled axial and circumferential welds in vessels. In contrast, flaws in cladding over embrittled plate material have the potential to be significant contributors to vessel failure. The significance of cladding flaws to the failure of vessels with embrittled plate regions may require further evaluation if vessel-specific calculations with the FAVOR code show significant contributions of such flaws to calculated failure probabilities. Conservative assumptions were made in the probabilistic fracture mechanics calculations. These calculations assumed that cladding flaws are preferentially located at the clad-base metal interface, and that these flaws are crack-like in nature with one crack tip positioned to grow the crack into the embrittled plate material. Although examinations of the PVRUF vessel showed flaws located at the clad-base metal interface, the morphology of these flaws (e.g., entrapped slag) had many characteristics of volumetric rather than crack-like flaws (i.e., blunted crack tips). A further assumption was that the local properties of the ferritic material at the interface are the same as the bulk properties of the embrittled plate material. In practice, the material at the interface is part of a weld fusion zone, which means that the material will have a local chemical composition and microstructure that would give a higher level of fracture toughness than that for the embrittled properties of the bulk of the plate material.

## 9 ALGORITHM TO GENERATE FLAW INPUT FILES FOR FAVOR

This section describes how PNNL applied the available data on fabrication flaws in combination with insights from the expert elicitation and PRODIGAL flow simulation model to develop an algorithm that generates computer files to serve as inputs to the ORNL-developed FAVOR code. Important details of the FAVOR code are described in Section 9.1; particular attention is given to the treatment of fabrication flaws. Details of the PNNL-developed algorithm (FORTRAN code) are presented in Section 9.2. Sample input and output files from the algorithm are provided in Section 9.3. Implementation of weld region and flaw type statistical correlations into the flaw distribution algorithm is described in Sections 9.4 through 9.6.

### 9.1 FAVOR Code Structure and Organization

As shown by Figure 9.1, FAVOR has three computational modules: (1) a deterministic load generator (FAVLoad), (2) a Monte Carlo probabilistic fracture mechanics (PFM) module (FAVPFM), and (3) a post-processor (FAVPost). Figure 9.1 also indicates the nature of the data streams that flow through these modules. This report concerns the probabilistic fracture mechanics module (FAVPFM) and the element of Figure 9.1 labeled *Flaw data*. The primary outputs of the module are shown in Figure 9.1 as conditional probabilities of fraction initiation (CPI) and of vessel failure (CPF) defined as a through-wall crack. The FAVPFM module is described below, based on documentation of the FAVOR code made available by ORNL. The other two modules of the FAVOR code are described only briefly.

#### 9.1.1 FAVLoad Module

The module FAVLoad uses inputs as generated by thermal-hydraulic calculations for the reactor coolant temperatures and pressures at the vessel inner wall. Based on vessel dimensions and material properties, FAVLoad calculates temperatures and stresses within the vessel wall, which, in turn are used to calculate crack tip stress intensity factors. These results become inputs to the probabilistic fracture mechanics calculations performed by the FAVPFM module.

The flaw categories of the FAVLoad module relate to the flaw input files. All flaws can be oriented in either the axial or circumferential direction. As indicated by Figure 9.2, FAVOR addresses three flaw categories:

- Category 1 – surface-breaking flaws:
  - infinite length – aspect ratio  $L/a = 4$
  - semi-elliptic – aspect ratio  $L/a = 2$
  - semi-elliptic – aspect ratio  $L/a = 6$
  - semi-elliptic – aspect ratio  $L/a = 10$
- Category 2 – embedded flaws – fully-elliptic geometry with inner crack tip located between the clad/base interface and  $1/8 t$  from the inner surface ( $t =$  thickness of the RPV wall)
- Category 3 – embedded flaws – fully-elliptic geometry with inner crack tip located between  $1/8 t$  and  $3/8 t$  from the inner surface.

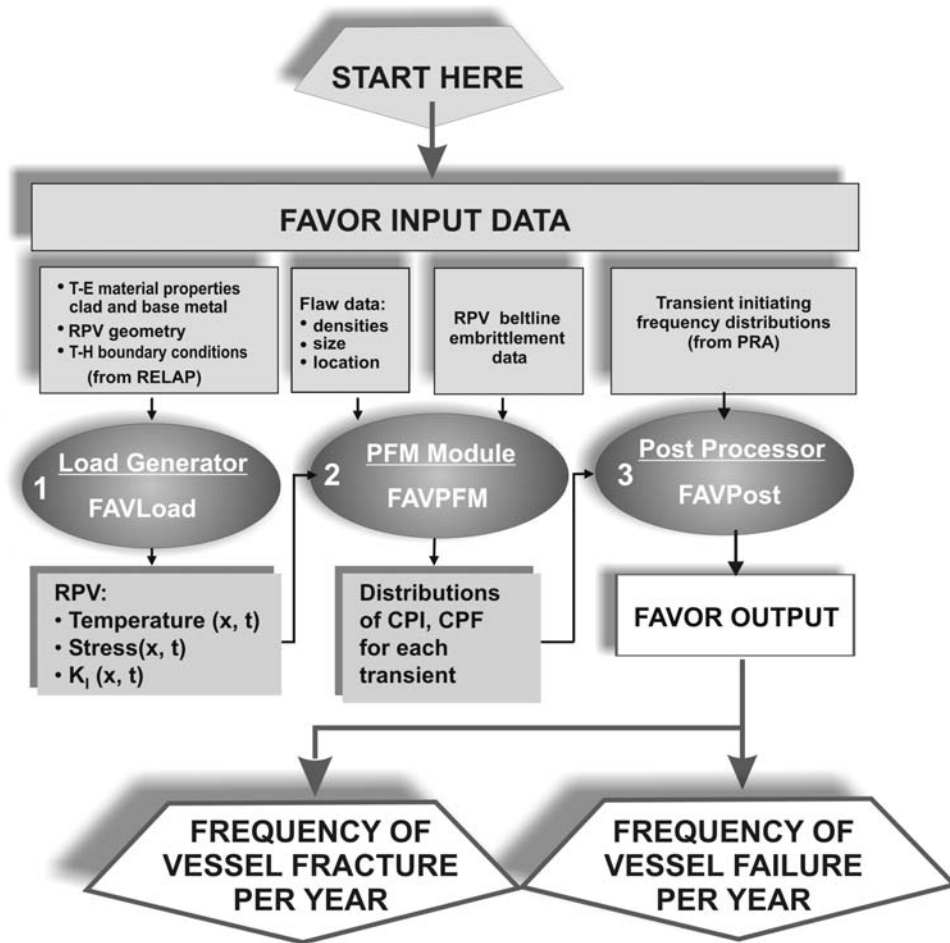


Figure 9.1. Data Streams for FAVOR Code Modules (1) FAVLoad, (2) FAVPFM, and (3) FAVPost

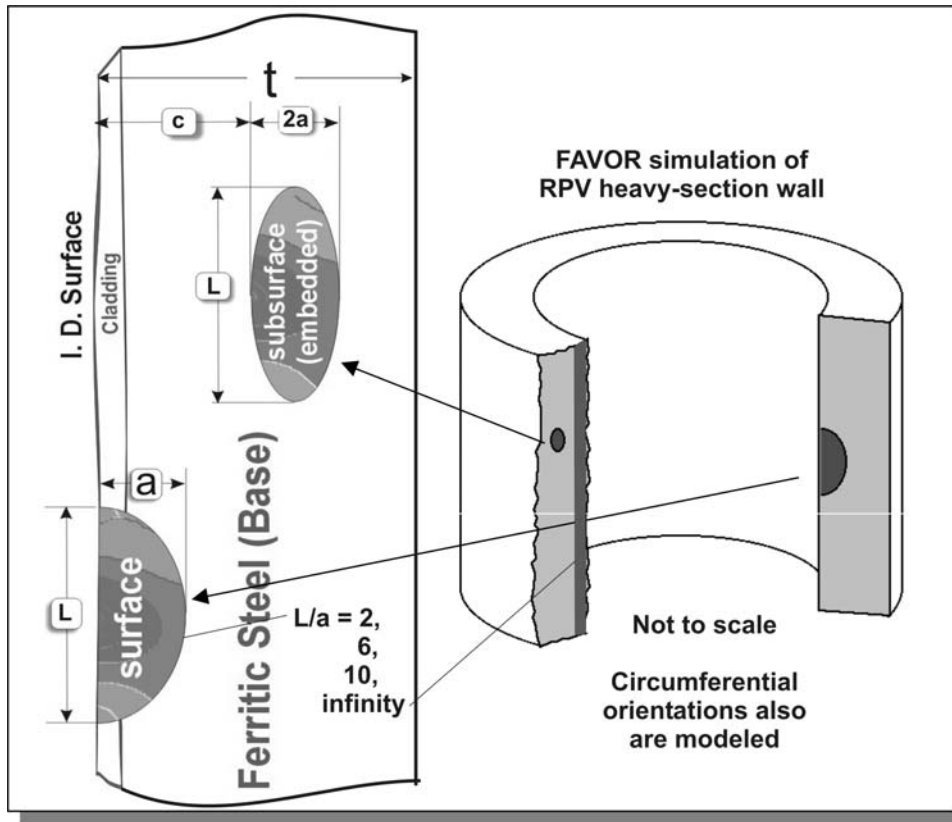


Figure 9.2. Flaw Models in the FAVOR Code

### 9.1.2 FAVPFM Module

The FAVOR code models the beltline of an RPV that is fabricated using either forged-ring segments or rolled plate segments, as shown by Figure 9.3. The vessel wall is lined with an internal cladding of austenitic stainless steel. Vessels made with forgings have only circumferential welds, while plate-type vessels have both circumferential and axial welds. Beltlines of plate-type vessels contain three major region categories to model: (1) axial welds, (2) circumferential welds, and (3) plate segments. Only that portion of a weld within the axial bounds of the core is addressed because the fast-neutron flux and associated radiation damage applied to a weld experience a steep attenuation beyond the fueled region. The potential growth of an axially-oriented flaw in a plate segment is limited by the height of the core but not by the height of the shell course. Therefore, the lengths of axial flaws in plate segments can become greater than those in axial welds. Circumferential flaws in circumferential welds are limited only by the full 360-degree arc-length of the weld. Due to the fabrication procedures for applying the cladding on the inner vessel surface, FAVOR assumes that all pre-existing surface-breaking flaws (in plate or weld subregions) are circumferential flaws. Embedded flaws can be either oriented axially or circumferentially, depending on the orientation of the weld. Fabrication flaws are assigned orientations as described by Table 9.1. Upon the initiation of crack growth, the growing cracks retain the original orientation of the fabrication flaws.

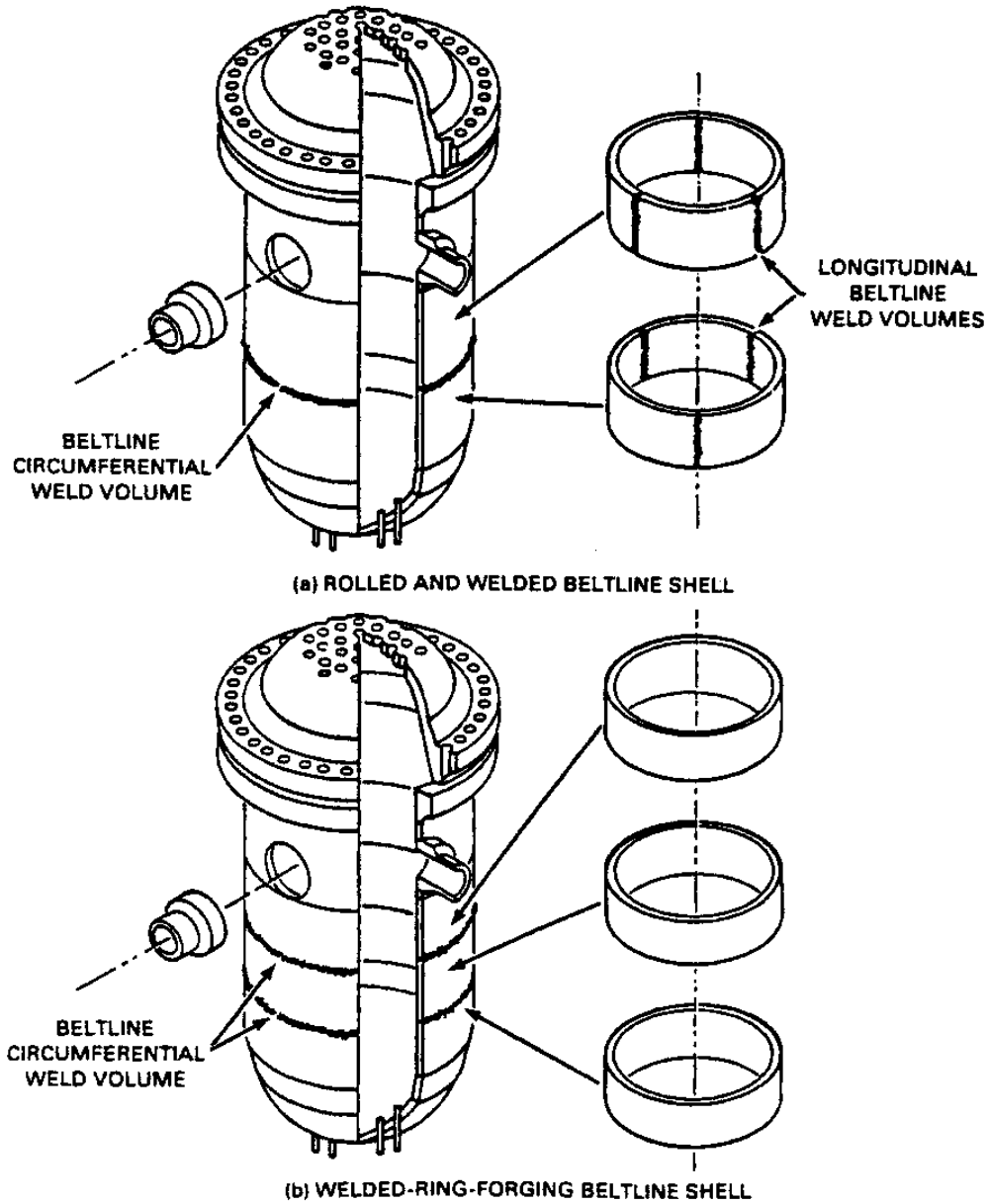


Figure 9.3. Fabrication Configurations of PWR Vessel Beltline Shells

Table 9.1. Applied Flaw Orientations by Major Regions			
Major Region	Flaw Category 1 <sup>(a)</sup>	Flaw Category 2 <sup>(b)</sup>	Flaw Category 3 <sup>(c)</sup>
Axial weld	Circumferential	Axial	Axial
Circumferential Weld	Circumferential	Circumferential	Circumferential
Plate/forging	Circumferential	Axial/circumferential <sup>d</sup>	Axial/circumferential <sup>(d)</sup>

(a) Surface-breaking flaw  
 (b) Embedded flaw in the base material between the clad/base interface and 1/8 t  
 (c) Embedded flaw in the base material between 1/8 t and 3/8 t  
 (d) Flaw Categories 2 and 3 in plates/forgings are divided equally between axial and circumferential orientations.

The FAVPFM probabilistic fracture mechanics model is based on the Monte Carlo technique, which performs deterministic fracture analyses for a large number of stochastically generated RPV trials or realizations. Each vessel realization can be considered to be a sample of the uncertain conditions of the specific RPV of interest. The uncertainties in the vessel include a number of the vessel's material properties along with the flaws in the vessel. Input uncertainties to the fracture mechanics analysis are described by statistical distributions. The RPV trials then propagate the input uncertainties along with their interactions through the model and thereby determine the probabilities of fracture and failure for a set of postulated PTS events at selected times during the vessel's operating history. The PFM model also provides estimates of the uncertainties in the estimated probabilities in terms of discrete statistical distributions. By repeating the RPV trials a large number of times, the output values constitute a random sample of the probability distribution induced by the combined probability distributions over the several input variables.

The assumed fracture mechanism for the RPV is stress-controlled cleavage fracture in the lower-transition temperature region of the vessel material. This mechanism is modeled under the assumption of linear-elastic fracture mechanics (LEFM). The predicted failure mechanism is of sufficient flaw growth either (1) to produce a net-section plastic collapse of the remaining ligament or (2) to advance the crack tip through a user-specified fraction of the wall thickness. Flaw growth can be due to either cleavage propagation or stable ductile tearing.

The Monte Carlo method involves sampling from probability distributions to simulate many possible combinations of flaw geometry and RPV material embrittlement. The PFM analysis is performed for the beltline of the RPV subjected to transient loading conditions. The RPV beltline is divided by FAVOR into *major regions* such as axial welds, circumferential welds, and plates or forgings that each have their own embrittlement-sensitive chemistries. The major regions are further discretized into *subregions* to accommodate detailed neutron fluence maps that include significant details regarding azimuthal and axial variations in neutron fluence. The general data streams that flow through the FAVPFM module are depicted in Figure 9.4. As shown, the FAVPFM module requires, as a key input, user-supplied data on flaw distributions.

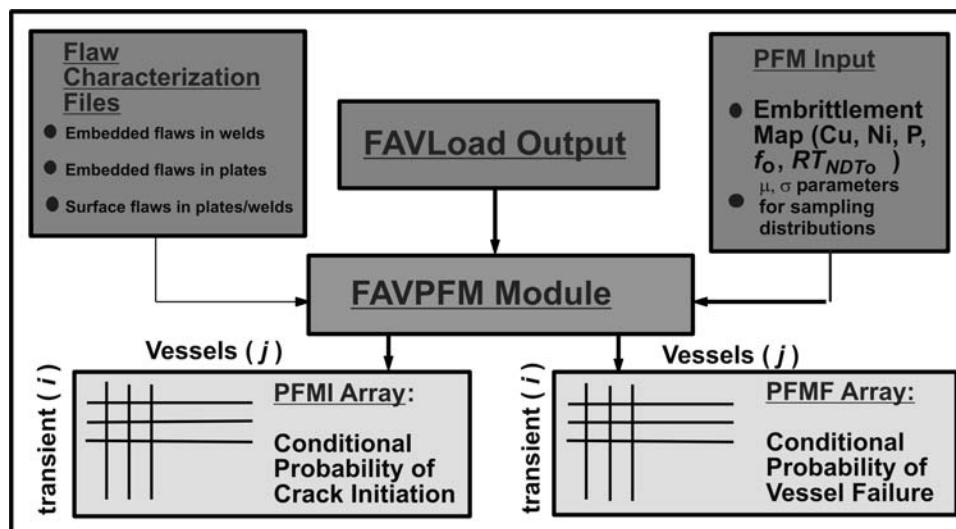


Figure 9.4. Input of User-Supplied Data on Flaw Distributions and Embrittlement and Output of Data on Vessel Failure Probabilities

The conditional probability of initiation,  $P(I|E)$ , was calculated in earlier versions of the FAVOR code by simply dividing the number of RPV trials predicted to experience cleavage fracture by the total number of trials. Similarly, the conditional probability of failure,  $P(F|E)$ , was calculated by dividing the number of RPV trials predicted to fail by the total number of failures. The current version of FAVOR now addresses the uncertainties in the calculated probabilities by calculating discrete distributions of RPV failure probabilities.

Because each RPV trial can be postulated to contain multiple flaws, one of the loops of the Monte Carlo simulation is indexed for the number of flaws for the particular trial. Each of the simulated flaws is positioned (through sampling) in a specific RPV beltline subregion that has its own distinguishing embrittlement parameters. The flaw geometry (depth, length, aspect ratio, and location within the RPV wall) is determined by sampling from appropriate distributions, as documented in this report. A deterministic fracture mechanics analysis is performed for each flaw for each of the PTS transients. The calculated probabilities are conditional probabilities in the sense that the transients are assumed to occur.

The discretization and organization of major regions and subregions of the beltline include a special treatment of weld *fusion lines*. The fusion lines represent the boundaries between the weld subregions and the neighboring plate or forging subregions. FAVOR checks for the possibility that the plate subregions adjacent to a weld subregion could have a higher degree of embrittlement than the weld. The  $RT_{NDT}$  values for the weld subregion of interest are compared to the corresponding values for the adjacent plate subregions. Each weld subregion will have at most two adjacent plate subregions. The embrittlement properties of the most limiting (either the weld or the adjacent plate subregion with the highest value of  $RT_{NDT}$ ) material are used when the fracture of the weld subregion is evaluated.

The method used to quantify the uncertainty in the flaw characterization is to include 1000 flaw-characterization file records in each of the three data files corresponding to the (1) the inner surface-breaking flaw, (2) embedded flaws in weld metal, and (3) embedded flaws in plate material. The flaw-characterization file for inner surface-breaking flaw is applicable to both weld and plate material regions. The RPV trials cycle through the flaw-characterization file records sequentially up to 1000, and then restart at the first file record.

Inner surface-breaking flaw density data are expressed by FAVOR in flaws per unit of RPV inner-surface area. The weld subregion embedded flaws are expressed as flaws per unit area of the fusion line between the weld and adjacent plate subregions. These conventions are consistent with the physical model used by PNNL to develop the flaw characterization data input to FAVOR. Embedded flaws within plate regions are expressed on a volumetric basis.

Figures 9.5a and 9.5b illustrate how FAVOR defines axial and circumferential weld subregion elements. For axial welds, the fusion lines are on the sides of the weld, whereas for circumferential welds, the fusion lines are on the top and bottom of the welds. A factor of 2 accounts for the fact that the input data developed by the PNNL procedure is in terms of the area for one side of the fusion line, whereas flaws can occur along fusion lines on both sides of the welds. All flaw densities are assumed to be uniform through the vessel wall thickness. The numbers of flaws in the plate subregion elements, as illustrated by Figure 9.5c, are calculated in a manner similar to that for welds, except that calculations are based on the flaws per unit volume of plate material.

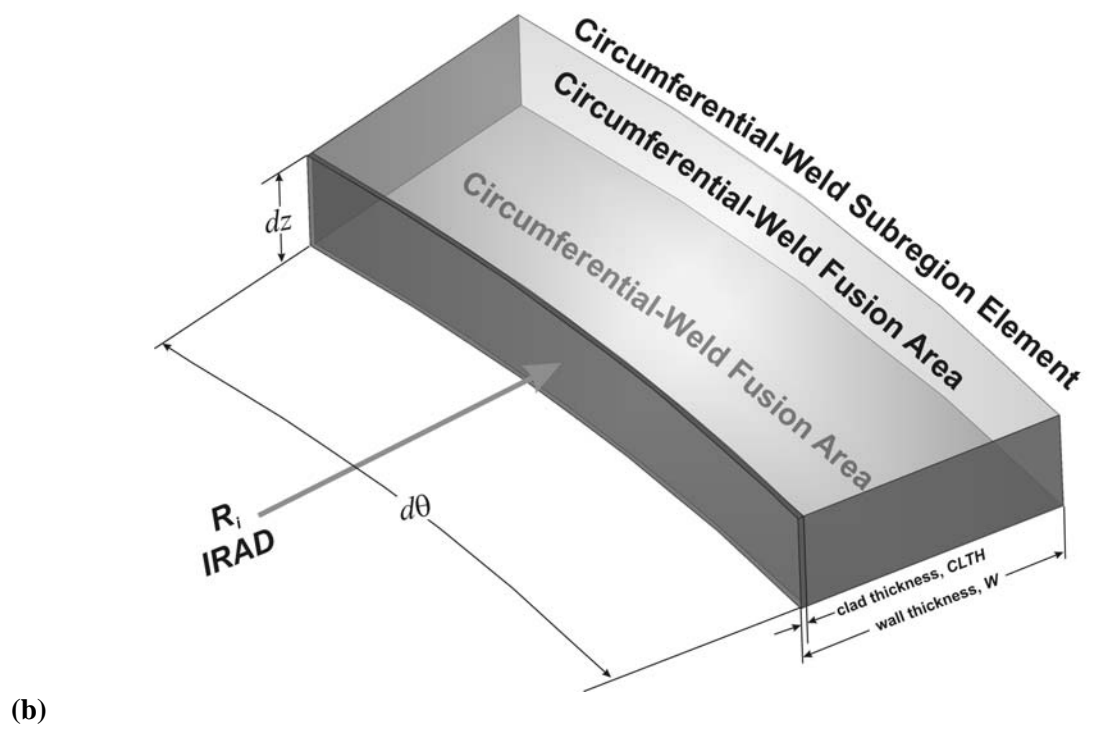
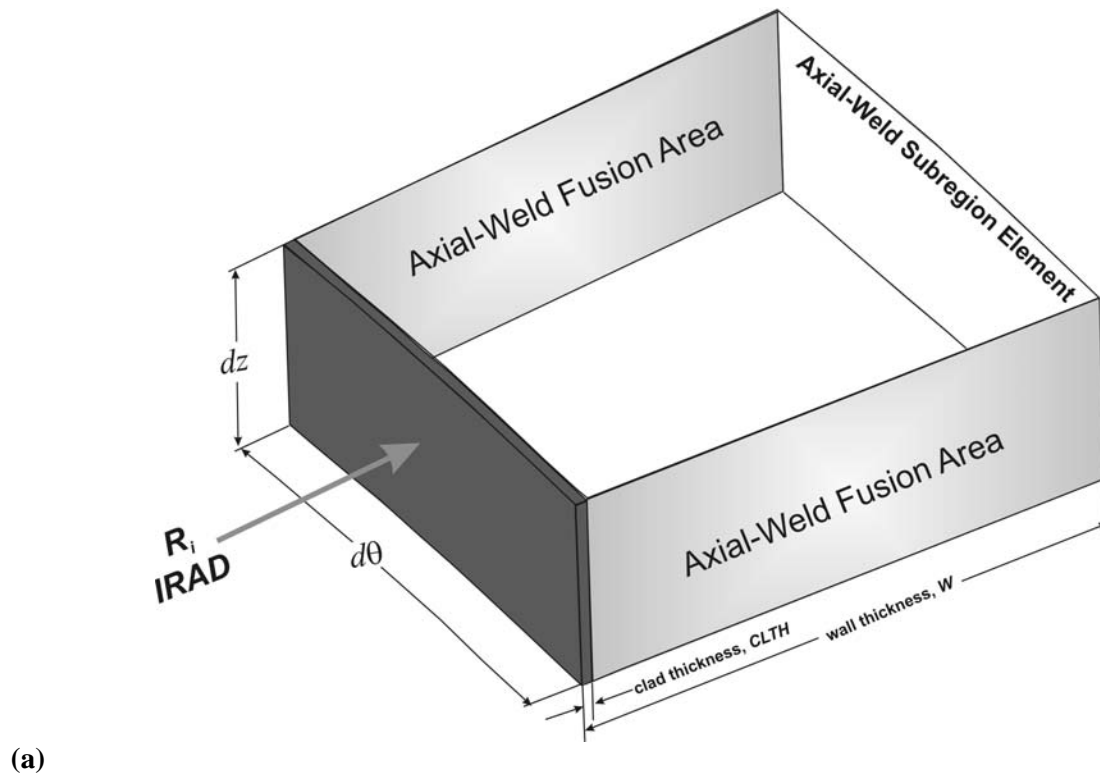


Figure 9.5. Weld Fusion Area Definitions for (a) Axial-Weld Subregion Elements and (b) Circumferential Subregion Elements

## Plate Subregion Element

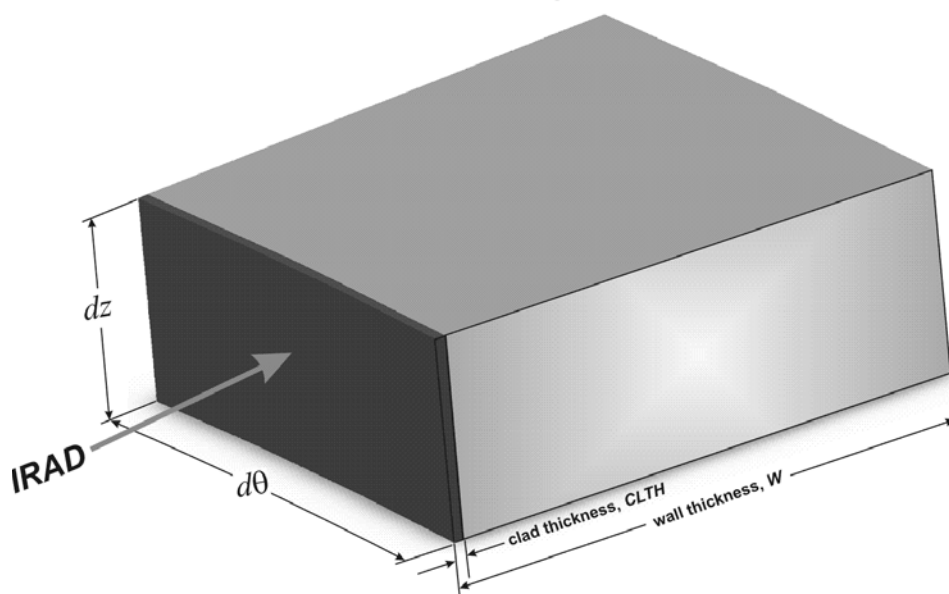


Figure 9.5 (contd). (c) Plate Subregion Element

### 9.1.3 FAVPost Module

The final module of the FAVOR code performs a post-processing of the results of the probabilistic fracture mechanics calculations and is not relevant to discussions of input files for flaw distributions. Distributions of transient-initiating frequencies obtained from PRA studies and the values of conditional probability of vessel failure and fracture (from FAVPFM) are combined by the FAVPost module to generate discrete distributions of frequencies of fracture initiation (crack growth) and failure (through-wall crack).

## 9.2 Required Input Files

The flaw model of the FAVOR code requires three input files to simulate the number, sizes, and locations of flaws in the beltline of a vessel as follows:

1. flaws in weld regions
2. flaws in base metal regions
3. surface-related flaws in the vessel cladding.

The number of flaws per unit area of weld fusion area or per unit volume of vessel material is specified to FAVOR using numerical tables of data. Statistical uncertainties in the flaw-related parameters are treated by generating 1000 tables that are based on the estimated uncertainties in the parameters of the flaw distributions. The tables describe the number of flaws per unit area or volume for defined ranges of flaw depth dimensions (expressed as a percentage of the vessel wall thickness) and for defined ranges of flaw aspect ratios (flaw length divided by flaw depth). Flaws are assumed to be located randomly through the thickness of the vessel wall.

Other inputs to FAVOR include the volumes and areas for the RPV subregions. From the assigned volumes and areas and from the inputs for the number of flaws per unit area or volume of each size category, the total numbers of flaws in the weld, base metal, or clad regions are calculated. Flaw locations relative to the vessel inner surface are assigned randomly. The FAVOR code also divides the vessel wall thickness into regions; the first region consists of the inner one-eighth of the wall thickness, and the second consists of the region from one-eighth to three-eighths of the vessel wall thickness. FAVOR assumes that flaws located outside the region three-eighths of the wall thickness make negligible contributions to vessel failure probabilities.

### **9.3 Computer Code for Generating Flaw Input Files**

A FORTRAN computer code was written by PNNL to perform calculations based on the flaw distribution functions (for flaw densities, flaw depth dimensions and flaw length or aspect ratios), as documented in Sections 6 through 8 of this report. The algorithm performs Monte Carlo calculations that simulate or sample from the uncertainty distributions for the parameters of the flaw distribution functions. Each application of the flaw distribution algorithm generates a data file for use as a possible input to the FAVOR code. Examples of input files that were supplied to ORNL for calculations with FAVOR are presented below.

The flaw distribution algorithm has three parts that individually address the three types of vessel regions (welds, base metal, and cladding). Inputs are provided in the form of batch input files. Each run of the algorithm addresses one category of vessel region. Discussions below describe each of the three parts of the code. The program logic for simulating flaws in weld regions is more complex and is described first. The corresponding logic for base metal flaws is a simple adaptation of the logic for weld flaws and requires only a brief explanation. Distributions for surface/clad flaws are treated in a deterministic manner, and the discussion of the logic for this category of flaws is again relatively brief.

Figure 9.6 describes the parameters and formats of the input file for the PNNL code. As indicated, the flaw distribution algorithm typically requires only five lines of input data. All input parameters are in metric units (mm), whereas output files can be in either metric or English units as requested by the user.

#### **9.3.1 Input File to PNNL Algorithm**

Inputs to the flaw distribution algorithm as described by Figure 9.6 include

- title line - A title of up to 80 characters allows the user to describe the calculation.
- number of material types - Allows the use of a rule-of-mixtures if a weld is made by more than one weld process (SAW, SMAW, and repair). Other inputs specify the welding processes in detail and the area or volume fractions contributed by each of the specified processes.
- number of Monte Carlo simulations - This parameter typically has been set at 1000 simulations to generate 1000 samples for the uncertainty analysis. The number of simulations can be specified to be other than 1000. If the number of simulations is prescribed to be zero, the calculation provides one flaw distribution corresponding to the best-estimate value from the uncertainty analysis.

```

C *****
C *****
C INPUT DATA FOR THE COMPUTER CODE VFLAW03.FOR
C *****
C *****
C DATA SET #1 CONTROL PARAMETERS
C *****
C COL. 1-80 NAME_REGION NAME OR TITLE FOR REGION
C (A80)
C
C COL. 1-11 N_SUBREGIONS NUMBER OF TYPES TO BE MIXED TOGETHER
C I10) WITHIN THE REGION
C
C COL. 11-20 N_SIMULATION = 0 BEST ESTIMATE CALCULATION
C (I10) > 0 UNCERTAINTY CALCULATION WITH
C WITH NUMBER OF MONTE CARLO
C TRIALS = N_SIMULATION
C
C COL. 21-30 WALL VESSEL TOTAL WALL THICKNESS (MM)
C (F10.4) (INCLUDING CLAD)
C
C COL. 31-40 IUNITS UNITS FOR OUTPUT FILES
C = 1 METRIC (FLAWS PER M^2 OR M^3)
C = 2 ENGLISH (FLAWS PER FT^2 OR FT^3)
C
C COL. 41-50 IVOLAREA UNITS FOR OUTPUT TABLES
C (10) (FOR WELD AND CLAD FLAWS)
C = 1 FLAWS PER UNIT VOLUME
C = 2 FLAWS PER UNIT AREA
C
C COL. 51-60 I_BASE_METAL = 0 NORMALLY
C (I10) = 1 JUNE 20, 2001 ASSUMPTIONS USED TO
C ADDRESS BASEMETAL FLAWS PER EXPERT
C JUDGMENT DATA AS ADJUSTMENT APPLIED
C TO WELD METAL DISTRIBUTION
C
C COL. 61-65 IORNL = 0 NORMALLY
C (I10) = 1 USE ORNL FORMAT FOR FLAW OUTPUT
C DATA FILE (W/O TWO HEADER LINES)
C
C COL. 66-75 UNIFORM_DENSITY FOR UNIFORM FLAW DEPTH DENSITY
C (F10.6) = 0.0 NORMALLY
C = USER SPECIFIED FLAWS
C PER UNIT AREA OR VOLUME
C FOR EACH CATEGORY OF
C ONE PERCENT OF WALL THICKNESS
C -----
C BASE METAL 1) DENSITY (INCLUDING UNCERTAINTY) OF SMALL FLAWS
C ASSUMPTIONS IN BASEMETAL IS 1/10 OF THAT FOR WELD METAL
C 2) DENSITY (INCLUDING UNCERTAINTY) OF LARGE FLAWS
C IN BASEMETAL IS 1/40 OF THAT FOR WELD METAL

```

**Figure 9.6. Input Instructions for Flaw Distribution Algorithm**

```

C *****
C DATA SET #2 MATERIAL TYPE CHARACTERISTICS
C (ONE DATA SET FOR EACH MATERIAL TYPE)
C *****
C
C COL. 1-10 VOLFRAC(N) VOLUME OR AREA FRACTION FOR MATERIAL TYPE
C (F10.4)
C
C COL. 11-15 IVESSEL(N) = 1 USE CORRELATIONS FROM PVRUF VESSEL
C (I5) = 2 USE CORRELATIONS FROM SHOREHAM VESSEL
C
C COL. 16-20 IMATERIAL(N) = 1 SAW (SUBMERGED METAL ARC WELD)
C (I5) = 2 SMAW(SHIELDED METAL ARC WELD)
C = 3 REPAIR WELD
C = 4 CLAD
C = 5 BASE METAL
C
C COL. 21-25 BEAD(N) BEAD SIZE (MM) FOR MATERIAL TYPE
C (F5.1)
C
C COL. 26-35 FACTOR(N) FACTOR ON FLAW FREQUENCIES APPLIED
C (F10.4) TO HARD WIRED FLAW DENSITIES
C (NORMALLY ASSIGNED AS 1.0)
C
C COL. 36-40 CLAD_THICK(N) CLAD THICKNESS (MM)
C (F5.1) (ONLY IF IMATERIAL(N) = 4)
C
C COL. 41-45 CLAD_WIDTH(N) CLAD BEAD WIDTH (MM)
C (F5.1) (ONLY IF IMATERIAL(N) = 4)
C
C COL. 46-50 N_LAYERS(N) NUMBER OF CLAD LAYERS
C (I5) (ONLY IF IMATERIAL(N) = 4)
C
C COL. 51-60 TRUNC(N) TRUNCATION ON FLAW DEPTH
C (F10.3) (MM)

```

**Figure 9.6. (contd)**

- vessel wall thickness - The wall thickness is the total thickness including the cladding.
- area or volume - Allows the output file to give flaw frequencies in terms of flaws per unit area of the weld fusion surface (for welds) or vessel inner surface (for clad/surface-breaking flaws). Alternatively, the output for weld regions can be requested in terms of flaws per unit volume. Base metal output is always in terms of flaw per unit volume. Clad/surface flaw frequencies also can be expressed in terms of flaws per unit volume. In this case, the density corresponds to the number of flaws in a given region of clad divided by the total volume of metal in the vessel wall beneath the region of the clad. It is noted that the FAVOR code made a change from using flaws per unit volume to flaws per unit area (for weld and clad/surface flaws). All subsequent applications of the PNNL flaw distribution algorithm have used the flaw per unit area approach. The PNNL algorithm has nevertheless retained the option of flaws per unit volume for purposes of sensitivity studies and to allow output files to be generated for PFM codes other than FAVOR that may be based on the flaws per unit volume concept.

- metric or English - Allows the output file to give flaw frequencies as either flaws per square meter or as flaws per square foot. If the flaw densities are expressed as flaws per unit volume, the units are flaws per cubic meter or flaws per cubic foot.
- base metal option - The current version of the algorithm does not explicitly treat flaws in base metal regions but first performs simulations of flaws as if the base metal were weld metal. The calculated flaw frequencies for welds are then reduced by hardwired factors of 10 for small flaws and 40 for large flaws.
- ORNL header option - The format prescribed by ORNL for the FAVOR input file of 1000 datasets (for the uncertainties in flaw distributions) does not allow for a header line to label the columns of the table. This parameter allows the header lines to be deleted.
- uniform depth density - This parameter normally is set to 0.0. Values other than zero should be used only for sensitivity studies. In this case, the output file arbitrarily assigns flaw frequencies that are independent of the flaw depth dimensions.

Each of the material types (as described above) requires one line for input parameters as follows:

- area or volume fraction - the area (or volume) fraction for each weld process (SAW, SMAW, or repair) for each material type of the weld - The sum of the area (or volume) fractions for all material types should add up to unity.
- vessel - Specifies if the parameters for the flaw densities and flaw dimensions are to be based on the data from the PVRUF vessel or from the Shoreham vessel.
- material type - Denotes the category of weld process (SAW, SMAW, or repair weld) for the material type of interest. This parameter also can direct the algorithm to perform calculations for clad material. In this case, the flaw densities are based on the number of clad layers and on the specified thickness and width of the clad weld beads. The flaw distribution algorithm has an inactive provision for base metal. The code instead treats base metal in an approximate manner as weld metal with the flaw densities reduced and the depth distributions truncated. The code currently stops and prints an error message if the user attempts to address base metal by use of this input parameter.
- bead size - Is the estimated bead size (through-wall dimension) for each weld material type (SAW, SMAW, and repair).
- factor - factor (normally set equal to 1.0) that is applied to the hardwired flaw densities - Values other than 1.0 should be used only for sensitivity studies.
- clad thickness - Is the total clad thickness and accounts for all layers, should the clad consist of more than one layer. This parameter needs to be specified only if the material type is clad rather than SAW, SMAW, and repair.
- clad width - Describes the bead width (or the width of the strip) for the cladding. This parameter needs to be specified only if the material type is clad rather than SAW, SMAW, and repair.

- number of clad layers - Specifies the number of clad layers and will specify only one layer for typical strip-type cladding. This parameter needs to be specified only if the material type is clad rather than SAW, SMAW, and repair.
- truncation on flaw depths - Describes the values of flaw depth dimensions, specified individually for SAW, SMAW, and repair welding, beyond which the flaw frequencies are set to zero. The truncation would be typically on the order of 25 mm for SAW and SMAW flaws and 50 mm for flaws in repair welds.

### 9.3.2 Output File from PNNL Algorithm

Output files from the PNNL algorithm provide the following information:

- display of the input data - The first part of the output file displays and identifies all of the input data the user has provided to the algorithm.
- first 10-sample flaw distributions from the uncertainty evaluation - The second part of the output file is a series of 10 tables corresponding to the first 10 (of a typical total of 1000) sample flaw distributions that are written on the large file for use as input to FAVOR.
- largest values from the 1000 simulated flaw distribution - the largest values (from a search through the 1000 simulated flaw distributions) for each element of the tables that describe the simulated distributions—This table does not correspond to any of the 1000 samples but only indicates the maximum values for the individual elements from all of the flaw distribution tables.
- median values from the 1000 simulated flaw distribution - the median values (from a search through the 1000 simulated flaw distributions) for each element of the tables that describe the simulated distributions—This table does not correspond to any of the 1000 samples but indicates only the median values for the individual elements from all of the flaw distribution tables.
- smallest values from the 1000 simulated flaw distribution - the smallest values (from a search through the 1000 simulated flaw distributions) for each element of the tables that describe the simulated distributions—This table does not correspond to any of the 1000 samples but indicates only the smallest values for the individual elements from all of the flaw distribution tables.
- 25<sup>th</sup> percentile values from the 1000 simulated flaw distribution - the 25<sup>th</sup> percentile values (from a search through the 1000 simulated flaw distributions) for each element of the tables that describe the simulated distributions—This table does not correspond to any of the 1000 samples but indicates only the 25<sup>th</sup> percentile values for the individual elements from all of the flaw distribution tables.
- 75<sup>th</sup> percentile values from the 1000 simulated flaw distribution - the 75<sup>th</sup> percentile values (from a search through the 1000 simulated flaw distributions) for each element of the tables that describe the simulated distributions—This table does not correspond to any of the 1000 samples but indicates only the 75<sup>th</sup> percentile values for the individual elements of the flaw distribution table.
- 5<sup>th</sup> percentile values from the 1000 simulated flaw distribution - the 5<sup>th</sup> percentile values (from a search through the 1000 simulated flaw distributions) for each element of the tables that describe the

simulated distributions—This table does not correspond to any of the 1000 samples but indicates only the 5<sup>th</sup> percentile values for the individual elements from all of the flaw distribution tables.

- 95<sup>th</sup> percentile values from the 1000 simulated flaw distribution - the 95<sup>th</sup> percentile values (from a search through the 1000 simulated flaw distributions) for each element of the tables that describe the simulated distributions—This table does not correspond to any of the 1000 samples but indicates only the 95<sup>th</sup> percentile values for the individual elements from all of the flaw distribution tables.

### **9.3.3 Output File from PNNL Algorithm for Inputs to FAVOR**

The second output file from the PNNL algorithm is generated for actual use as an input file by FAVOR. This relatively large file is not intended to be printed as a hard copy. It contains the flaw distribution tables for all of the samples of flaw distributions that are calculated by the Monte Carlo simulation. The output file as described in Section 9.3.2 provides the user with the first 10 of the large number (e.g., 1000) of samples.

## **9.4 Procedure for Weld Regions**

Section 6 of this report documents the flaw data and statistical correlations that were developed to describe the flaws observed in the welds of the PVRUF and Shoreham vessels. The following paragraphs describe the implementation of the statistical correlations into the flaw distribution algorithm.

### **9.4.1 Treatment of Weld Flaws**

Weld regions of concern to RPV integrity are the axial and circumferential seam welds in the high neutron fluence region of the vessel beltline. These welds can be fabricated by the SAW process or by the SMAW process. Typically, a given seam weld will have some welding from both processes, but the largest fraction (e.g., >90%) of the weld will usually be deposited by the automatic SAW process. The flaw model accounts for the differences between the flaw densities and size distributions for these weld processes. In this regard the identification of local regions as produced by specific welding processes requires information not generally available from vessel fabrication records. Therefore, calculations with FAVOR have assumed a random mixture of SAW and SMAW materials plus a small fraction of repair welding. The fractions have been based on trends observed from the vessels examined by PNNL.

In practice, some flaws are located randomly within the volume of weld metal, and other flaws are located along the fusion lines that separate the weld metal from the adjoining base metal. While many flaws are within the volume of the weld, PNNL data have shown that very few of these flaws have significant through-wall dimensions. Most larger weld flaws are located along the weld fusion line. FAVOR therefore assumes that all weld flaws are located along fusion lines. Only a small fraction of these fusion line flaws has through-wall dimensions approaching or exceeding the size of a single weld bead.

A single flaw input file is used by FAVOR to address both axial and circumferential welds. Flaws for axial welds are assumed in FAVOR to have axial orientations, and flaws for circumferential welds are assumed to have circumferential orientations.

Although repair welding makes up only a small percentage of the weld metal in a typical vessel, most of the larger flaws (depth dimensions greater than a weld bead) have been associated with weld repairs. Typical repairs are ground-out regions that have been filled by a manual welding process. The repairs can

be entirely within seam welds or entirely within base metal, but will most typically span both weld metal and base metal because repairs are generally made to the defects that reside along the weld fusion lines. Observed repairs have been made from both the inside and the outside surfaces of vessels. It has not been considered practical for FAVOR calculations to identify specific locations of repairs, although such information can be obtained from construction records. The repairs have therefore been assumed to occur at random locations, such that the repair flaws are blended into the population of flaws associated with the normal welding processes. However, the small amount of material from repair welding nevertheless makes the dominant contribution to the estimated number of larger flaws.

### 9.4.2 Flow Chart for Welds

Figure 9.7 is a flow chart for the steps in the Monte Carlo simulation for flaws in welds. Details of the calculations are as follows:

- PVRUF versus Shoreham vessel - There is an option to base the simulation of the parameters of the flaw distributions and the associated uncertainties in these distributions on the data from either the PVRUF or the Shoreham vessel.
- weld type - The weld process can be either SAW or SMAW, or repair weld, or a mixture of these processes. An implied assumption is that a given local region has a random chance of being composed of any of the specified weld types.
- bead size - An input to the calculations allows the user to specify the weld bead size (through thickness dimension) for each category of weld material. This permits vessel specific information on the welding process to be accounted for in the estimates of flaw distributions. If the calculations are to be based on the observed bead sizes for the PVRUF or Shoreham vessels, the following inputs can be used as default inputs:

<b>Weld Type</b>	<b>Bead Size (mm) PVRUF Vessel</b>	<b>Bead Size (mm) Shoreham Vessel</b>
Submerged Arc (SAW)	6.5	5.0
Shielded Metal Arc (SMAW)	3.5	3.5
Repair	3.5	3.5

- vessel simulation - The Monte Carlo simulation ensures that uncertainties in the parameters of the statistical flaw distribution functions are simulated only once per vessel. For example, in reference to Figure 9.7, one conditional depth distribution for small flaws (and likewise for large flaws) applies to all flaw types (SAW, SMAW and repair) for each simulated vessel. The length distributions for repair flaws are assumed to be the same as that for SMAW welds. The Monte Carlo simulation samples the parameters for this distribution only once for both weld types.

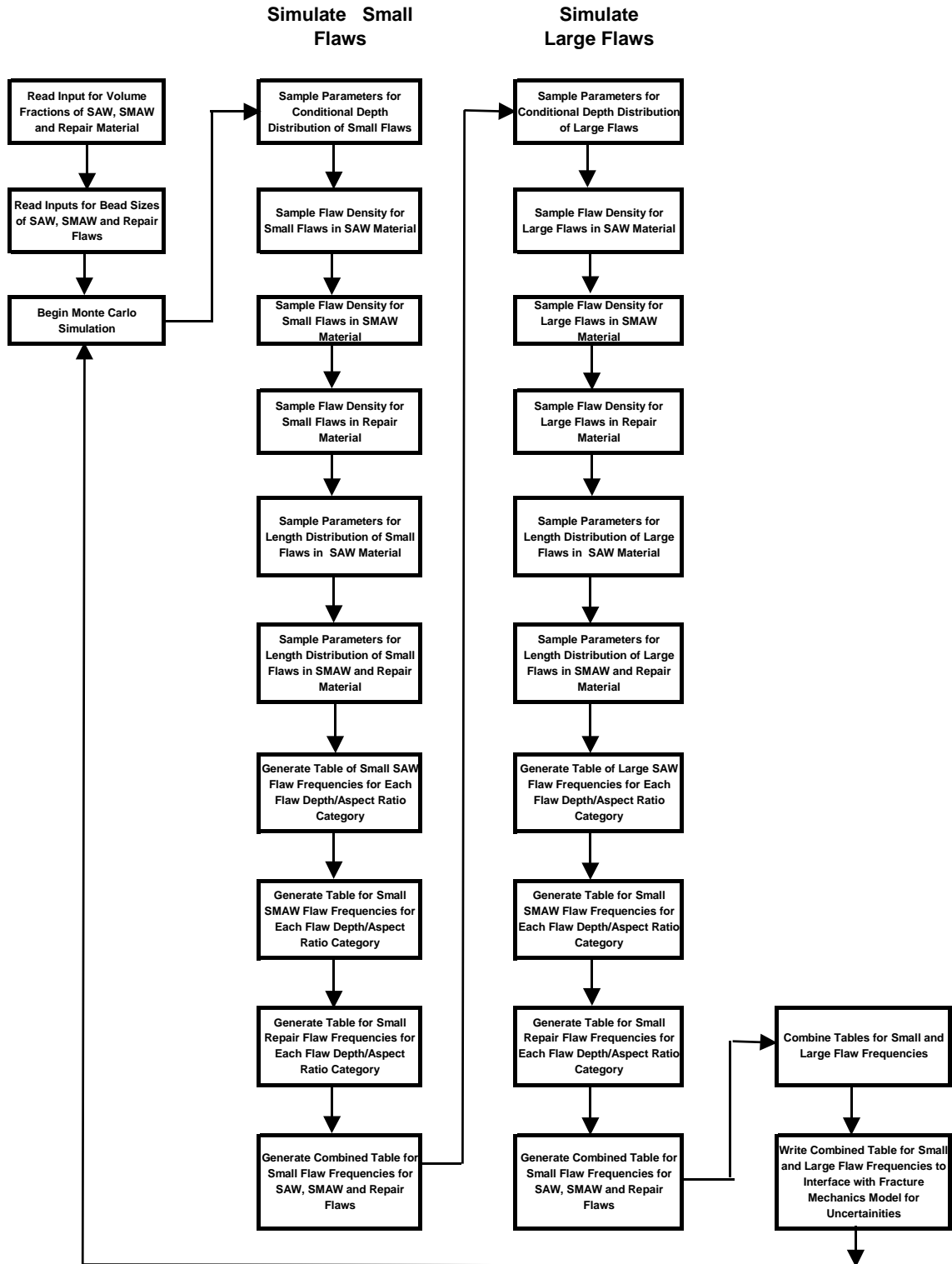


Figure 9.7. Flow Chart for Weld Flaws

- large and small flaws - As indicated in Figure 9.7, there are independent elements of the model that address the parameters for the distributions of small and large flaws. Small flaws are those with through-wall depths that are less than one weld bead dimension, whereas the large flaws are greater than one bead dimension. Results for the two depth categories are combined in the final step of the calculation. The resulting tables for use as inputs to FAVOR do not differentiate between large and small flaws.
- flaw densities - Six separate simulations address uncertainties in the densities (flaws per square meter or cubic meter) of SAW, SMAW, and repair flaws for both small and large flaws. The uncertainties in the densities for small flaws are relatively small because the PNNL examinations found a large number of small flaws. The uncertainties in the densities of large flaws are much larger because the vessel examinations found relatively few large flaws.
- conditional depth distribution - The conditional depth distribution (as normalized with respect to the weld bead dimension) was assumed to be the same for SAW, SMAW, and repair flaws. Different distribution functions and parameters are used to describe the depths of large versus small flaws. Because the number of observed large flaws was very small, the uncertainties in the parameter for the exponential distribution for the depths of large flaws were relatively large. The uncertainties in the depths of small flaws were relatively small.
- aspect ratio distribution - The database for validated measurements of aspect ratios for small and large flaws in the PVRUF vessel was relatively small, and the uncertainties were correspondingly large. Data showed that most SAW flaws in the PVRUF welds tended to be about 1:1, whereas the aspect ratios of these flaws in SMAW welds were much larger. A separate data analysis was performed for aspect ratios for flaws in the welds of the Shoreham vessel. The Shoreham vessel (compared to the PVRUF vessel) showed a trend of larger aspect ratios for small flaws in the SAW welds. Differences in aspect ratios for SMAW and SAW flaws were relatively small for the Shoreham vessel. It was assumed for both the PVRUF and Shoreham vessel that flaws in repair and SMAW welds have the same distribution of aspect ratios.

### 9.4.3 Sample Input and Output File for Welds

Figures 9.8 through 9.10 present inputs and outputs for a sample calculation for welds by the PNNL flaw distribution algorithm. This particular example was based on the uncertainty distribution obtained from an analysis of the Shoreham flaw data and presents (Figure 9.10) the first simulated distribution of a total of 1000 tables from sampling for the uncertainty analysis. The Monte Carlo simulation, as performed by the FORTRAN computer code, generates a file consisting of a large number of tables (e.g., 1000) corresponding to Figure 9.10.

The rows of Figure 9.10 come from a binning into 100 bins of the data from the continuous flaw distributions generated by the algorithm. Each bin corresponds to a depth category defined by 1% increments of the vessel wall thickness. For example, the bin designated by the label “1” in Figure 9.10 gives the number of flaws per square foot of fusion surface that have depth dimensions between 1% and 2% of the vessel wall thickness. There are 40.614 flaws per square foot for this depth category, whereas the number of very large flaws with depths between 9% and 10% of the vessel wall thickness is only 0.0017841 flaws per square foot. There are no flaws with depths greater than 23% of the vessel wall thickness, consistent with the specified truncation depth for flaws in repair welds.

OCONEE-1	OCTOBER 29, 2002	WELD	FLAW/FT^2	SHOREHAM TRUNCATED	
3	1000	219.10	2	2	0 1 0.0
0.9700	2	1 4.76	1.0		25.4
0.0100	2	2 5.33	1.0		25.4
0.0200	2	3 3.56	1.0		50.8

**Figure 9.8. Sample Flaw Distribution Input File for Weld Region**

```

GENERATION OF FLAW DISTRIBUTION INPUT FILE FOR THE ORNL FAVOR CODE

NAME OF REGION = OCONEE-1 OCTOBER 29, 2002 WELD    FLAW/FT^2    SHOREHAM
TRUNCATED

NUMBER OF SUBREGIONS =      3
UNCERTAINTY CALCULATION
NUMBER OF MONTE CARLO SIMULATIONS =    1000
VESSEL TOTAL WALL THICKNESS (MM) =    219.10
ENGLISH UNITS - FLAWS PER FT^2 OR FLAWS PER FT^3
WELD DENSITY OPTION - FLAWS PER UNIT AREA
BASE_METAL APPROXIMATION NOT USED

OUTPUT FILE REFORMATTED FOR INPUT TO ORNL FAVOR CODE

SUBREGION NUMBER    1
  VOLUME FRACTION =    .9700
  SHOREHAM VESSEL PARAMETERS
  SAW (SUBMERGED METAL ARC WELD)
  BEAD SIZE (MM)      =    4.76
  FACTOR ON FLAW FREQUENCIES =    1.0000 (DEFAULT = 1.0)
  CLAD THICKNESS(MM) =    .0000 (USED ONLY FOR CLAD)
  CLAD BEAD WIDTH (MM) =    .0000 (USED ONLY FOR CLAD)
  NUMBER OF CLAD LAYERS =    0 (USED ONLY FOR CLAD)
  TRUNCATION ON FLAW DEPTH (MM) =    25.4000

SUBREGION NUMBER    2
  VOLUME FRACTION =    .0100
  SHOREHAM VESSEL PARAMETERS
  SMAW (SHIELDED METAL ARC WELD)
  BEAD SIZE (MM)      =    5.33
  FACTOR ON FLAW FREQUENCIES =    1.0000 (DEFAULT = 1.0)
  CLAD THICKNESS(MM) =    .0000 (USED ONLY FOR CLAD)
  CLAD BEAD WIDTH (MM) =    .0000 (USED ONLY FOR CLAD)
  NUMBER OF CLAD LAYERS =    0 (USED ONLY FOR CLAD)
  TRUNCATION ON FLAW DEPTH (MM) =    25.4000

SUBREGION NUMBER    3
  VOLUME FRACTION =    .0200
  SHOREHAM VESSEL PARAMETERS
  REPAIR WELD
  BEAD SIZE (MM)      =    3.56
  FACTOR ON FLAW FREQUENCIES =    1.0000 (DEFAULT = 1.0)
  CLAD THICKNESS(MM) =    .0000 (USED ONLY FOR CLAD)
  CLAD BEAD WIDTH (MM) =    .0000 (USED ONLY FOR CLAD)
  NUMBER OF CLAD LAYERS =    0 (USED ONLY FOR CLAD)
  TRUNCATION ON FLAW DEPTH (MM) =    50.8000

```

**Figure 9.9. Sample from Flaw Distribution File for Weld Region**

FLAW DISTRIBUTION FOR SIMULATION NUMBER 1

N	FLAWS/FT**2	1.0-1.25	1.25-1.5	1.5-2.0	2.0-3.0	3.0-4.0	4.0-5.0	5.0-6.0	6.0-8.0	8.0-10.0	10.0-15.0	>15.0
1	.40614E+02	2.285	2.232	4.310	8.039	7.322	6.671	6.078	10.588	8.798	16.044	27.633
2	.311174E+01	6.680	6.230	11.230	18.275	13.849	10.504	7.973	10.654	6.153	6.294	2.157
3	.29780E+00	13.925	11.939	19.043	24.477	13.479	7.486	4.186	3.687	1.189	.548	.040
4	.84188E-01	20.384	16.106	22.883	23.709	9.749	4.095	1.746	1.077	.204	.047	.001
5	.24607E-01	28.213	19.981	24.412	19.303	5.558	1.708	.550	.244	.028	.004	.000
6	.10494E-01	36.682	22.971	23.618	13.574	2.481	.514	.119	.037	.003	.000	.000
7	.59722E-02	43.742	24.483	21.487	9.116	1.016	.131	.020	.004	.000	.000	.000
8	.38645E-02	49.281	24.949	19.069	6.225	.438	.034	.003	.000	.000	.000	.000
9	.26093E-02	53.918	24.832	16.718	4.322	.200	.010	.001	.000	.000	.000	.000
10	.17841E-02	58.006	24.354	14.523	3.018	.095	.003	.000	.000	.000	.000	.000
11	.12243E-02	61.693	23.631	12.521	2.108	.046	.001	.000	.000	.000	.000	.000
12	.84087E-03	65.047	22.736	10.724	1.470	.022	.000	.000	.000	.000	.000	.000
13	.57784E-03	68.101	21.724	9.140	1.025	.011	.000	.000	.000	.000	.000	.000
14	.39709E-03	70.887	20.637	7.757	.713	.005	.000	.000	.000	.000	.000	.000
15	.27288E-03	73.430	19.510	6.561	.496	.002	.000	.000	.000	.000	.000	.000
16	.18752E-03	75.751	18.369	5.534	.345	.001	.000	.000	.000	.000	.000	.000
17	.12886E-03	77.869	17.233	4.658	.239	.001	.000	.000	.000	.000	.000	.000
18	.88555E-04	79.803	16.118	3.913	.166	.000	.000	.000	.000	.000	.000	.000
19	.60855E-04	81.567	15.035	3.282	.115	.000	.000	.000	.000	.000	.000	.000
20	.41819E-04	83.177	13.993	2.750	.080	.000	.000	.000	.000	.000	.000	.000
21	.28738E-04	84.647	12.996	2.302	.056	.000	.000	.000	.000	.000	.000	.000
22	.19749E-04	85.988	12.049	1.925	.039	.000	.000	.000	.000	.000	.000	.000
23	.13571E-04	87.212	11.153	1.609	.027	.000	.000	.000	.000	.000	.000	.000
24	.00000E+00	100.000	.000	.000	.000	.000	.000	.000	.000	.000	.000	.000
25	.00000E+00	100.000	.000	.000	.000	.000	.000	.000	.000	.000	.000	.000
26	.00000E+00	100.000	.000	.000	.000	.000	.000	.000	.000	.000	.000	.000
27	.00000E+00	100.000	.000	.000	.000	.000	.000	.000	.000	.000	.000	.000
28	.00000E+00	100.000	.000	.000	.000	.000	.000	.000	.000	.000	.000	.000
29	.00000E+00	100.000	.000	.000	.000	.000	.000	.000	.000	.000	.000	.000
30	.00000E+00	100.000	.000	.000	.000	.000	.000	.000	.000	.000	.000	.000
31	.00000E+00	100.000	.000	.000	.000	.000	.000	.000	.000	.000	.000	.000
32	.00000E+00	100.000	.000	.000	.000	.000	.000	.000	.000	.000	.000	.000
33	.00000E+00	100.000	.000	.000	.000	.000	.000	.000	.000	.000	.000	.000
34	.00000E+00	100.000	.000	.000	.000	.000	.000	.000	.000	.000	.000	.000
35	.00000E+00	100.000	.000	.000	.000	.000	.000	.000	.000	.000	.000	.000
36	.00000E+00	100.000	.000	.000	.000	.000	.000	.000	.000	.000	.000	.000
37	.00000E+00	100.000	.000	.000	.000	.000	.000	.000	.000	.000	.000	.000
38	.00000E+00	100.000	.000	.000	.000	.000	.000	.000	.000	.000	.000	.000
39	.00000E+00	100.000	.000	.000	.000	.000	.000	.000	.000	.000	.000	.000
40	.00000E+00	100.000	.000	.000	.000	.000	.000	.000	.000	.000	.000	.000
41	.00000E+00	100.000	.000	.000	.000	.000	.000	.000	.000	.000	.000	.000
42	.00000E+00	100.000	.000	.000	.000	.000	.000	.000	.000	.000	.000	.000
43	.00000E+00	100.000	.000	.000	.000	.000	.000	.000	.000	.000	.000	.000
44	.00000E+00	100.000	.000	.000	.000	.000	.000	.000	.000	.000	.000	.000
45	.00000E+00	100.000	.000	.000	.000	.000	.000	.000	.000	.000	.000	.000
46	.00000E+00	100.000	.000	.000	.000	.000	.000	.000	.000	.000	.000	.000
47	.00000E+00	100.000	.000	.000	.000	.000	.000	.000	.000	.000	.000	.000
48	.00000E+00	100.000	.000	.000	.000	.000	.000	.000	.000	.000	.000	.000
49	.00000E+00	100.000	.000	.000	.000	.000	.000	.000	.000	.000	.000	.000
50	.00000E+00	100.000	.000	.000	.000	.000	.000	.000	.000	.000	.000	.000
51	.00000E+00	100.000	.000	.000	.000	.000	.000	.000	.000	.000	.000	.000
52	.00000E+00	100.000	.000	.000	.000	.000	.000	.000	.000	.000	.000	.000
53	.00000E+00	100.000	.000	.000	.000	.000	.000	.000	.000	.000	.000	.000
54	.00000E+00	100.000	.000	.000	.000	.000	.000	.000	.000	.000	.000	.000
55	.00000E+00	100.000	.000	.000	.000	.000	.000	.000	.000	.000	.000	.000
56	.00000E+00	100.000	.000	.000	.000	.000	.000	.000	.000	.000	.000	.000
57	.00000E+00	100.000	.000	.000	.000	.000	.000	.000	.000	.000	.000	.000
58	.00000E+00	100.000	.000	.000	.000	.000	.000	.000	.000	.000	.000	.000
59	.00000E+00	100.000	.000	.000	.000	.000	.000	.000	.000	.000	.000	.000
60	.00000E+00	100.000	.000	.000	.000	.000	.000	.000	.000	.000	.000	.000
61	.00000E+00	100.000	.000	.000	.000	.000	.000	.000	.000	.000	.000	.000
62	.00000E+00	100.000	.000	.000	.000	.000	.000	.000	.000	.000	.000	.000
63	.00000E+00	100.000	.000	.000	.000	.000	.000	.000	.000	.000	.000	.000
64	.00000E+00	100.000	.000	.000	.000	.000	.000	.000	.000	.000	.000	.000
65	.00000E+00	100.000	.000	.000	.000	.000	.000	.000	.000	.000	.000	.000
66	.00000E+00	100.000	.000	.000	.000	.000	.000	.000	.000	.000	.000	.000
67	.00000E+00	100.000	.000	.000	.000	.000	.000	.000	.000	.000	.000	.000
68	.00000E+00	100.000	.000	.000	.000	.000	.000	.000	.000	.000	.000	.000
69	.00000E+00	100.000	.000	.000	.000	.000	.000	.000	.000	.000	.000	.000
70	.00000E+00	100.000	.000	.000	.000	.000	.000	.000	.000	.000	.000	.000
71	.00000E+00	100.000	.000	.000	.000	.000	.000	.000	.000	.000	.000	.000
72	.00000E+00	100.000	.000	.000	.000	.000	.000	.000	.000	.000	.000	.000
73	.00000E+00	100.000	.000	.000	.000	.000	.000	.000	.000	.000	.000	.000
74	.00000E+00	100.000	.000	.000	.000	.000	.000	.000	.000	.000	.000	.000
75	.00000E+00	100.000	.000	.000	.000	.000	.000	.000	.000	.000	.000	.000
76	.00000E+00	100.000	.000	.000	.000	.000	.000	.000	.000	.000	.000	.000
77	.00000E+00	100.000	.000	.000	.000	.000	.000	.000	.000	.000	.000	.000
78	.00000E+00	100.000	.000	.000	.000	.000	.000	.000	.000	.000	.000	.000
79	.00000E+00	100.000	.000	.000	.000	.000	.000	.000	.000	.000	.000	.000
80	.00000E+00	100.000	.000	.000	.000	.000	.000	.000	.000	.000	.000	.000
81	.00000E+00	100.000	.000	.000	.000	.000	.000	.000	.000	.000	.000	.000
82	.00000E+00	100.000	.000	.000	.000	.000	.000	.000	.000	.000	.000	.000
83	.00000E+00	100.000	.000	.000	.000	.000	.000	.000	.000	.000	.000	.000
84	.00000E+00	100.000	.000	.000	.000	.000	.000	.000	.000	.000	.000	.000
85	.00000E+00	100.000	.000	.000	.000	.000	.000	.000	.000	.000	.000	.000
86	.00000E+00	100.000	.000	.000	.000	.000	.000	.000	.000	.000	.000	.000
87	.00000E+00	100.000	.000	.000	.000	.000	.000	.000	.000	.000	.000	.000
88	.00000E+00	100.000	.000	.000	.000	.000	.000	.000	.000	.000	.000	.000
89	.00000E+00	100.000	.000	.000	.000	.000	.000	.000	.000	.000	.000	.000
90	.00000E+00	100.000	.000	.000	.000	.000	.000	.000	.000	.000	.000	.000
91	.00000E+00	100.000	.000	.000	.000	.000	.000	.000	.000	.000	.000	.000
92	.00000E+00	100.000	.000	.000	.000	.000	.000	.000	.000	.000	.000	.000
93	.00000E+00	100.000	.000	.000	.000	.000	.000	.000	.000	.000	.000	.000
94	.00000E+00	100.000	.000	.000	.000	.000	.000	.000	.000	.000	.000	.000
95	.00000E+00	100.000	.000	.000	.000	.000	.000	.000	.000	.000	.000	.000
96	.00000E+00	100.000	.000	.000	.000	.000	.000	.000	.000	.000	.000	.000
97	.00000E+00	100.000	.000	.000	.000	.000	.000	.000	.000	.000	.000	.000
98	.00000E+00	100.000	.000	.000	.000	.000	.000	.000	.000	.000	.000	.000
99	.00000E+00	100.000	.000	.000	.000	.000	.000	.000	.000	.000	.000	.000
100	.00000E+00	100.000	.000	.000	.000	.000	.000	.000	.000	.000	.000	.000

Figure 9.10. Sample Flaw Data Output File for Weld Region

Columns 3 through 13 of Figure 9.10 give information on the simulated aspect ratios for each of the flaw depth categories. In the case of the first row of the table (the depth category corresponding to flaws with depths between 0% and 1% of the vessel wall), it is seen that 2.285% of the flaws in this category have aspect ratios between 1:1 and 1.25:1. From the final column of Figure 9.10, it is seen that 27.633% of this category of small flaws have aspect ratios greater than 15:1. It is seen in Figure 9.10 that most of the relatively deep flaws have small aspect ratios.

Figure 9.11 is a sample plot of estimated flaw frequencies (expressed here in terms of flaws per cubic foot) as estimated for a representative vessel. This plot addresses flaws for all categories including welds, base metal and clad/surface flaws. The flaw depth distributions of Figure 9.11 are truncated to preclude extrapolations of curves to flaw depths that are significantly larger than the depth dimensions of flaws that were detected in the PNNL examinations of vessel materials.

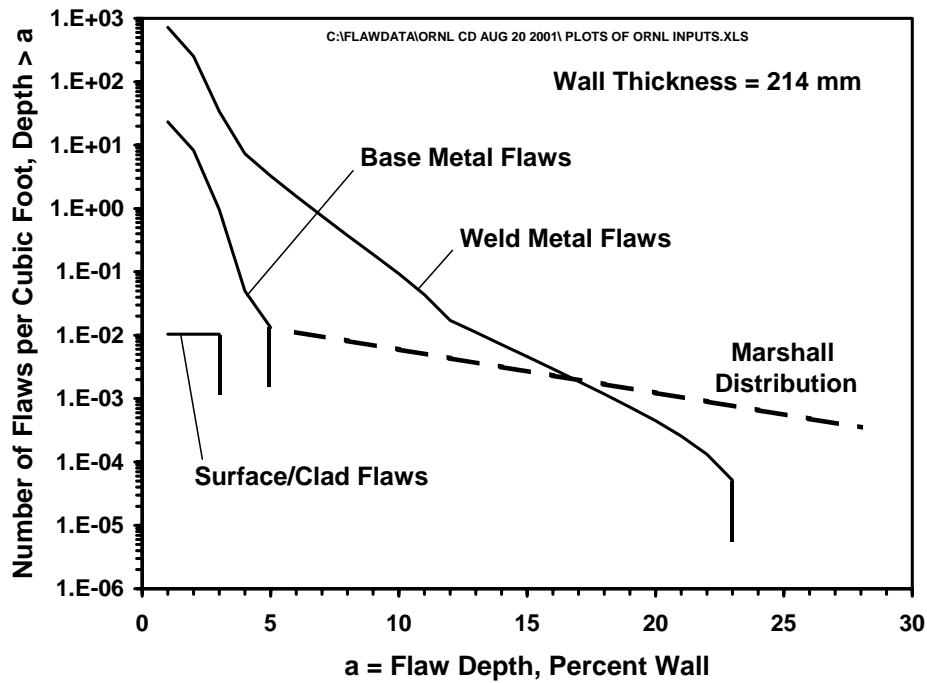


Figure 9.11. Flaw Distribution for Various Vessel Regions (Median Values from Uncertainty Analyses)

## 9.5 Procedure for Base Metal Regions

Section 7 of this report describes the approach for developing statistical distributions for flaws in base metal regions. The implementation of the statistical formulation into the flaw distribution algorithm is described in the following paragraphs.

### 9.5.1 Treatment of Base Metal Flaws

Flaws are observed to occur at much lower rates in base metal (per unit volume of metal) than in welds. It has also been observed that the largest flaws in plate and forging materials have orientations parallel to the surfaces of the vessel. This orientation is related to the rolling and forming operations used to fabricate the vessel plates and forged rings. Although these laminar-type flaws can be quite large, they

have no significance to vessel integrity. In this discussion, the base metal flaws of concern are therefore only those flaws that have some through-wall dimension. As discussed above in Section 7, PNNL's examinations of plate materials show that flaws occur at lower rates per unit volume (by a factor of 10 or greater) than in welds.

### 9.5.2 Flow Chart for Base Metal

Because the flow chart for base metal flaws is essentially the same as the flow chart for weld metal flaws (see Figure 9.7), a separate chart is not needed. The only difference is that the flaw densities for base metal (flaws per unit volume) are reduced by a factor of 10 for small flaws and by a factor of 40 for large flaws relative to values simulated for weld metal. In accordance with the questions posed during expert judgment elicitation, flaw estimates for plate materials are based on adjustments to distributions derived from the data from the PVRUF vessel rather than from the Shoreham vessel. The input file for FAVOR (1000 datasets) for base metal flaws has the same treatment of statistical uncertainties as developed for the PVRUF data for weld flaws. Truncations for maximum depths of base metal flaws (as described in Section 7) are different than the truncations for weld flaws, such that recommended truncations for base metal flaws occur at much smaller flaw depths than for weld flaws.

### 9.5.3 Sample Input and Output Files for Base Metal

Figures 9.12 through 9.14 present inputs and outputs for a sample calculation for base metal by the PNNL flaw distribution algorithm. As indicated in Figure 9.13, this example was based on the flaw distribution parameters and the uncertainty distributions obtained from analyses of the PVRUF data. Figure 9.14 is the first simulated distribution of a total of 1000 such tables corresponding to sampling for the uncertainty analysis.

As for the weld flaws, the rows of Figure 9.14 come from a binning into 100 bins of the data from the continuous flaw distributions generated by the algorithm. Each bin corresponds to a depth category defined by 1% increments of the vessel wall thickness. For example, the bin designated by the label "1" gives the number of flaws per cubic foot that have depth dimensions between 1% and 2% of the vessel wall thickness. There are 17.505 flaws per cubic foot for this depth category, whereas the number of very large flaws with depths between 4% and 5% of the vessel wall thickness is only 0.014037 flaws per cubic foot. There are no flaws with depths greater than 5% of the vessel wall thickness, consistent with the specified truncation flaw depths.

Columns 3 through 13 of Figure 9.14 give information on the aspect ratios for each of the flaw depth categories. Considering the first row of the table (the depth category corresponding to flaws with depths between 0% and 1% of the vessel wall), it is seen that 46.753% of the flaws in this category have aspect ratios between 1:1 and 1.25:1. From the final column of the table, it is seen that only 1.340% of this category of small flaws have aspect ratios greater than 15:1.

Figure 9.11 includes a sample plot of estimated flaw frequencies (flaws per cubic foot) as estimated for base metal. The flaw depth distributions of Figure 9.11 are truncated to preclude extrapolations of curves to flaw depths that are much larger than the depth dimensions of any flaws that were detected in the PNNL examinations of vessel materials.

OCONEE-1 OCTOBER 29, 2002 - BASE METAL						FLAWS/FT <sup>3</sup>		
	3	1000	219.10	2	1	1	1	0.0
0.9300	1	1	6.5	1.0			11.00	
0.0500	1	2	3.5	1.0			11.00	
0.0200	1	3	3.5	1.0			11.00	

**Figure 9.12. Sample from Flaw Distribution Input File for Base Metal Region**

```

GENERATION OF FLAW DISTRIBUTION INPUT FILE FOR THE ORNL FAVOR CODE

NAME OF REGION = OCONEE-1 OCTOBER 29, 2002 - BASE METAL   FLAWS/FT^3

NUMBER OF SUBREGIONS =      3
UNCERTAINTY CALCULATION
NUMBER OF MONTE CARLO SIMULATIONS = 1000
VESSEL TOTAL WALL THICKNESS (MM) = 219.10
ENGLISH UNITS - FLAWS PER FT^2 OR FLAWS PER FT^3
WELD DENSITY OPTION - FLAWS PER UNIT VOLUME
BASE_METAL APPROXIMATION IS USED

OUTPUT FILE REFORMATTED FOR INPUT TO ORNL FAVOR CODE

SUBREGION NUMBER  1
  VOLUME FRACTION = .9300
  PVRUF VESSEL PARAMETERS
  SAW (SUBMERGED METAL ARC WELD)
  BEAD SIZE (MM) = 6.50
  FACTOR ON FLAW FREQUENCIES = 1.0000 (DEFAULT = 1.0)
  CLAD THICKNESS(MM) = .0000 (USED ONLY FOR CLAD)
  CLAD BEAD WIDTH (MM) = .0000 (USED ONLY FOR CLAD)
  NUMBER OF CLAD LAYERS = 0 (USED ONLY FOR CLAD)
  TRUNCATION ON FLAW DEPTH (MM) = 11.0000

SUBREGION NUMBER  2
  VOLUME FRACTION = .0500
  PVRUF VESSEL PARAMETERS
  SMAW (SHIELDED METAL ARC WELD)
  BEAD SIZE (MM) = 3.50
  FACTOR ON FLAW FREQUENCIES = 1.0000 (DEFAULT = 1.0)
  CLAD THICKNESS(MM) = .0000 (USED ONLY FOR CLAD)
  CLAD BEAD WIDTH (MM) = .0000 (USED ONLY FOR CLAD)
  NUMBER OF CLAD LAYERS = 0 (USED ONLY FOR CLAD)
  TRUNCATION ON FLAW DEPTH (MM) = 11.0000

SUBREGION NUMBER  3
  VOLUME FRACTION = .0200
  PVRUF VESSEL PARAMETERS
  REPAIR WELD
  BEAD SIZE (MM) = 3.50
  FACTOR ON FLAW FREQUENCIES = 1.0000 (DEFAULT = 1.0)
  CLAD THICKNESS(MM) = .0000 (USED ONLY FOR CLAD)
  CLAD BEAD WIDTH (MM) = .0000 (USED ONLY FOR CLAD)
  NUMBER OF CLAD LAYERS = 0 (USED ONLY FOR CLAD)
  TRUNCATION ON FLAW DEPTH (MM) = 11.0000

```

**Figure 9.13. Sample Flaw Distribution Output File for Base Metal Region**



## 9.6 Procedure for Surface/Clad Flaws

Section 8 of this report describes the approach for developing statistical distributions for flaws in clad regions. The implementation of the statistical formulation into the flaw distribution algorithm is described in the following paragraphs.

### 9.6.1 Treatment of Surface/Clad Flaws

As described in Section 8, the numbers and sizes of clad/surface-breaking flaws at the inner surface of a vessel have been estimated from data on flaws that have been detected during examinations of vessel cladding. These flaws can occur randomly in the cladding applied over both weld and base metal. Because most of the vessel inner surface consists of base metal, all but a small fraction of the clad (or surface-related) flaws will be adjacent to base metal rather than at weld metal locations. All of the surface/clad flaws are assumed to have circumferential orientations consistent with the direction of the weld beads that make up the clad. The flaw depths are assumed to be equal to the full thickness of the clad and are assigned to the depth dimension bin that approximates the clad thickness.

### 9.6.2 Flow Chart for Surface/Clad Flaws

The computational procedure for generating the distribution tables for surface/clad flaws is relatively simple compared to the flow chart of Figure 9.2. Section 8 describes the procedure in detail. The underlying methodology is designed to provide flaw distribution tables in terms of flaws per unit area of vessel inner surface. However, to be consistent with the FAVOR code, these distributions can be converted to surface flaws per unit volume or unit area based on the material for the full thickness of the vessel wall.

### 9.6.3 Sample Input and Output Files for Surface/Clad Flaws

Figures 9.15 through 9.17 present inputs and outputs for a sample calculation for clad/surface flaws generated by the PNNL flaw distribution algorithm. This table was the first of a total of 1000 such tables that make up the input file for FAVOR. Because there was no evaluation of statistical uncertainties for the flaw distribution parameters for surface/clad flaws, all 1000 datasets are identical. However, the FAVOR code is structured to address uncertainties in the distributions, should it become possible in the future to quantify these uncertainties.

The rows of Figure 9.17 come from a binning of the data from the continuous flaw distributions into 100 bins. Each bin corresponds to a depth category defined by 1% increments of the vessel wall thickness. For example, the bin designated by the label "1" on Figure 9.17 gives the number of flaws per square foot that have depth dimensions between 1% and 2% of the vessel wall thickness. In this case, there are zero flaws per square foot for this depth category because the depth of a flaw extending through the full clad thickness does not correspond to this particular bin. Rather, the specified clad thickness of 4.77 mm results in flaws having depths within the bin of 2% to 3% of the vessel wall thickness. In this case, there are 0.0036589 clad/surface flaws per square foot of clad surface, and all flaws are within the bin corresponding to 2% to 3% of the vessel wall. The value of flaw density of 0.0036589 is relatively small because it accounts for the factor of 1000 ratio (as discussed in Section 8) between the total clad flaw density (including clad flaws of all depth dimensions) versus the small number of through-clad flaws that are sufficiently large to contribute to vessel failure.

```

OCONEE-1  CLAD  OCTOBER 29, 2002  SINGLE LAYER  FLAWS/FT^2
          1    1000  219.10          2          2          0  1          0.0
1.0000    1    4 4.77          1.0 4.77 25.4    1    200.0

```

**Figure 9.15. Sample Flaw Distribution Input File for Surface/Clad Flaws**

```

GENERATION OF FLAW DISTRIBUTION INPUT FILE FOR THE ORNL FAVOR CODE

NAME OF REGION =  OCONEE-1  CLAD  OCTOBER 29, 2002  SINGLE LAYER  FLAWS/FT^2

NUMBER OF SUBREGIONS =      1
UNCERTAINTY CALCULATION
NUMBER OF MONTE CARLO SIMULATIONS =  1000
VESSEL TOTAL WALL THICKNESS (MM) =  219.10
ENGLISH UNITS - FLAWS PER FT^2 OR FLAWS PER FT^3
WELD DENSITY OPTION - FLAWS PER UNIT AREA
BASE_METAL APPROXIMATION NOT USED

OUTPUT FILE REFORMATTED FOR INPUT TO ORNL FAVOR CODE

SUBREGION NUMBER  1
  VOLUME FRACTION =  1.0000
  PVRUF VESSEL PARAMETERS
  CLAD
  BEAD SIZE (MM)      =  4.77
  FACTOR ON FLAW FREQUENCIES =  1.0000  (DEFAULT = 1.0)
  CLAD THICKNESS(MM)  =  4.7700  (USED ONLY FOR CLAD)
  CLAD BEAD WIDTH (MM) =  25.4000  (USED ONLY FOR CLAD)
  NUMBER OF CLAD LAYERS =  1  (USED ONLY FOR CLAD)
  TRUNCATION ON FLAW DEPTH (MM) =  200.0000

```

**Figure 9.16. Output File for Surface/Clad Flaws**

It is also seen in Figure 9.17 that 67.45% of the flaws have aspect ratios equal to 2:1. The final column of the table indicates that 7.817% of the flaws have aspect ratios that should be treated as infinite by FAVOR.

Figure 9.11 includes a plot of the clad/surface flaw distribution. The flaw depth distribution is flat and is truncated at a flaw depth dimension corresponding to the thickness of the clad.



## 10 CONCLUSIONS

An improved model for postulating fabrication flaws in reactor pressure vessels has been developed that is based on empirical data representative of fabrication practices in the U.S. from the late 1960s through early 1980s. This model addresses three broad categories of flaws: (1) weld flaws, (2) base metal flaws, and (3) cladding flaws. A separate set of input data corresponding to each flaw category is provided as input to the FAVOR code for PTS calculations. The input files describe the number of flaws per unit of weld fusion surface or per cubic volume of metal, the distribution of flaw depth dimensions, and the distribution of flaw aspect ratios. Other key features of the flaw model are as follows:

1. The flaw model treats the flaw locations as uniformly distributed through the thickness of the vessel wall and does not make the conservative assumption that the flaws are inner-surface breaking.
2. Weld flaws are assumed in the FAVOR code to lie along the weld fusion line in a manner to allow them to potentially grow into either the weld material or base metal, whichever is more limiting from the standpoint of fracture toughness.
3. Clad materials are assumed to have sufficient fracture toughness to preclude the growth of flaws within the cladding material, which implies that the clad flaws are structurally significant only if they extend up to or penetrate beyond the clad-to-base metal interface.
4. Underclad cracks in base metal are not addressed, although the model could be enhanced in the future to evaluate vessels of concern to PTS for which underclad cracking is considered a credible mechanism of cracking.
5. Flaws of most concern to failure of base metal regions include both the flaws associated with weld fusion line and the flaws associated with cladding in addition to flaws within the base metal itself.

Data files have been prepared for use by ORNL for PTS calculations with the FAVOR code. Calculations have been performed for several representative vessels that have considered plants from the major nuclear steam supply system suppliers. Although most calculations have been for vessels for which the weld material is the most limiting from the standpoint of embrittlement, one vessel has had base metal as the most limiting material.

## 11 REFERENCES

Bishop BA. 1993. *Benchmarking of Probabilistic Fracture Mechanics Analyses of Reactor Vessels Subjected to Pressurized Thermal Shock Loading*, EPRI Research Project 2975-5, Electric Power Research Institute, Palo Alto, CA.

Chapman OJV. 1993. "Simulation of Defects in Weld Construction," *Reliability and Risk in Pressure Vessels and Piping*, PVP-Vol. 251, pp. 81-89, American Society of Mechanical Engineers, New York.

Chapman OJV, and FA Simonen. 1998. *RR-PRODIGAL - A Model for Estimating the Probabilities of Defects in Reactor Pressure Vessel Welds*, NUREG/CR-5505, U.S. Nuclear Regulatory Commission, Washington, DC.

Chapman OJV, MA Khaleel, and FA Simonen. 1996. "A Simulation Model for Estimating Probabilities of Defects in Welds," *Fatigue and Fracture - 1996 - Volume 1*, PVP Vol. 323, pp. 375-391, American Society of Mechanical Engineers, New York.

Crawford SL, GJ Schuster, AF Pardini, and SR Doctor. 2000. "Initial Studies in Developing Fabrication Flaw Rates for Base Metal of Pressure Vessels," presented at the 2<sup>nd</sup> *International Conference on NDE in Relation to Structural Integrity for Nuclear and Pressurized Components*, New Orleans, LA (May 24-26, 2000).

Dickson TL. 1994. *FAVOR: A Fracture Mechanics Analysis Code for Nuclear Reactor Pressure Vessel, Release 9401*, ORNL/NRC/LTR/94/1, Martin Marietta Energy Systems, Inc., Oak Ridge National Laboratory, Oak Ridge, TN.

Dickson TL, and FA Simonen. 1997. "Inclusion of Embedded Flaws in Pressurized Thermal Shock Analyses of Nuclear Reactor Pressure Vessels," *Fatigue and Fracture - 1997 - Volume 2*, PVP Vol. 346, pp. 197-205, American Society of Mechanical Engineers, New York.

Dickson TL, SNM Malik, JW Bryson, and FA Simonen. 1999. "Revisiting the Integrated Pressurized Thermal-Shock Studies of an Aging Pressurized Water," *Fracture, Design Analysis of Pressure Vessels, Heat Exchangers, Piping Components and Fitness for Service - 1999*, PVP Vol. 388, American Society of Mechanical Engineers, New York.

Halmshaw R, and CA Hunt. 1975. "Can Cracks Be Found by Radiography?," *British Journal of Nondestructive Testing*, May 1975, pp. 71-75.

Jackson DA, and L Abramson. 2000. *Report on the Preliminary Results of the Expert Judgment Process for the Development of a Methodology for a Generalized Flaw Size and Density Distribution for Domestic Reactor Pressure Vessels*, MEB-00-01, PRAB-00-01, U.S. Nuclear Regulatory Commission, Washington, DC.

Jackson DA, and SR Doctor. 2000. "Developing a Generic Flaw Distribution for Reactor Pressure Vessels," 2<sup>nd</sup> *International Conference on NDE in Relation to Structural Integrity for Nuclear and Pressurized Components*, New Orleans, LA (May 24-26, 2000).

- Jackson DA, L Abramson, SR Doctor, FA Simonen, and GJ Schuster. 2001. "Developing a Generalized Flaw Distribution for Reactor Pressure Vessels," *Nuclear Engineering and Design*, Vol. 208, pp. 123-131.
- Li YY, and WR Mabe. 1998. "Defect Distribution in Weld-Deposited Cladding," *Fatigue, Environmental Factors, and New Materials*, PVP Vol. 374, pp. 75-90, American Society of Mechanical Engineers, New York.
- Marshall Committee. 1982. *An Assessment of the Integrity of PWR Vessels*, Second Report by a Study Group under the Chairmanship of DW Marshall, published by the U.K. Atomic Energy Commission.
- Pardini AF, GJ Schuster, SL Crawford, and SR Doctor. 2000. "Validation of Fabrication Flaws in Weld metal from PVRUF," *2<sup>nd</sup> International Conference on NDE in Relation to Structural Integrity for Nuclear and Pressurized Components*, New Orleans, LA (May 24-26, 2000).
- Schuster GJ, SR Doctor, and PG Heasler. 1998. *Characterization of Flaws in U.S. Reactor Pressure Vessels: Density and Distribution of Flaw Indications in PVRUF*. NUREG/CR-6471, Vol. 1, U.S. Nuclear Regulatory Commission, Washington, DC.
- Schuster GJ, SR Doctor, SL Crawford, and AF Pardini. 1999. *Characterization of Flaws in U.S. Reactor Pressure Vessels: Density and Distribution of Flaw Indications in the Shoreham Vessel*, NUREG/CR-6471, Vol. 3, U.S. Nuclear Regulatory Commission, Washington, DC.
- Schuster GJ, SR Doctor, SL Crawford, and AF Pardini. 2000a. *Characterization of Flaws in U.S. Reactor Pressure Vessels: Validation of Flaw Density and Distribution in the Weld Metal of the PVRUF Vessel*, NUREG/CR-6471, Vol. 2, U.S. Nuclear Regulatory Commission, Washington, DC.
- Schuster GJ, AF Pardini, SL Crawford, and SR Doctor. 2000b. "Overview of Fabrication Flaw Studies on RPV Material from Four Canceled Nuclear Power Plants," *2<sup>nd</sup> International Conference on NDE in Relation to Structural Integrity for Nuclear and Pressurized Components*, New Orleans, LA (May 24-26, 2000).
- Schuster GJ, and SR Doctor. 2001a. "Fabrication Flaw Rate Estimates for Base Metal of Pressure Vessels and Initial Validation Results," *3<sup>rd</sup> International Conference on NDE in Relation to Structural Integrity for Nuclear and Pressurized Components*, Seville, Spain.
- Schuster GJ, and SR Doctor. 2001b. "Use of SAFT-UT in Characterizing Fabrication Flaws in Nuclear Reactor Pressure Vessels," *3<sup>rd</sup> International Conference on NDE in Relation to Structural Integrity for Nuclear and Pressurized Components*, Seville, Spain.
- Simonen FA, KI Johnson, AM Liebetrau, DW Engel, and EP Simonen. 1986. *VISA-II-A Computer Code for Predicting the Probability of Reactor Pressure Vessel Failure*, NUREG/CR-4486, U.S. Nuclear Regulatory Commission, Washington, DC.
- Simonen FA, and KI Johnson. 1993. "Effects of Residual Stresses and Underclad Flaws on the Reliability of Reactor Pressure Vessels," *Reliability and Risk in Pressure Vessels and Piping*, PVP Vol. 251, pp. 91-100, American Society of Mechanical Engineers, New York.

Simonen FA, SR Doctor, GJ Schuster, DA Jackson, and L Abramson. 2001. "Flaws in Vessel Cladding and Their Potential Contributions to Vessel Failure Probabilities," *Service Experience, Fabrication, Residual Stresses and Performance*, PVP Vol. 427, pp. 21-32, American Society of Mechanical Engineers, New York.

## **Appendix A**

# **STATISTICAL EQUATIONS FOR FLAW DISTRIBUTION FUNCTIONS AND UNCERTAINTY ANALYSES**

## Appendix A

# STATISTICAL EQUATIONS FOR FLAW DISTRIBUTION FUNCTIONS AND UNCERTAINTY ANALYSES

This appendix describes the basis of a Monte Carlo methodology to simulate uncertainty in flaw distribution estimates. This methodology relies on the “generalized flaw distribution model” that NRC developed (Jackson and Abramson 2000) to describe flaws in a RPV. The objective is to develop a methodology for producing a set of flaw distribution functions along with a characterization of the statistical uncertainties in the parameters of the functions. The FAVOR code performs a random sampling to incorporate the uncertainty into vessel evaluations. Because such a strategy implicitly views the flaw density and size distribution functions as random, it is natural to utilize a Bayesian estimation methodology. Under a Bayesian methodology, the data are summarized in terms of a posterior distribution, and a Monte Carlo sampling of the posterior will produce a set of results that describe uncertainty.

### A.1 Definitions

The function  $\gamma(x, \alpha)$ : represents a gamma density function parameterized by the vector  $\alpha$ . as defined by the formula

$$\gamma(x:\alpha) = \frac{\alpha_1^{\alpha_2} x^{\alpha_2-1}}{\Gamma(\alpha_2)} \exp(-\alpha_1 x) \quad (\text{A.1})$$

The function  $DIR(p : \alpha)$  is a Dirichlet distribution, which is defined as

$$DIR(p:\alpha) = \frac{\Gamma(\alpha_+)}{\Gamma(\alpha_1)\Gamma(\alpha_2)\dots\Gamma(\alpha_m)} p_1^{\alpha_1-1} p_2^{\alpha_2-1} \dots p_m^{\alpha_m-1} \quad (\text{A.2})$$

### A.2 Distributional Families Required for Modeling

This section presents three distributional families that are required to model the available flaw data. These are Poisson, exponential, and multinomial. The Poisson distribution is used to model flaw density data, while the other two are used to describe the flaw depth and length data. The following describes the standard posteriors for each distributional family.

#### A.2.1 Posterior for a Poisson Density Parameter

A flaw density parameter  $\rho$  is to be estimated from count data; a total of  $N$  flaws are observed in a volume  $V$  of material. The count  $N$  is assumed to be Poisson distributed, so the conditional distribution is

$$f(N|\rho) = \exp(-\rho V) \frac{(\rho V)^N}{N!} \quad (\text{A.3})$$

The standard conjugate prior employed for such a distribution is a two-parameter gamma distribution. Assume that the prior distribution is

$$p(\rho) = \gamma(\rho : \alpha) \quad (\text{A.4})$$

Then the posterior distribution is given by

$$f(\rho|N) = \gamma(\rho : \alpha_1 + V, \alpha_2 + N) \quad (\text{A.5})$$

The standard noninformative prior assigns  $\alpha_1 = 0$ , and  $\alpha_2 = 0$ , so that the posterior is the same as the likelihood. However, if one uses this improper prior, the posterior will not exist when  $N = 0$ . We do not expect to encounter such situations with the current dataset, so we will employ the above prior distribution for analysis.

This means that the posterior distribution we will employ for the flaw density parameter is

$$f(\rho|N) = \gamma(\rho : V, N) \quad (\text{A.6})$$

### A.2.2 Posterior for an Exponential Distribution Parameter

A set of data,  $(x_i, i = 1, 2, 3, \dots, n)$  is observed from an exponential distribution with rate parameter  $\lambda$ . In other words, the conditional distribution for  $x_i$  is given by

$$f(x_i|\lambda) = \lambda \exp(-\lambda x) \quad (\text{A.7})$$

The standard conjugate prior distribution on  $\lambda$  is a gamma of the form

$$p(\lambda) = \gamma(\lambda : \alpha) \quad (\text{A.8})$$

and this results in a posterior distribution of

$$f(\lambda|x) = \gamma(\lambda : S + \alpha_1, n + \alpha_2) \quad (\text{A.9})$$

where  $S = \sum_i x_i$  is the sufficient statistic for the data.

### A.2.3 Posterior for Multinomial Distribution Parameters

Let  $X_i, i = 1, 2, 3, \dots, m$  represent multinomial variates, with conditional distribution

$$f(X|\beta) = \frac{X_+!}{X_1! X_2! \dots X_m!} \beta_1^{N_1} \beta_2^{N_2} \dots \beta_m^{N_m} \quad (\text{A.10})$$

The parameter vector,  $\beta$ , must sum to one.

The conjugate family for this distribution is the Dirichlet, which is denoted as  $DIR(p : \alpha)$ . If the prior distribution is given by

$$p(\beta) = DIR(\beta : \alpha) \quad (\text{A.11})$$

then the posterior is given by

$$f(\beta|X) = DIR(\beta : \alpha + X) \quad (\text{A.12})$$

The standard noninformative prior is produced by setting  $\alpha_i = 0$ . With the noninformative assignment, the posterior will not exist if any  $X_i$  is zero. Because we intend to use the multinomial on small flaws only, which are quite numerous,  $X_i$  is not expected to be zero, so we will set alpha to zero. The posterior employed on multinomial data is therefore

$$f(\beta|X) = DIR(\beta : X) \quad (\text{A.13})$$

### **A.3 Reference**

Jackson DA, and L Abramson. 2000. *Report on the Preliminary Results of the Expert Judgment Process for the Development of a Methodology for a Generalized Flaw Size and Density Distribution for Domestic Reactor Pressure Vessels*, MEB-00-01, PRAB-00-01, U.S. Nuclear Regulatory Commission, Washington, DC.

## **Appendix B**

### **LIST OF EXPERTS ON VESSEL FLAWS**

## Appendix B

### LIST OF EXPERTS ON VESSEL FLAWS

Name	Affiliation	Area of Expertise
Frank Ammirato	Manager, Electric Power Research Institute (EPRI) NDE Center	Non-Destructive Examination
Francis Berry	Consulting Engineer Retired, Chicago Bridge & Iron	Non-Destructive Examination, Reactor Vessel Fabrication
Spencer Bush, PhD.	President, Review & Synthesis Associates Retired, Pacific Northwest National Laboratory	ASME Code, Non-Destructive Examination, Metallurgy
Domenic Canonico, PhD.	Industry Consultant	ASME Code, Failure Analysis, Forgings, Metallurgy, Reactor Vessel Fabrication, Welding
O.J. Victor Chapman	President, OJVC Consultancy Retired, Rolls Royce	Expert Elicitation, Failure Analysis, Non-Destructive Examination, Statistics, Welding
Robert DeNale	Naval Surface Warfare Center Head, Metals Department	Failure Analysis, Metallurgy, Non-Destructive Examination, Welding
John Lareau	Westinghouse formerly Combustion Engineering	ASME Code, Non-Destructive Examination, Reactor Vessel Fabrication
Carl Lundin, PhD.	Professor of Metallurgy, University of Tennessee Consultant	Failure Analysis, Metallurgy, Welding
Harry Lunt	Consulting Metallurgist Retired, Burns & Roe	Forgings, Failure Analysis, Metallurgy, Non-Destructive Examination, Welding
Edward Nisbett	Consultant Retired, National Forge Co.	ASME Code, Failure Analysis, Forgings, Metallurgy
Robert B. Pond, PhD	President, M-Structures Adjunct Faculty, Johns Hopkins University, American Society of Metals, Loyola College	ASME Code, Expert Elicitation Process, Failure Analysis, Metallurgy, Non-Destructive Examination, Welding
Stan Rosinski	EPRI NDE Center, Program Manager	Metallurgy
James Sims, P.E.	Consultant Retired, Chicago Bridge & Iron	Reactor Vessel Fabrication, Welding
Kenneth Stuckey	Framatome	ASME Code, Reactor Vessel Fabrication
Helmut Thielsch, P.E. (deceased April 2003)	President, Thielsch Engineering	Failure Analysis, Metallurgy, Non-Destructive Examination

<b>Name</b>	<b>Affiliation</b>	<b>Area of Expertise</b>
David Thomas	Consultant Retired, Chairman Arcos Corporation	Welding Materials, Metallurgy, Welding.
Robert Warke	Senior Research Engineer Southwest Research Institute	ASME Code, Failure Analysis, Forgings, Metallurgy, Welding

## DISTRIBUTION

No. of  
Copies

No. of  
Copies

OFFSITE

30 Pacific Northwest National Laboratory

L. Abramson  
NRC/RES  
Mail Stop 10E50

M. T. Anderson  
S. E. Cumblidge  
A. A. Diaz  
S. R. Doctor (23)  
S. R. Gosselin  
P. G. Heasler  
G. J. Schuster  
F. A. Simonen

J. Hixon  
NRC/RES  
Mail Stop T-10E10

10 D. Jackson  
NRC/RES  
Mail Stop T-10E10

10 M. Kirk  
NRC/RES  
Mail Stop T-10E10

**BIBLIOGRAPHIC DATA SHEET**

*(See instructions on the reverse)*

1. REPORT NUMBER  
**(Assigned by NRC, Add Vol., Supp., Rev.,  
and Addendum Numbers. if anv.)**

2. TITLE AND SUBTITLE

3. DATE REPORT PUBLISHED

MONTH

YEAR

4. FIN OR GRANT NUMBER

5. AUTHOR(S)

6. TYPE OF REPORT

7. PERIOD COVERED *(Inclusive Dates)*

8. PERFORMING ORGANIZATION - NAME AND ADDRESS *(If NRC, provide Division, Office or Region, U.S. Nuclear Regulatory Commission, and mailing address; if contractor, provide name and mailing address.)*

9. SPONSORING ORGANIZATION - NAME AND ADDRESS *(If NRC, type "Same as above"; if contractor, provide NRC Division, Office or Region, U.S. Nuclear Regulatory Commission, and mailing address.)*

10. SUPPLEMENTARY NOTES

11. ABSTRACT *(200 words or less)*

12. KEY WORDS/DESCRIPTORS *(List words or phrases that will assist researchers in locating the report.)*

13. AVAILABILITY STATEMENT

**unlimited**

14. SECURITY CLASSIFICATION

*(This Page)*

**unclassified**

*(This Report)*

**unclassified**

15. NUMBER OF PAGES

16. PRICE